

## STABILITY OF ADSORBENTS FOR DIRECT AIR CAPTURE (DAC): CHALLENGES AND PERSPECTIVES

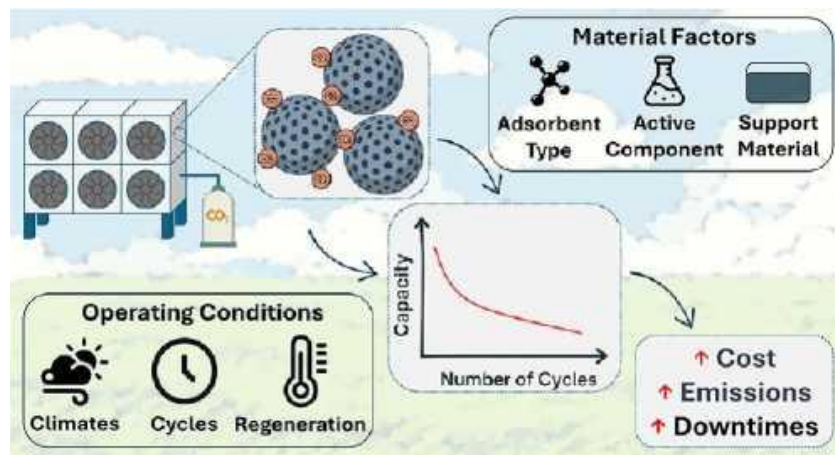
Salar Fakhreddinfakhriazar, Cristhian Molina-Fernandez, and Gregoire Leonard\*

Salar Fakhreddinfakhriazar - *Department of Chemical Engineering, Université de Liege, 4000 Liege, Belgium; orcid.org/0009-0005-8363-3691*

Cristhian Molina-Fernández - *Department of Chemical Engineering, Université de Liege, 4000 Liege, Belgium*

Grégoire Léonard - *Department of Chemical Engineering, Université de Liege, 4000 Liege, Belgium; orcid.org/0000-0003-2237-8306*

**ABSTRACT:** Direct air capture (DAC) technologies, particularly adsorption-based systems, are advancing rapidly as a form of negative emission technologies (NETs). DAC technologies represent a promising engineering approach to addressing diffuse CO<sub>2</sub> emissions and provide several deployment advantages, including flexibility and scalability. However, a critical yet often overlooked challenge of adsorption-based DAC is the limited stability of CO<sub>2</sub> sorbent materials, which undermines sustainability and hinders large-scale deployment. While most research has focused on developing adsorbents with high CO<sub>2</sub> selectivity and capacity, stability remains a crucial criterion, investigated in some studies through multicycle testing and exposure to accelerated degradation environments. This review provides a brief overview of DAC adsorbent types, followed by a detailed analysis of existing studies on the stability of solid sorbents under DAC operating conditions, highlighting key findings and research gaps. The thermal, oxidative, and hydro(thermal) stability of different adsorbents are discussed, along with the influence of operational variables on degradation mechanisms. Findings indicate that, while thermal degradation is generally not the primary concern at the moderate regeneration temperatures typical of DAC, oxidative degradation in the presence of oxygen can be severe, particularly for amine-based sorbents. Hydro(thermal) stability is found to depend largely on the properties of the support material. Ultimately, this review aims to guide the development of efficient and durable CO<sub>2</sub> adsorbents, contributing to the design of more sustainable DAC systems.



## 1. Introduction

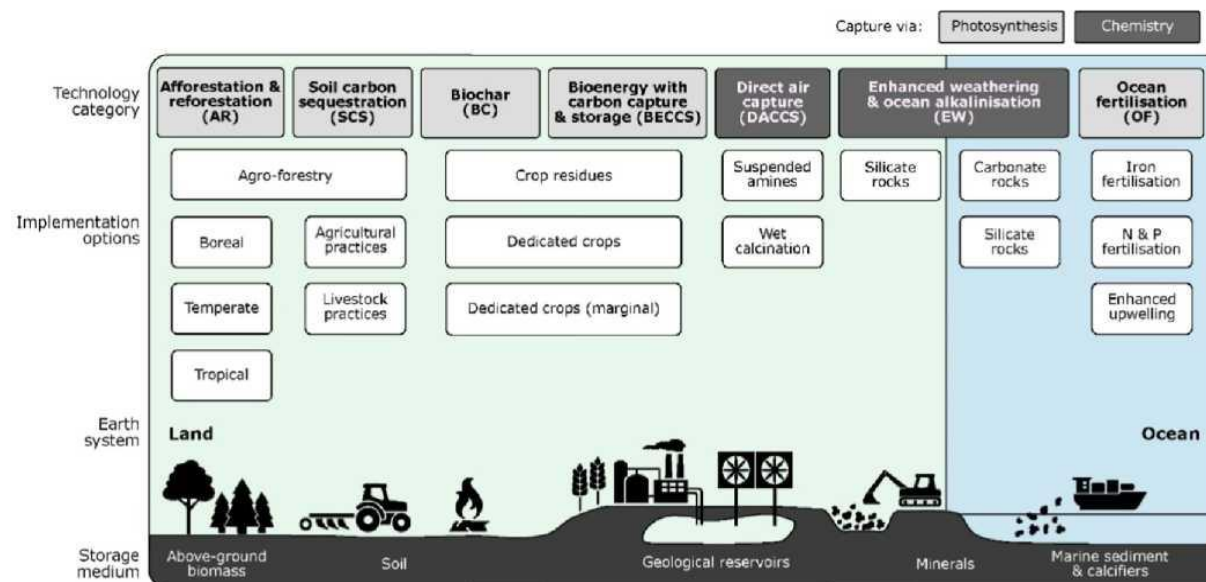
Mitigating the negative effects of global warming and preventing further anthropogenic climate change are among the most critical challenges of the 21st century. The concentration of carbon dioxide (CO<sub>2</sub>) in the atmosphere has increased by about 50% since the beginning of the Industrial Revolution, from 280 to 427 ppm in December 2025.<sup>1</sup> Prospects of human population and economic growth point toward a steady increase in atmospheric CO<sub>2</sub> concentration unless a rapid global response is deployed. According to the Intergovernmental Panel on Climate Change (IPCC), and in parallel to other actions, it now appears essential to employ negative emission technologies (NETs) to meet the strict 1.5°C temperature increase target.<sup>2</sup> With 2024 marking the first calendar year where global mean temperature rose by more than 1.5°C (approximately by 1.55 °C) above preindustrial levels,<sup>3</sup> the role of NETs becomes even more critical to avoid exceeding the upper limit of a 2 °C temperature increase.

The most important NETs are afforestation/reforestation, soil carbon sequestration, bioenergy with carbon capture and storage (BECCS), all of them often classified as indirect air capture technologies, and direct air capture with carbon sequestration (DACCS), see Figure 1.<sup>4</sup> Enhanced weathering (EW) and ocean fertilization (OF) have also been studied as potential approaches for achieving negative emissions.<sup>5,6</sup> To achieve the defined temperature increase, a mixed technology portfolio is necessary.<sup>7</sup> Afforestation/reforestation and soil carbon sequestration are regarded as more natural solutions.<sup>8</sup> Still, massive deployment of afforestation/reforestation would be accompanied by intensive land and material (water and fertilizer) usage. Widespread BECCS implementation would also be hampered by the same issue.<sup>7</sup> Compared to indirect air capture technologies, direct air capture (DAC) stands out by its lower land and water requirements as well as lower primary energy per sequestered ton of CO<sub>2</sub>.<sup>9</sup> Capturing 10 Gt<sub>CO</sub> /year employing BECCS requires land equivalent to the surface of the European continent, while DAC technology would need a land area of the size of Ireland. DAC also matches intermittent renewable energy sources, and its prospective cost is less than 100 \$/t<sub>CO2</sub>.<sup>9</sup> Moreover, the International Energy Agency (IEA) special report of 2022 introduced DAC as one of the essential approaches for fulfilling the net zero policies by the year 2050.<sup>10</sup> Finally, several pioneering companies such as Climeworks, Global Thermostat, and Carbon Engineering have shown that DAC is technically viable. Increasingly, due to the slow action of human societies and continuing increase in atmospheric CO<sub>2</sub> concentrations, direct separation of CO<sub>2</sub> from air appears unavoidable to keep global warming within the limits set at the 21st Conference of the Parties (COP21) in Paris.<sup>11,12</sup>

On the other hand, DAC faces challenges as it is an energyintensive technology, and it requires deployment of new infrastructures on a large-scale. The high energy requirements of DAC installations come from the electrical energy needed to power the fans that feed air to the system and overcome its pressure drop, but also from the energy needed for regenerating the CO<sub>2</sub> capture agent. Although known to treat the CO<sub>2</sub> emissions from concentrated industrial fumes, the gas separation techniques employed in DAC must cope with lower levels of CO<sub>2</sub> concentration (around 0.04%, i.e., at least 100 times more diluted than most industrial fumes). This level of dilution leads to an increase in the minimum thermodynamic work required to perform this separation which is of the order of 2 to 4 times more important than for concentrated CO<sub>2</sub>.<sup>13</sup> However, the work to be done is not proportional to the level of dilution which keeps the energy requirements of DAC to a high level but still worth considering. Obviously, the energy required by the DAC plants should be provided from renewable energies to prevent CO<sub>2</sub> penalty emissions that could otherwise lead to larger emissions than what can be captured, as shown in a previous

study.<sup>14</sup> Moreover, the DAC process is highly sensitive to ambient conditions, i.e., the properties of the air from which CO<sub>2</sub> is removed. These properties include variables such as temperature and humidity, which can vary significantly in different locations.

**Figure 1.** Classification and comparison of NETs. Reproduced from ref 7. Available under a CC-BY license. Copyright 2018 Minx et al.

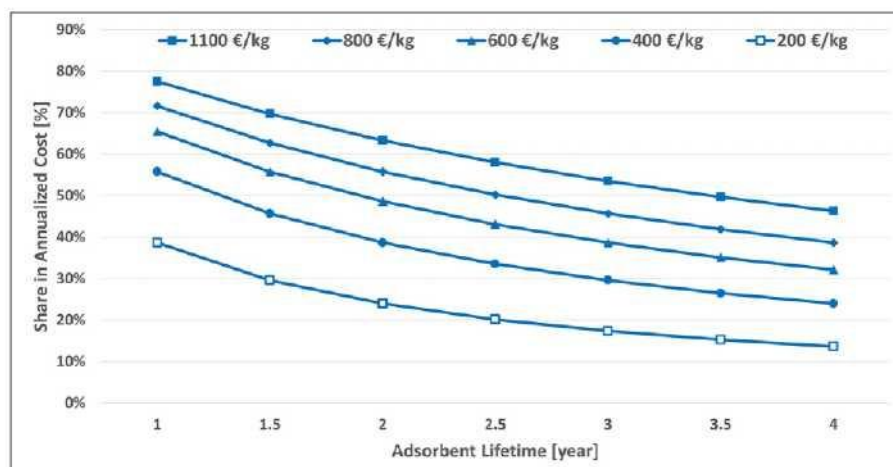


Absorption in liquid solvents and adsorption on solid sorbents are the two most mature technologies available for the separation of CO<sub>2</sub> from diluted sources, and both are currently employed by companies active in the DAC field. A typical DAC system operates in three main steps: (1) ambient air is drawn into the unit by fans and contacted with a solid or liquid sorbent; (2) CO<sub>2</sub> is selectively captured until the sorbent becomes saturated, after which CO<sub>2</sub>-depleted air is released back to the atmosphere; and (3) the saturated sorbent is regenerated by desorption, producing a concentrated CO<sub>2</sub> stream for utilization or geological storage and restoring the sorbent for subsequent cycles. Comparing adsorption and absorption technologies in energy terms, the regeneration of a CO<sub>2</sub>-loaded liquid solvent is more energy-demanding because of the stronger bonds with CO<sub>2</sub> and the noticeable amount of water present in the solvent.<sup>15-17</sup> Moreover, adsorption capture units can be easily modularized, enabling mass-manufacturing, and unlike solvent-based installations, they do not suffer from water loss or corrosion problems.<sup>4,16</sup> The present paper will thus focus on adsorbents, although its conclusions could be relevant for liquid solvent systems on a case-by-case basis.

Traditionally, DAC adsorption systems can be classified according to the contactor type, i.e., how the solid adsorbent is placed in contact with the air. Additionally, adsorption systems are differentiated based on the mechanism of sorbent regeneration. Both classifications are detailed here. First, as large air volumes have to be treated to capture enough CO<sub>2</sub>, it is essential to have energy- and cost-efficient means of ensuring intimate contact between air and the adsorbent. The air contactor must allow acceptable mass and heat transfer that is required for adsorption and regeneration steps, without a prohibiting pressure drop.<sup>4</sup> The contactors used for DAC are fixed bed, moving bed, and fluidized bed. In the fixed-bed system, there are several columns in parallel, and different stages are carried out in each column. Moving bed

systems are operated in a continuous manner, where the bed is moved between adsorption and regeneration steps. Finally, in the fluidized bed, the individual adsorbent is moved in a fluidized form between adsorption and desorption columns. While Climeworks patented a fixed-bed system,<sup>18,19</sup> Global Thermostat patented a hybrid moving and fixed-bed process design.<sup>20</sup> Although Svante has achieved a technology readiness level (TRL) of 7 for its rotating packed bed contactor in pointsource carbon capture,<sup>21</sup> the application of rotary adsorbers for DAC remains at a lower TRL.<sup>22</sup> Finally, Klomp et al. carried out DAC in a fluidized pilot facility with a capacity of 10 kgCO<sub>2</sub>/day.<sup>23</sup>

**Figure 2.** Share of adsorbent cost in the annualized CAPEX at different adsorbent prices (per kg) as a function of adsorbent lifetime (operating conditions: 18 DAC units; inlet air CO<sub>2</sub> concentration: 400 ppm (dry), adsorption temperature: 20 °C, adsorption pressure: 1 bar, blowdown pressure: 330 mbar, air throughput ≈2580 m<sup>3</sup>/h, capture rate: 2460 kgCO<sub>2</sub>/day, adsorption/regeneration/cooling cycle times ≈109/112/105 min (4 cycles/day), and regeneration temperature: 90 °C).



Regardless of the contactor configuration, the capture process could be carried out under different modes. The main DAC methods can be categorized as follows: temperature swing adsorption (TSA) or temperature concentration swing adsorption (TCSA), temperature-vacuum swing adsorption (TVSA) or temperature-vacuum concentration swing adsorption (TVCSA), moisture swing adsorption (MSA), electro-swing adsorption,<sup>24</sup> microwave-assisted desorption,<sup>25,26</sup> and electrically driven temperature swing adsorption (ETSA).<sup>27,28</sup> The regeneration step in these methods differs in the nature or agents used to trigger the release of CO<sub>2</sub> from the material. The selection of regeneration method depends on several factors such as the desired purity of the final CO<sub>2</sub> product, availability of waste heat or low-pressure steam, and the characteristics of the adsorbent (i.e., isotherms and temperature and moisture stability).<sup>4</sup> During TSA cycles, the temperature is increased to break the bonds between CO<sub>2</sub> and the solid adsorbents, whereas in TVSA cycles the temperature is raised after applying vacuum. In the TCSA process, besides elevating temperature, an inert gas is used to purge the system. The DAC process can be also performed using steam-assisted TSA and TVSA (S-TSA and S-TVSA), where the steam can be employed to provide the heat required for the regeneration as well as being used as the purge gas.<sup>29,30</sup> In ETSA, the required temperature increase is instead generated in situ via direct Joule heating of electrically conductive supports, such as coated carbon fiber.<sup>28</sup> Analogously, in MSA, after CO<sub>2</sub> is captured from dry air, moisture

is introduced to the system to release the adsorbed CO<sub>2</sub>.<sup>31</sup> More comprehensive information can be found in the review paper published by Low and co-workers.<sup>4</sup>

Efforts in the domain of adsorbent development are mostly dedicated to enhancing adsorbent capacity and selectivity. These properties are of paramount importance as they directly influence the required amount of solid sorbent for a given capture scale and the purity of the recovered CO<sub>2</sub>, respectively. The stability of the CO<sub>2</sub> adsorbents is also a key factor in the evaluation of adsorbent performance.<sup>32</sup> Though many adsorbents are suggested to be suitable for DAC, stability analysis (longevity tests) of these sorbents was only conducted superficially. Most adsorbents have been tested in a very limited number of cycles, often less than 100 cycles. During these cycles, the sorbent is usually exposed to idealized conditions such as the use of an inert atmosphere, which is translated into a likely overestimation of the material lifetime and overlooking the effect of oxygen (O<sub>2</sub>) presence on the stability of the adsorbent.

To evidence the potential effect of stability on the cost, some calculations are performed using data from the work by Kim and Léonard.<sup>33</sup> In that paper, the Climework's Hinwil plant with a capacity of 2460 kg of CO<sub>2</sub>/day was modeled. Based on their assumption of using about 550 kg adsorbent in this plant and considering 2.5 years of stability and adsorbent price near 1100 €/kg, it appears that the sorbent cost contributes to 58% of the annualized capital expenditure (CAPEX). Based on these values, different scenarios assuming different stability times and adsorbent costs are evaluated and illustrated in Figure 2. In this regard, by increasing the adsorbent's lifetime up to 4 years, the share of this cost can be decreased to 46% of annualized CAPEX, which is still very significant. Thus, adsorbent stability seems to have an important impact on the economics of DAC capture. Similarly, Holmes et al.<sup>34</sup> presented an economic model that included the effects of adsorbent degradation and reduced capacity, showing that levelized costs increased with higher deactivation rates. Indeed, the analysis indicated that optimizing replacement time results in a cost difference of approximately \$700 per ton of net CO<sub>2</sub> captured between the lowest and highest degradation scenarios, highlighting the potential impact of sorbent stability on the economics of DAC. Readers are encouraged to refer to their study for further details. Additionally, degradation of the solid adsorbents may cause complexities in the systems, efficiency loss, secondary emissions, and undesirable shutdowns, which in turn further increases the capture cost.<sup>17</sup> Consequently, the stability of amine-based carbon capture adsorbents has been described as "a multifaceted puzzle" by Jahandar Lashaki and coauthors<sup>35</sup> in their review article published in 2019.

Although numerous reviews have addressed DAC and solid sorbents for CO<sub>2</sub> capture, focusing on material classes, synthesis strategies, and performance metrics such as adsorption capacity and kinetics,<sup>36-40</sup> the stability and long-term durability of adsorbents have received comparatively limited attention. To date, only two reviews have explicitly focused on sorbent stability. The comprehensive review by Jahandar Lashaki et al.<sup>35</sup> primarily focuses on post-combustion CO<sub>2</sub> capture adsorbents and predates many recent studies conducted under DAC-relevant conditions, while the more recent review by Zhao et al.<sup>41</sup> provides a relatively brief assessment; notably, both reviews are limited to amine-based adsorbents. In contrast, the present review offers a DAC-specific and broader perspective, critically examining the stability of all major classes of solid adsorbents relevant to DAC. Particular emphasis is placed on degradation mechanisms and characterization methods to elucidate the degradation mechanisms, with the aim of supporting the development of more robust DAC adsorbents and informing the selection of operating conditions that minimize performance degradation.

Since this review is intended to serve as a resource for both experts and early-stage researchers, it begins by outlining and classifying the various DAC adsorbent materials. Then, the different deactivation mechanisms are thoroughly discussed. The main deactivation routes (thermal, oxidative, and hydrothermal) are examined in three dedicated sections. These sections examine different materials, including metalorganic frameworks (MOFs), supported amines (impregnated, grafted, or in situ polymerized), commercial materials such as Lewatit, and carbonate-based adsorbents. Moreover, the significance of interactions between the active component and the solid support is emphasized. Additionally, the main solid and gaseous byproducts formed during each degradation pathway are identified. Although not performed under DAC conditions, some works were also included due to their relevance to the subject. Overall, this review provides a comprehensive summary of the state of the art and highlights the research still needed in terms of adsorbent stability to support DAC deployment.

## 2. DAC adsorbents: Types and characteristics

CO<sub>2</sub> capture adsorbents are generally classified as physical or chemical adsorbents (known as physisorbent or chemisorbent). The difference originates from the mechanism involved in the bonding of the CO<sub>2</sub> molecule to the sorbent functional groups. While physical adsorbents rely on weak van der Waals forces, chemical adsorbents form covalent bonds after a chemical reaction has taken place. As adsorption is a surface phenomenon, porous materials are particularly suitable due to their high specific surface area. Chemical adsorbents are more selective and present higher loading capacity; however, due to their stronger connection to CO<sub>2</sub>, their regeneration energy is higher than physisorbents. Physical adsorbents, as their equilibrium loading of CO<sub>2</sub> is a function of the gas partial pressure, are less suitable for application in DAC.<sup>17</sup> Apart from

being less selective, the heat of adsorption of these adsorbents is lower, resulting in low adsorption capacity under ultradilute DAC conditions.<sup>42</sup> Physical adsorbents without reactive functional groups include zeolites, carbon-based materials, MOFs, and covalent organic frameworks (COFs). In contrast, among chemical adsorbents, solids incorporating amino functionalities are particularly relevant. Other basic functional groups, such as carbonates, have also been reported.<sup>43,44</sup>

Different indicators can be used to evaluate the quality of an adsorbent. First, the heat or enthalpy of adsorption (also known as the isosteric heat or isosteric enthalpy of adsorption) is the most important thermodynamic parameter of adsorption. A higher heat of CO<sub>2</sub> adsorption indicates a greater energy requirement for its desorption.<sup>45</sup> In physisorption, the heat of adsorption remains low (less than 0.40 eV or 1-40 kJ/mol) due to weak binding forces between the adsorptive and adsorbent. Conversely, chemisorption results in a higher heat of adsorption (greater than 0.41 eV or 40-800 kJ/mol) because it involves strong chemical bond formation.<sup>46</sup> Then, high CO<sub>2</sub> uptake capacity, high CO<sub>2</sub> selectivity, acceptable stability, low regeneration energy, fast adsorption and desorption kinetics are further characteristics of a suitable carbon capture adsorbent.<sup>17</sup> Generally, the selection of appropriate carbon capture adsorbents depends on several key performance indicators (KPIs) which are listed by Saenz Cavazos and co-workers and depicted in Figure 3: (1) intrinsic material properties, (2) adsorbent performance parameters and (3) process performance indicators.<sup>47</sup> It should be noted that the primary focus of this review is the stability of adsorbents. Readers are therefore

referred to other comprehensive studies for detailed discussions of additional KPIs and related adsorbent characteristics. In the following section, the main classes of sorbent materials relevant to DAC are introduced, beginning with physisorbents and followed by chemisorbents, including amine-functionalized adsorbents.

**Figure 3.** Key performance indicator (KPI) classification for carbon capture adsorption processes. Reproduced from ref 47. Available under a CC-BY license. Copyright 2023 Saenz Cavazos et al.

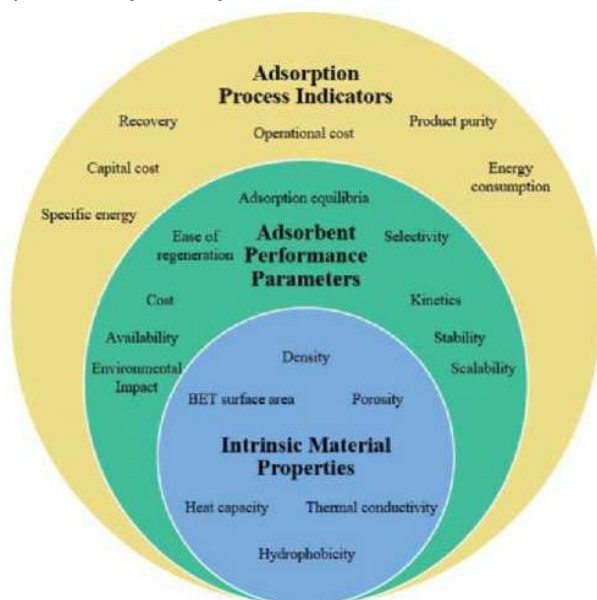


**Table 1.** Summary of Zeolite Adsorbents Evaluated under DAC-Relevant Conditions

framework	zeolite	cation	$T_{ads}$ (°C)	$q_{CO_2}$ (mmol/g) at 400 ppm (dry/wet) (RH %)	$Q_{st}$ (kJ/mol) or $T_{reg}$ (°C) g	stability observation	refs
FAU	APG-III	Na <sup>+</sup>	22	0.51/-	31.7 ± 1.3 kJ/mol	no degradation reported during regeneration-adsorption tests	63
FAU	Na-X (Siliporite Nitroxy 5)	Na <sup>+</sup>	20 -20	0.30 <sup>a</sup> / -1.10 <sup>a</sup> / -	44-49 kJ/mol 49-54 kJ/mol	stable operation demonstrated in repeated TVSA runs (7 consecutive experiments between 58 °C and -58 °C)	60
FAU	Li-X (Siliporite Nitroxy SXSDM)	Li <sup>+</sup>	20 -20	0.31 <sup>a</sup> / -0.77 <sup>a</sup> / -			
FAU	13X	Na <sup>+</sup>	25	0.23/-	-	-	59
FAU	13X	Na <sup>+</sup>	-20	2.83/-	200 °C	stable (5 cycles, TSA)	59
FAU	FAU1 (13X)	Na <sup>+</sup>	25	0.41/-	-	-	58
FAU	13X (Si/Al = 1.2)	Na <sup>+</sup>	22	0.44/0.015 <sup>b</sup> (5%)	45-50 kJ/mol 100 °C	retained 47% of dry uptake capacity (5 humid cycles, TSA)	64

FAU	Na-Y (Si/Al $\approx$ 15)	Na <sup>+</sup>	25	0.08/-	195 °C <sup>c</sup>	-	65
LTA	4A	Na <sup>+</sup>	25	0.41/-	-	-	59
LTA	4A	Na <sup>+</sup>	-20	2.09/-	200 °C	-	59
LTA	5A	Ca <sup>2+</sup>	25	0.16/-	-	-	59
LTA	5A	Ca <sup>2+</sup>	-20	1.92/1.3 (70%)	200 °C	capacity loss after first cycle, then stabilizes over 5 TSA cycles	59
MER	K-MER3.6 (Si/Al = 3.6)	K <sup>+</sup>	22	0.28/0.0009 <sup>b</sup> (5%)	45-50 kJ/mol	retained 73% of dry uptake capacity (5 humid cycles, TSA)	64
MOR	MOR5 (Si/Al $\approx$ 5)	Na <sup>+</sup>	25 -11	1.15/- 2.02/-	30 kJ/mol	-	58
MOR	MOR4 (Si/Al $\approx$ 4)	Na <sup>+</sup>	25	1.13/-	-	-	58
MOR	MOR6 (CBV10A)	Na <sup>+</sup>	25	0.77/-	-	stable over 6 cycles	58
MOR	Na-Mordenite (Si/Al $\approx$ 20)	Na <sup>+</sup>	25	0.18/-	215 °C <sup>c</sup>	-	65
MFI	MFI12 (ZSM-5)	Na <sup>+</sup>	25	0.57/-	-	-	58
MFI	Na-ZSM-5 (Si/Al = 16)	Na <sup>+</sup>	25	0.37/-	275 °C <sup>c</sup>	-	65
MFI	Na-ZSM-5 (Si/Al = 11.5)	Na <sup>+</sup>	25	0.38/0.2 <sup>d</sup>	275 °C <sup>c</sup> , 450 °C <sup>e</sup>	stable over 20 dry cycles	65
*BEA	BEA5	Na <sup>+</sup>	25	0.23/-	-	-	58
*BEA	Na-Beta (Si/Al $\approx$ 12.5)	Na <sup>+</sup>	25	0.14/-	210 °C <sup>c</sup>	-	65
MAZ	MAZ3 (Omega-1)	Na <sup>+</sup>	25	0.65/-	-	-	58
FER	FER10 (ZSM-35)	Na <sup>+</sup>	25	0.11/-	-	-	58
MEL	MEL15 (ZSM-11)	Na <sup>+</sup>	25	0.17/-	-	-	58

<sup>a</sup> Measured at 420 ppm of CO<sub>2</sub>. <sup>b</sup> Dynamic column breakthrough experiment at 30 °C. <sup>c</sup> Desorption peak temperatures. <sup>d</sup> Atmospheric humid air in Gwangju, Korea at 27 °C. <sup>e</sup> Regeneration temperature for wet condition.

## 2.1 PHYSISORBENTS (PHYSISORPTION MATERIALS)

Physisorption occurs through weak physical interactions that capture CO<sub>2</sub> on the adsorbent surface. Therefore, materials with high porosity or nanoscale structures are ideal for achieving high capture performance.<sup>48,49</sup> Such porous architectures enhance the intermolecular attraction between CO<sub>2</sub> and the material surface, with ultramicropores (<0.7 nm) being identified as the most effective for CO<sub>2</sub> adsorption.<sup>40</sup>

**2.1.1. Zeolites.** These materials are microporous (<2 nm) crystalline frameworks with a regular pore structure, formed by tetrahedral AlO<sub>4</sub> or SiO<sub>4</sub> building blocks interconnected via bridging oxygen atoms.<sup>50</sup> The aluminum in the silicate framework of zeolites creates negative charges that require compensating cations.<sup>51</sup> For CO<sub>2</sub> capture, the necessary charge balance is most often provided by alkali cations, particularly Na<sup>+</sup> and Li<sup>+</sup>.<sup>52,53</sup> Several factors impact the capture performance of zeolites including size, charge density, and cations' arrangement in the porous framework.<sup>54</sup> Low CO<sub>2</sub> uptake, particularly in the presence of water (H<sub>2</sub>O), along with a strong temperature dependence of adsorption capacity and limited selectivity over N<sub>2</sub> have been identified as limitations of zeolites.<sup>55,56</sup> Although the use of zeolites

for carbon capture is generally more suitable for gas streams containing moderate to high CO<sub>2</sub> concentrations (i.e., 15% and 50%),<sup>55</sup> their application in DAC has recently attracted increasing interest, owing to demonstrated high capture capacities in low- temperature, cold-climate conditions.<sup>57</sup> Table 1 summarizes zeolite adsorbents evaluated under DAC-relevant conditions. The summary tables report KPIs, including the CO<sub>2</sub> adsorption capacity ( $q_{CO_2}$ ) and the corresponding adsorption temperature ( $T_{ads}$ ), the isosteric heat of adsorption ( $Q_{st}$ ) and/ or regeneration temperature ( $T_{reg}$ ), as well as any relevant stability observations. It is worth noting that the adsorption enthalpy ( $\Delta H_{ads}$ ) is defined as the negative of the isosteric heat of adsorption ( $\Delta H_{ads} = -Q_{st}$ ).<sup>62</sup>

**Table 2.** Summary of Unfunctionalized MOFs Evaluated under DAC-Relevant Conditions

MOF	$T_{ads}$ (°C)	$q_{CO_2}$ (mmol/g) at 400ppm (dry/wet) (RH %)	$Q_{st}$ (kJ/mol) or $T_{reg}$ (°C)	stability observation	refs
HKUST-1	25	0.05/-	34 kJ/mol	degraded under humidity: Brunauer-Emmett-Teller (BET) surface area and CO <sub>2</sub> uptake decrease after 1-14 days at 40 °C, 75% RH	83,84
Mg-MOF-74	25	0.14/-	39-47 kJ/mol	highly moisture-sensitive	87,96
SIFSIX-3-Cu	25	1.24/stable <sup>a</sup> (74%)	54 kJ/mol	CO <sub>2</sub> /N <sub>2</sub> breakthrough selectivity unchanged at humid conditions; powder X-ray diffraction (PXRD) retained after ≥4 dry/humid runs	95
SIFSIX-3-Zn	25	0.13/stable <sup>a</sup> (74%)	45 kJ/mol	-	
SIFSIX-2-Cu-i	25	0.07/-	32 kJ/mol	-	
SIFSIX-3-Ni	25	0.39/0.18 <sup>b</sup> (49% and 75%)	45 kJ/mol	significant CO <sub>2</sub> /H <sub>2</sub> O competition; high H <sub>2</sub> O uptake under DAC conditions; 7% BET surface area decrease after accelerated stability test (40 °C, 75% RH, up to 14 days)	83,97
SIFSIX-18-Ni-β	25	0.4/0.3 <sup>c</sup> (74%)	52 kJ/mol	5% capacity decrease over 6 cycles at 1000 ppm of CO <sub>2</sub> ; no performance decline over 100 cycles at 1 bar CO <sub>2</sub> ; 10% capacity decrease over 6 cycles at 1000 ppm of CO <sub>2</sub>	96
NbOFFIVE-1-Ni	25	1.3/1.27 <sup>d</sup> (75%)	54 kJ/mol	CO <sub>2</sub> uptake conserved over repeated dry/humid cycles; promising hydro stability; similar isotherm recorded after 6 months water immersion; in situ variable humidity PXRD also confirmed hydro stability	98
TIFSIX-3-Co	25	1.05/-	100 °C	PXRD unchanged after regeneration; thermally stable up to 245 °C	103
TIFSIX-3-Ni	25	0.79-1.21/0.44 <sup>e</sup> (35-51%)	56 kJ/mol	crystal structure degradation onset at 230 °C; significant degradation observed over 50 cycles in ambient air with varying RH: loss of porosity, crystallinity, and CO <sub>2</sub> uptake; visible color change after long-term cycling	99

<sup>a</sup>No loss in humid breakthrough at 1000 ppm of CO<sub>2</sub>. <sup>b</sup>Not directly measured at 400 ppm; temperature-programmed desorption (TPD) after humid air exposure. <sup>c</sup>Not measured at 400 ppm; evaluated by dynamic breakthrough at 1000 ppm of CO<sub>2</sub> and 74% RH. <sup>d</sup>Not measured at 400 ppm; evaluated by dynamic breakthrough at 1000 ppm of CO<sub>2</sub> and 75% RH. <sup>e</sup>Postcyclic CO<sub>2</sub> isotherm value at 400 ppm following multiple TSA cycles under ambient air at 30 °C.

**2.1.2. Carbonaceous Adsorbents.** Carbon-based porous materials include several classes, among which activated carbons (ACs), carbon nanotubes (CNTs), and graphene are widely studied.<sup>66-68</sup> Activated carbon is a predominantly amorphous carbon material with a partially graphitic structure, characterized

by a high specific surface area and a hierarchical pore system dominated by micropores.<sup>66,69</sup> ACs exhibit tunable physicochemical properties, wide availability at reasonable cost, and a porous structure that is intrinsically linked to their microcrystalline arrangement.<sup>66,70</sup> Due to the acidic nature of both AC and CO<sub>2</sub> molecules, these adsorbents exhibit limited capture capacity.<sup>71</sup> Their CO<sub>2</sub> uptake at low concentrations is limited, and they show lower selectivity compared to zeolites.<sup>72,73</sup> However, their ability to adsorb large quantities of CO<sub>2</sub> at high partial pressures makes them suitable alternative for use in pressure swing adsorption (PSA) processes.<sup>74,75</sup> Similar to zeolites, moisture adversely affects their CO<sub>2</sub> adsorption.<sup>76,77</sup> It is worth noting that carbon fibers are also used as support for amine components in electrically operated DAC systems.<sup>27,28,78</sup>

**2.1.3. Metal-Organic Frameworks (MOFs).** These materials consist of highly organized frameworks of metal atoms or clusters that serve as nodes, linked together by organic ligands. The combination of metal nodes with organic linkers makes it possible to precisely control the properties of the framework, particularly, pore size and shape, and other tunable surface properties, enabling facile and predictable customization of pore functionality and surface area.<sup>79</sup> The outstanding gas adsorption capacities of MOFs, including CO<sub>2</sub>, attracted a lot of attention in the field of CO<sub>2</sub> capture. The tunable structural and chemical properties of MOFs also make them promising candidates for DAC applications.<sup>80,81</sup> Nonetheless, not all MOFs have exhibited acceptable performance for CO<sub>2</sub> capture from dilute streams and gas mixtures.<sup>79</sup>

Although MOFs containing open metal sites have demonstrated substantial single-component CO<sub>2</sub> adsorption capacities at high partial pressures, resulting from the Lewis acidity associated with partially positively charged metal centers,<sup>82</sup> their adsorption performance is often hindered at low CO<sub>2</sub> concentrations and in the presence of moisture.<sup>83-87</sup> MOF-74 series with different metal centers (including Mg,<sup>88</sup> Ni,<sup>89,90</sup> Co,<sup>90</sup> and Zn<sup>91</sup>), HKUST-1,<sup>83</sup> and MIL-101 (Cr)<sup>92,93</sup> have demonstrated high CO<sub>2</sub> capture capacities at higher concentrations.

Fluoride-based MOFs represent another class of physisorbent MOFs composed of metal centers linked by pyrazine-based or nitrogen-containing organic linkers and pillared by fluorine-containing inorganic anions (such as SiF<sub>6</sub><sup>2-</sup>, TiF<sub>6</sub><sup>2-</sup>, or NbOF<sub>5</sub><sup>2-</sup>).<sup>79,94</sup> High CO<sub>2</sub> capture performance under DAC-relevant conditions has been reported for these materials, including the SIFSIX, TIFSIX, and NbOFFIVE series.<sup>95-98</sup> In particular, SIFSIX-3-Cu exhibits significant CO<sub>2</sub> adsorption at low partial pressures, which is attributed to strong electrostatic interactions between the electronegative F ions lining the pores and the electropositive carbon atom of the CO<sub>2</sub> molecule.<sup>79</sup> Nevertheless, the CO<sub>2</sub> adsorption performance of these materials can be adversely affected by the presence of moisture in the gas stream.<sup>96,99-101</sup> For further details on design strategies, physicochemical properties, and performance metrics under DAC-relevant conditions, readers are referred to existing literature.<sup>62,79,102</sup> Table 2 provides an overview of physisorbent MOFs evaluated under DAC-relevant conditions.

**2.1.4. Covalent Organic Frameworks (COFs).** These frameworks are crystalline porous polymers in which the building units comprised of light elements (such as C, N, O, B, Si) are linked through strong covalent bonds, forming extended two-dimensional (2D) or three-dimensional (3D) networks.<sup>104</sup> As COFs are constructed from light elements, they are characterized by low framework density. Compared with other porous adsorbents, COFs offer high structural and functional tunability along with high specific surface areas and large porosity. These properties arise from the variety of organic monomers, resulting in design flexibility of organic building blocks, as well as from the well-defined ordered crystalline

architecture and the diversity of covalent bonds.<sup>104-107</sup>

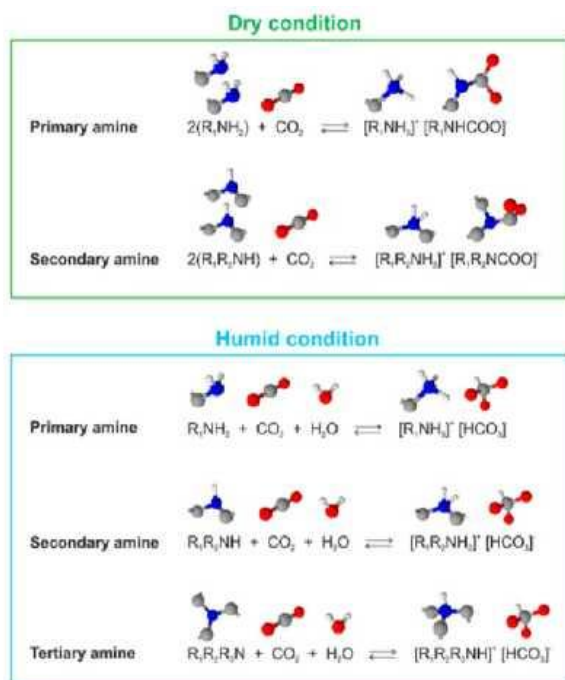
In 2D COFs, monomers are covalently linked within a plane to form layered frameworks. These layers are stacked through  $\pi$ - $\pi$  interactions, leading to extended conjugation between layers.<sup>108,109</sup> In contrast, 3D COFs are constructed through covalent bonding in all directions, resulting in infinite frameworks with regular periodic structures that extend throughout three-dimensional space.<sup>110-112</sup> 3D COFs featuring medium-sized pores offer high surface areas, substantial pore volumes, and significant porosity, making them promising candidates for gas adsorption applications, including CO<sub>2</sub> capture.<sup>113</sup> Nevertheless, large-scale synthesis, understanding of CO<sub>2</sub> adsorption kinetics, and developing a broader array of 3D COF structures suitable for DAC remain key challenges to their widespread application.<sup>40</sup>

Among the various classes of COFs, boron-based, triazine-based, imine-based, and polyimide-linked frameworks have been investigated for carbon capture applications.<sup>114,115</sup> Amide-linked COFs have also demonstrated high CO<sub>2</sub> capture potential, which has been attributed to high polarity of carbonyl bonds and strong framework-CO<sub>2</sub> interactions.<sup>116,117</sup> In addition, the incorporation of metal ions onto the pore walls of COFs has been proposed as a strategy to enhance affinity of framework toward CO<sub>2</sub> and to improve adsorption kinetics.<sup>118,119</sup> For a comprehensive discussion of COF synthesis methods, structural and physicochemical features, carbon capture performance and DAC-oriented developments, readers are referred to recent review articles in the literature.<sup>113,120-122</sup> Despite their potential in gas separation, unfunctionalized COFs have seen limited application in DAC due to inadequate CO<sub>2</sub> uptake at atmospheric concentrations<sup>109,117,123-125</sup> and the need for further optimization to enable effective adsorption under humid conditions.<sup>122</sup> As a result, their stability is not considered in this review.

## 2.2 CHEMISORBENTS (CHEMISORPTION MATERIALS)

**2.2.1. Amine-Functionalized Adsorbents.** Among the different adsorbent classes mentioned, amine-functionalized porous materials have been extensively studied owing to their high affinity for CO<sub>2</sub> and strong resistance to humidity.<sup>126,127</sup> Amines are incorporated into carrier materials with high surface area and porosity, forming a uniform dispersion. As a result, the modified materials exhibit the beneficial properties of both the amine and the support.<sup>128</sup> Amine groups act as Lewis bases and nucleophiles that can chemically interact with CO<sub>2</sub>, a Lewis acid, leading to the formation of carbamate and/ or carbamic acid species.<sup>129,130</sup> Primary and secondary amines generally exhibit stronger Lewis basicity toward CO<sub>2</sub> than tertiary amines, which do not react with CO<sub>2</sub> under dry conditions.<sup>62</sup> Water is known to facilitate the reaction of primary and secondary amines with CO<sub>2</sub> and enhance the performance of the adsorbent. In dry conditions, two amine molecules capture one carbon molecule, whereas in the humid environment, one amine reacts with one CO<sub>2</sub> molecule (Scheme 1).<sup>17</sup> In addition, increased capture efficiency of amine-based sorbents in humid conditions is attributed to the formation of more carbamate ions<sup>131</sup> or bicarbonate<sup>132,133</sup> species.

**Scheme 1.** CO<sub>2</sub> Adsorption Reactions in Dry and Humid Environments<sup>a</sup>



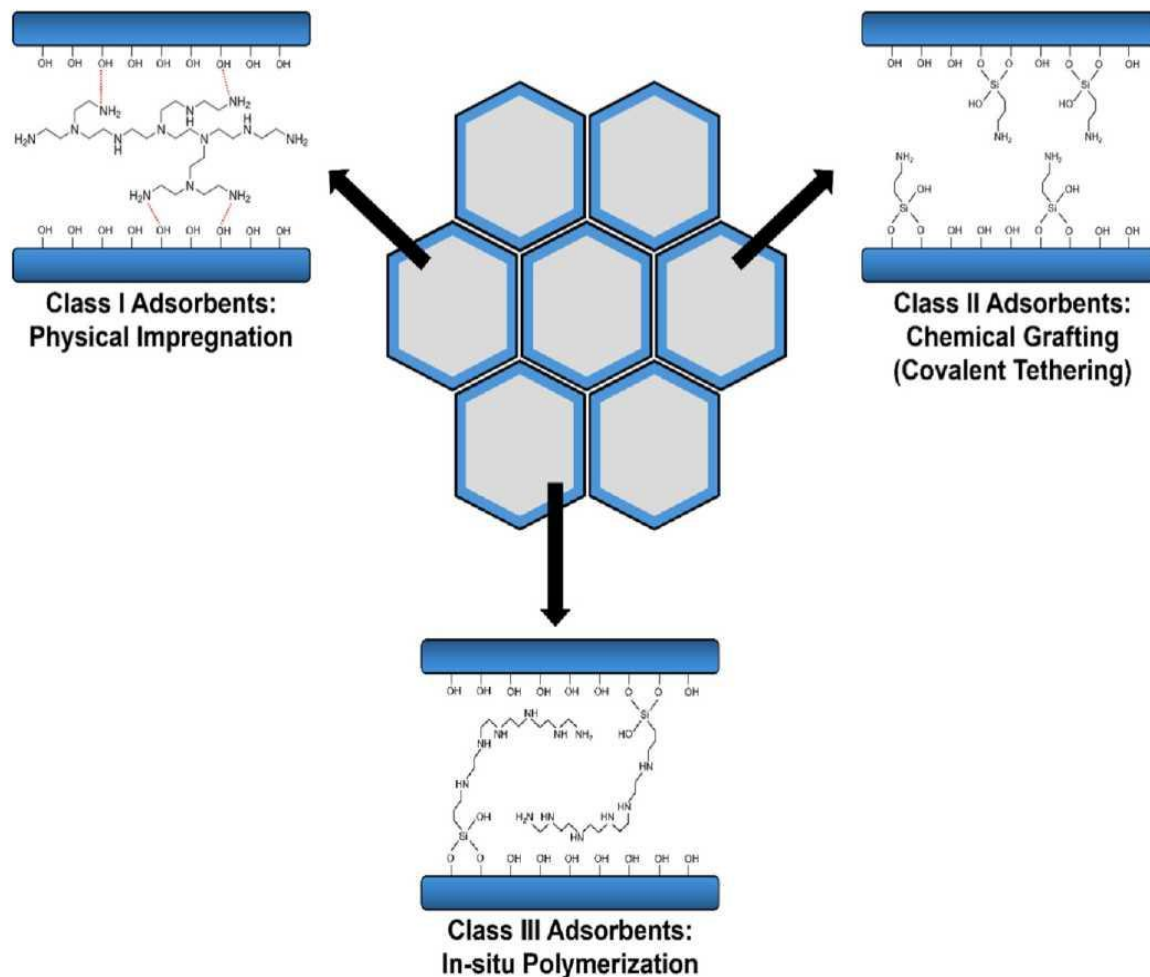
<sup>a</sup>Reproduced from ref 128. Available under a CC-BY 4.0 license. Copyright 2022 Hack et al.

Various porous support materials have been functionalized by amine components: silica,<sup>134,135</sup> zeolite,<sup>136,137</sup> carbon material,<sup>27,28</sup> resin,<sup>138-140</sup> MOF,<sup>141-143</sup> and COF.<sup>144,145</sup> Silica is the most common support used for synthesizing aminebased carbon capture and DAC adsorbents (known as aminosilica adsorbents) due to their high performance and tunable structural and chemical properties.<sup>146,147</sup> The performance of amine functionalized materials is mainly affected by the synthesis method and process parameters. Supports can be functionalized via physical impregnation (Class I), chemical grafting (Class II), in situ polymerization (Class III), or a combined grafting-impregnation approach (Class IV).<sup>148</sup> The difference in interactions between the support and amine material in these methods is depicted in Figure 4. These types of functionalization methods are further detailed in the next sections. Due to the uneven stacking of amines, which inhibits and reduces the diffusion of CO<sub>2</sub>, the actual capture efficiency of amine-based adsorbents (CO<sub>2</sub> loading/theoretical CO<sub>2</sub> loading) is significantly lower than the potential theoretical maximum of 0.5.<sup>39</sup> Still, the amine loading efficiency (amine loaded/amine used in the preparation) of impregnated samples is reported to be higher than that of grafted adsorbents, with 89.10% efficiency for 50% PEI loading on MCM-41 compared to 23.18% for the same loading when grafted with (3-aminopropyl)triethoxysilane (APTES).<sup>149</sup>

**2.2.1.1. Impregnation.** Impregnated adsorbents (also referred to as class I adsorbents) are synthesized by physical impregnation of amine material into the existing pore window of a mesoporous solid support<sup>39</sup> and, typically, there is no direct chemical bond between the carrier and the amino component.<sup>150</sup> The amine loading inside the support pores is affected by the available pore volume of the support as well as the amine group density.<sup>148</sup> Amine selection is an important criterion that highly influences the performance of the adsorbents. Aminopolymers and small amine molecules are suitable for the synthesis of amine-impregnated adsorbents and short-chain aminopolymers have been frequently used for impregnation.<sup>39</sup> Aminopolymers can be tailored under various synthesis conditions to adjust their molecular weight (Mw) and chain type, where tuning the chain structure yields different amine groups

(i.e., primary, secondary, and tertiary amines).<sup>39</sup> Examples of aminopolymers and amine molecules used for the preparation of amine-impregnated DAC adsorbents are summarized in Table 3 and their chemical structure is illustrated in Charts S1 and S2 in Supporting Information.

**Figure 4.** Amine-based porous solid adsorbent schematic and interactions between the support material and the amine component.



**2.2.1.2. Grafting.** Unlike physical impregnation, in amine-grafted adsorbents (also known as class II adsorbents) covalent bonds are formed between the active amine component and the support. Moreover, it appears that most amine-grafted adsorbents investigated in the literature contain Si bonds. In this method, the aminosilanes, amine molecules containing the silane group, are chemically attached on the surface of the porous support by silylation reactions (condensation reaction) between aminosilanes and the hydroxyl groups on support material.<sup>39,148</sup> In grafted adsorbents, CO<sub>2</sub> capture capacity is inherently limited by aminosilane surface saturation due to the restricted number of hydroxyl anchoring sites available on the support.<sup>151</sup> The grafting reactions of APTES onto silica support<sup>152</sup> are depicted in Scheme S2. In some cases, silylation can be carried out by cross-coupling reactions.<sup>153</sup> Examples of aminosilanes employed in the synthesis of amine-grafted DAC adsorbents are listed in Table 4, with their corresponding chemical structures shown in Chart S3 of the Supporting Information.

**2.2.1.3. In Situ Polymerization.** This approach combines advantages of both impregnation and grafting methods.<sup>154</sup> The adsorbents synthesised using this technique (also named class III adsorbents) are prepared by in situ ring-opening polymerization (ROP) of amine-containing monomers, i.e., ethyl- enimine (aziridine) in the pores of the support which results in forming covalent bonds between aminopolymers and the support.<sup>154-156</sup> Cationic ROP of aziridine to form branched poly(ethylenimine) (bPEI) is depicted in Scheme S3. Similar to grafted adsorbents, amines are chemically attached to the support. However, adsorbents produced in this way are bound to the support via C-O bonds and have a higher capture capacity due to the greater amine loading resulting from the in situ formation of long polymer chains containing many N sites.<sup>155</sup> However, aziridine is toxic and its polymerization reaction is fast, which makes it difficult to control the polymer formation, reducing the attractiveness of this method to the laboratory scale.<sup>148</sup>

**Class IV Adsorbents.** Certain adsorbents are fabricated using both impregnation and grafting methods. In some works, they are referred to as double-functionalized or class IV adsorbents.<sup>148</sup> In this double functionalization technique, the amine-grafted adsorbent is later coated with another amine component to increase the available active adsorption sites.<sup>101,157</sup>

**2.2.1.5. Amine-Functionalized MOFs.** Researchers have also functionalized MOFs with amine groups to act as chemisorbents, achieving higher adsorption capacities. Primary amines experience less steric hindrance than secondary amines, which favorably influences CO<sub>2</sub> uptake kinetics. Amines with longer N-substituted alkyl chains typically show enhanced Lewis basicity, while polyamines containing multiple amino groups along a single alkyl chain increase the density of chemisorption sites within MOFs. Consequently, highly porous MOFs with large pore sizes are particularly well suited for amine functionalization.<sup>62</sup>

Amine-functionalized MOFs can be synthesized through several approaches: (1) incorporation of amine-bearing linkers during framework synthesis,<sup>62,79,143,184</sup> (2) postsynthetic attachment of amines to open metal sites (also known as postsynthetic grafting on secondary building units),<sup>62,79,185</sup> and (3) loading or encapsulation of amines within the MOF pores.<sup>62,186</sup> The IRMOF-74-III series is an example of MOFs synthesized using linkers that contain amines. These materials possess a hexagonal channel pore structure similar to that of Mg-MOF-74, with the key distinction being the incorporation of linkers bearing pendant amine groups. Although IRMOF- 74-III exhibits lower CO<sub>2</sub> capture capacity compared to other amine-functionalized MOFs, its adsorption performance remains largely unaffected by the presence of moisture.<sup>184</sup>

Several MOFs have been functionalized via postsynthetic attachment of amines to open metal sites,<sup>187,188</sup> among which Mg<sub>2</sub>(dobpdc) (structurally similar to M-MOF-74 with larger pores) has been extensively studied.<sup>85, 142, 189-191</sup> *N,N'*- dimethylethylenediamine (DMEDA, commonly denoted as mmen in the literature)-grafted Mg<sub>2</sub>(dobpdc) (mmen- Mg<sub>2</sub>(dobpdc)), has been reported to exhibit a CO<sub>2</sub> uptake of approximately 2 mmol/g at 400 ppm.<sup>85,185</sup> Additional examples of amine-functionalized MOFs are summarized in Table 5, and readers are referred to the existing literature for detailed discussions and comprehensive information on synthesis strategies, performance metrics, and adsorption mechanisms.<sup>192,193</sup>

**Table 3.** Summary of Impregnated (Class I) Adsorbents Evaluated under DAC-Relevant Conditions

support	amine component	amine loading	T <sub>ads</sub> (°C)	q <sub>CO2</sub> at 400 ppm (dry/wet) (RH %)	Q <sub>st</sub> (kJ/mol)/T <sub>reg</sub> (°C) (regeneration atmosphere)	stability observation	refs
SBA-15	branched poly(ethylenimine) (bPEI)	50 wt %	25	1.14-1.34/2.16 (60%)	55-70/80 (He)	stable (10 humid cycles)	158
mesocellular silica foam (MCF)	bPEI	39 wt %	25	1.08/-	-/110 (Ar)	stable (3 cycles, TSA) <sup>a</sup>	159
fumed silica	bPEI	50 wt %	25	1.67/-	83/85 (air)	stable (4 cycles, TSA)	160
hierarchical meso/macroporous silica (H-SiO <sub>2</sub> )	bPEI	2.62 gPEI/gsorben t	30	2.34/3.36 (19%)	-/110 (He)	Stable (dry); gradual loss under humidity (5 cycles, TSA)	161
silica gel	bPEI	30-50 wt %	40	1.6-1.9 <sup>b</sup> /-	115-141/100 (N <sub>2</sub> )	≈2-3% amine loss (26 cycles, TSA); less loss for higher loading	162
silica gel	bPEI	40 wt %	40	1.85 <sup>b</sup> /-	113-120/100 (N <sub>2</sub> )	stable (26 cycles, TSA)	162
CARiACT G-10	bPEI	40 wt %	25	1.38/-	-/100 (N <sub>2</sub> )	≈0.8% capacity decrease (50 cycles, TSA)	147
resin HP20	bPEI	50 wt %	25	2.26/-	-/100 (N <sub>2</sub> )	stable (5 cycles, TSA)	138
γ-alumina	bPEI	20-40 wt %	25	0.58-1.33/0.87-2.0 (70%)	-/50-110 (He or Ar)	stable (3-5 cycles, TSA.)	133,163
γ-alumina	bPEI	20-40 wt %	-20	0.47-0.49/1.26-1.8 (70%)	-/50-60 (He)	stable (10 cycles, TSA)	133
SBA-15	linear poly(ethylenimine) (IPEI)	50 wt %	35	0.75/-	-/110 (Air)	60-80% amine efficiency and capacity loss after accelerated oxidation	164
fumed silica	IPEI	44.5-48 wt %	25	0.73-1.21/-	42-53/55 and 75 (N <sub>2</sub> )	stable performance for highest Mw sample (>100 cycles, TSA) <sup>c</sup>	165
SBA-15	branched poly(propyleneimine) (bPPI)	32-43 wt %	35	0.10-0.58 <sup>d</sup> /-	110 (Air)	17% capacity decline after a 12 h oxidation at 110 °C	166
SBA-15	linear poly(propyleneimine) (IPIPI)	50 wt %	35	1.25/-	105/110 (N <sub>2</sub> )	<0.3% of amine loss (50 cycles, TSA)	164
SBA-15	poly(propylene guanidine) (PPG)	28-50 wt %	30	0.25-0.63/-	70/100 and 120 (He)	56% (120 °C) and 25% (100 °C) capacity loss (5 cycles, TSA)	167
SBA-15	poly(glycidyl amine) (PGA)	35-55 wt %	35	0.14-0.33 <sup>d</sup> /-	-/90 (He)	10-16% capacity decline (20 cycles, TSA.) <sup>a</sup>	168

SBA-15	tetraethylenepentamine (TEPA)	50 wt %	25	1.2-2.3/2.12 (60%)	-/90-110 (N <sub>2</sub> or He)	≈20% capacity loss (20 dry cycles, TSA.); Stable (10 humid cycles)	158,169,1
hierarchical silica (HS)	TEPA	70 wt %	30	5.20/5.88 (50 ± 3%)	104/110 (N <sub>2</sub> )	≈22% capacity loss (10 cycles, TSA.)	171
CARiACT G-10	TEPA	40 wt %	25	2.15/-	-/100 (N <sub>2</sub> )	≈29% capacity loss (50 cycles, TSA.)	147
γ-alumina	TEPA	20-40 wt %	25	1.2-1.8/1.5-2.5 (70%)	-/70 (He)	stable (5 cycles, TSA)	133
γ-alumina	TEPA	20-40 wt %	-20	0.9-1.2/1.88-0.65 (70%)	-/60 (He)	stable (10 dry and 5 humid cycles, TSA)	133
γ-alumina	TEPA	50 wt %	25	1.5/-	-/100 (N <sub>2</sub> )	≈37% capacity loss (20 cycles, TSA.)	170
SBA-15	triethylenetetramine (TETA)	50 wt %	25	1.7-1.8/1.80 (60%)	-/80 (He)	≈18% capacity decay (10 humid cycles, TSA.)	158
SBA-15	tripropylentetramine (TPTA)	20-40 wt %	35	0.1-1.3 <sup>d</sup> /-	-/70 (N <sub>2</sub> )	<5% capacity loss (4 cycles, TSA)	172
silica gel	pentaethylenehexamine (PEHA)	40 wt %	40	1.8 <sup>b</sup> /-	108-125/100 (N <sub>2</sub> )	≈11% amine loss (26 cycles, TSA) <sup>e</sup> ; enhanced stability at higher loading of 50 wt %: ≈5% amine loss (26 cycles, TSA)	162
MCF	poly(allylamine) (PAA)	41 wt %	25	0.86/-	-/110 (He)	stable (3 cycles, TSA) <sup>a</sup>	161

<sup>a</sup> Cycles conducted at 10% CO<sub>2</sub>. <sup>b</sup> Measured at 5% CO<sub>2</sub>. <sup>c</sup> Cycles conducted at 10% and 95% CO<sub>2</sub>;  $T_{reg} \geq 55$  °C. <sup>d</sup> Values originally reported per g SiO<sub>2</sub> were converted to per g adsorbent using reported amine loading. <sup>e</sup> Cycles at  $T_{ads} = 75$  °C.

**Table 4.** Summary of Grafted and In Situ Polymerized Chemisorbents (Class II and III) Evaluated under DAC-Relevant Conditions

support	amine component	amine loading/number of amine sites	$T_{ads}$ (°C)	$q_{CO_2}$ at 400 ppm (dry/wet) (RH %)	$Q_t$ (kJ/mol)/ $T_{reg}$ (°C) (regeneration atmosphere)	stability observation	refs
SBA-15	(3-aminopropyl)triethoxysilane (APTES)	2.4-2.7 mmolN/g	35	0.05/-	-/110 (He)	40% capacity loss after oxidation 24 h at 130 °C	173
MCM-41	APTES	50 wt %	25	2.41 <sup>a</sup> /-	-/100 (-)	19% capacity loss (5 cycles, TVSA)	149
Hierarchical silica	APTES	5.68 mmolN/g	30	0.82/1.7 (50%)	65/110 (N <sub>2</sub> )	≈13% capacity loss (5 cycles, TSA.)	174
polysilsesquioxane-based hybrid silica	APTES	4.5 mmolN/g	30	-/1.68 (60%)	85 ± 5/60-80 (He)	stable (50 cycles, TSA)	175
titania/silsesquioxane composite aerogel	APTES	8.47 mmolamine/g	30	1.64/-	-/90 (N <sub>2</sub> )	stable (15 cycles, TSA)	176

SBA-15	3-(aminopropyl)trimethoxysilane (APTMS)	1.1-2.13 mmol <sub>Si</sub> /g <sup>b</sup>	25	0.04-0.21/-	-/110 (He)	loading-dependent oxidative stability	177
SBA-15	( <i>N,N</i> -dimethylaminopropyl)trimethoxysilane (DMAPS)	≈2.4-2.7 mmolN/g	35	0.02/-	-/110 (He)	-	173
SBA-15	( <i>N</i> -methylaminopropyl)-trimethoxysilane (MAPS)	≈2.4-2.7 mmolN/g	35	0.02/-	-/110 (He)	-	173
hierarchical bimodal mesoporous silica	<i>N</i> 1-(3-trimethoxy-silylpropyl)diethylenetriamine (TRI)	50 wt %	25	1.04/-	-/90 (He)	stable (10 cycles, TSA)	178
hierarchical silica	TRI	9.68 mmol <sub>N</sub> /g	30	1.54/2.08 (50%)	46/110 (N <sub>2</sub> )	≈15% capacity loss (5 cycles, TSA.)	174
silica gel	TRI	5.12 mmol <sub>N</sub> /g	25	0.773/1.098 (60%)	-/90 (He)	stable (17 cycles, TSA)	179
γ-alumina	TRI	<i>N</i> content = 7.12 wt %	25	0.39/0.76 (73%)	44.6/90 (N <sub>2</sub> )	≈17% capacity loss (60 cycles, TSA.)	180
nanofibrillated cellulose (NFC)	<i>N</i> -(2-aminoethyl)-3-aminopropylmethylmethoxysilane (AEAPDMS)	5.9 mmol <sub>N</sub> /g	30	-/0.90 <sup>c</sup> (60%)	-/90 (vacuum)	≤5% capacity loss (100 cycles, TVSA) <sup>d</sup> , ≈30% capacity loss (oxidative degradation)	181
NFC	AEAPDMS	4.2 mmol <sub>N</sub> /g	23	1.11/2.13 (60%)	50-73/90 (N <sub>2</sub> )	-	182
large-pore AIMCM-41 aluminosilicate	PEI (grafted via CPTMS, class II)	32	20	0.49/-	-/100 (N <sub>2</sub> )	≈1.5% capacity loss (50 cycles, TSA)	183
large-pore AIMCM-41 aluminosilicate	cation ring-opening polymerization of 2-ethyl-2-oxazoline (EtOX) (in situ polymerization)	49	20	0.81/-	-/100 (N <sub>2</sub> )	0.3% capacity (50 cycles, TSA)	183

<sup>a</sup> Measured under pure CO<sub>2</sub>. <sup>b</sup> Silane loading. <sup>c</sup> Average during cycling; ambient air 400-530 ppm. <sup>d</sup> Adsorption at 30 °C in humid air, desorption at 90 °C under vacuum, 30 mbar.

**Table 5.** Summary of Amine-Functionalized MOFs and COFs Evaluated under DAC-Relevant Conditions

adsorbent	amine incorporation mode	amine component	amine loading/number of amine sites	$T_{ads}$ (°C)	$q_{CO_2}$ at 400 ppm (dry/wet) (RH %)	$Q_{st}$ (kJ/mol)/ $T_{reg}$ (°C) (regeneration atmosphere)	stability observation	refs
IR-MOF-74-III-NH <sub>2</sub>	amine-decorated linker	-NH <sub>2</sub>	one amine per linker	25	0.01/-	-	-	198
IR-MOF-74-III-CH <sub>2</sub> NH <sub>2</sub>	amine-decorated linker	-CH <sub>2</sub> NH <sub>2</sub>	one amine per linker	25	0.05/-	-/90-95 (N <sub>2</sub> )	preserved CO <sub>2</sub> breakthrough time under 65% RH; PXRD unchanged after dry and wet cycles	198
MIL-101(Cr)-SO <sub>3</sub> H-TAEA	postsynthetic	tris(2-aminoethyl)amine (TREN)	-	20	1.12/-	87/-	stable CO <sub>2</sub> uptake and preserved PXRD (15 dry cycles, TVSA) <sup>a</sup>	143
ED-Mg/DOBDC or ED-Mg-MOF-74	amine-appended MOF nodes	ethylenediamine (ED)	≈5.5 wt % (≈1-3 ED per unit cell)	25	1.51/-	-/110 (Ar)	stable CO <sub>2</sub> capacity (4 cycles, TSA)	141
ED-Mg <sub>2</sub> (dobdc) or ED-Mg-MOF-74	amine-appended MOF nodes	ED	1.8 ED per Mg <sub>2</sub> (dobdc) formula unit	25	0.82 ± 0.10/1.07 ± 0.13 (1.9 vol %) <sup>b</sup>	-/100-120 (N <sub>2</sub> )	stable (18 dry cycles, TSA); 74% capacity decrease (18 wet cycles, TSA)	199
MIL-101(Cr)-TREN	amine-appended MOF nodes	TREN	2.63 mmol/g <sub>MOF</sub>	25	0.35/-	-/110 (He)	Stable capacity (3 cycles, TSA)	186
MIL-101(Cr)-TREN (impregnated)	encapsulated amine (physical impregnation)	TREN	5.67 mmol/g <sub>MOF</sub>	25	2.8/-	-/110 (He)	≈ 15% capacity loss (3 dry cycles, TSA)	186
MIL-101(Cr)-PEI-800	encapsulated amine	bPEI	1.06 mmol/g <sub>MOF</sub>	25	1.1/-	70/110 °C (He)	5% capacity loss (3 cycles, TSA); stable at 32% RH	186
en-Mg <sub>2</sub> (dobpdc)	amine-appended MOF nodes	ED	≈1.6 ED per Mg <sub>2</sub> (dobpdc) formula unit	25	2.83 <sup>c</sup> /-	49-51/120 (vacuum; Ar)	≈4% capacity loss (20 cycles, TVSA.) <sup>d</sup> ; ≈5% capacity loss (5 cycles involving 100% RH, TSA) <sup>e</sup>	142
mmen-Mg <sub>2</sub> (dobpdc)	amine-appended MOF nodes	<i>N,N'</i> -Jimethylethylenedi-	≈1.6 mmen per Mg <sub>2</sub> (dobpdc) formula	25	2.0 <sup>c</sup> /-	71/150 (N <sub>2</sub> )	Stable capacity (10 cycles, TSA)	85

		amine (DMEDA; "mmen")	unit					
2-ampd-Mg <sub>2</sub> (dobpdc)	amine-appended MOF nodes	2-(aminomethyl)piperidine (2-ampd)	≈1 diamine per Mg site	40	0.64 <sup>f</sup> /2.2 <sup>g</sup> (2.6 vol %)	73 ± 2/140 (humid pure CO <sub>2</sub> )	≈6% diamine loss (750 humid cycles, TSA.) <sup>h</sup>	200
COF-609	covalent incorporation into COF backbone (postsynthetic)	Tris(3-aminopropyl)amine (TRPN)	one TRPN per linker site	25	0.304/0.393 (50%)	-	moderate H <sub>2</sub> O uptake (4.66 mmol/g at 50% RH)	144
COF-709	covalently bound bPEI inside COF pores via C-S bonds (postsynthetic)	thiol-modified branched polyethylenimine (SH-bPEI)	9.24 mmol/g sorbent	25	0.48/1.13 (50%)	41-50/95 (N <sub>2</sub> )	stable capacity (10 cycles humid, TSA)	196
COF-999	covalently attached polyamines within COF pores (postsynthetic)	ring-opening polymerization of aziridine	average ≈3 ethylenimine repeat units per linker side chain	25	0.96 ± 0.03/2.05 ± 0.03 (50%)	53/60 (N <sub>2</sub> )	no loss in CO <sub>2</sub> capacity, crystallinity, or breakthrough behavior (100 cycles, TSA) <sup>i</sup>	145

<sup>a</sup>Desorption at 0.4 mbar and 80 °C. <sup>b</sup>Dynamic column breakthrough. <sup>c</sup>Measured at 390 ppm. <sup>d</sup>Cycles at  $T_{ads} = 40$  and  $T_{reg} = 120$  °C under vacuum (<102 kPa). <sup>e</sup>Cycles at  $T_{ads} = 40$  and  $T_{reg} = 130$  °C. <sup>f</sup>Measured at 0.4% CO<sub>2</sub>. <sup>g</sup>Dynamic column breakthrough under humid 4% CO<sub>2</sub>. <sup>h</sup>Cycles at 4% CO<sub>2</sub>;  $T_{ads} = 40$  °C and  $T_{reg} = 140$  °C. <sup>i</sup>Cycling performed under outdoor air with 28-51% RH and 410517 ppm of CO<sub>2</sub>

**2.2.1.6. Amine-Functionalized COFs.** COFs can also be functionalized with active groups, including amines, through two primary approaches: bottom-up synthesis<sup>194,195</sup> and postsynthetic modification.<sup>144,145,196,197</sup> In the bottom-up approach, functional groups are incorporated directly into the COF monomers prior to framework construction enabling uniform distribution of functionalities throughout the backbone. Nevertheless, synthesizing functionalized monomers is often challenging and may complicate COF formation due to changes in monomer rigidity or symmetry. In contrast, postsynthetic modification involves the introduction of functional groups into preformed COFs containing reactive or coordinative sites, typically via coordination interactions or covalent chemical transformations. This method generally provides less control over functional group distribution and results in reduced pore size and surface area; however, the enhanced reactivity of the introduced functionalities can partially compensate for these limitations.<sup>115</sup> In this context, Yaghi's group has developed COF-609,<sup>144</sup> COF-999,<sup>145</sup> and COF-709<sup>196</sup> as sorbents for DAC (Table 3).

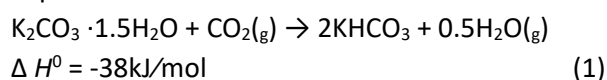
**2.2.1.7. Commercial Adsorbents.** Commercially available resin-based adsorbents have been also used for DAC applications. Lewatit VP OC1065 (referred to as Lewatit in this paper), Purolite A109, and Purolite A110 aminoresins are among these solid sorbents. Lewatit is widely recognized as the benchmark sorbent for DAC applications and is believed to be similar to the adsorbent used by Climeworks.<sup>201</sup> Lewatit is a commercial anion exchange resin with application in the selective removal of acids from process streams, the decolorization of sugar starch and protein solutions and the adsorption of aldehydes.<sup>202</sup> This material displays an acceptable performance in the adsorption of atmospheric CO<sub>2</sub>, with adsorption loading of 1 mmol/g at 25°C under dry conditions.<sup>203</sup>

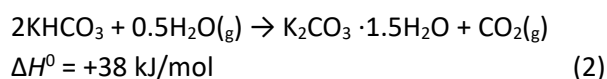
Both Lewatit and Purolite adsorbents are ion exchange resins that are composed of divinylbenzene-cross-linked poly(styrene), which is functionalized with primary amines via covalent bonding to the polymeric support.<sup>23,201</sup> CHN elemental analysis (EA) (Table 6) revealed that Lewatit contains more nitrogen than Purolite A109 but less than A110, which explains the higher capacity of Purolite A110 compared to Lewatit.<sup>204,205</sup> The higher water adsorption in A110 also contributed to its greater CO<sub>2</sub> uptake. In addition, Purolite A110 exhibited a lower heat of CO<sub>2</sub> adsorption compared to Lewatit.<sup>204</sup> Due to intellectual property constraints, in-depth information about their molecular structure and manufacturing process remains unavailable.

**Table 6.** CHN EA of Lewatit, Purolite A109 and A110<sup>204,205</sup>

Aminoresin	C (wt %)	H (wt %)	N (wt %)	Q <sub>st</sub> (kJ/mol)
Lewatit VP OC1065	82.5	8.1	8.3	107 ± 8
Purolite A109	81.28	7.37	6.13	N.A.
Purolite A110	79.6	8.2	10.2	104 ± 9

**2.2.2. Carbonate-Based Adsorbents.** Carbonate-based adsorbents are an inorganic type of chemisorbents prepared by the deposition of carbonate salts (i.e., K<sub>2</sub>CO<sub>3</sub> and Na<sub>2</sub>CO<sub>3</sub>) onto a support.<sup>206-210</sup> CO<sub>2</sub> adsorption on carbonate functionalized adsorbents takes place by the formation of potassium or sodium bicarbonate, thus, a certain level of moisture is required.<sup>211</sup> The CO<sub>2</sub> adsorption and desorption reactions are presented in Reactions 1 and 2, respectively, along with their corresponding reaction enthalpies.<sup>212</sup>





In addition to being inexpensive, these sorbents are more eco-friendly than amine-loaded sorbents since they do not emit harmful byproducts and have better oxidative stability. However, their high regeneration energy requirements and slow kinetics limit their deployment.<sup>213</sup> Additionally, their CO<sub>2</sub> adsorption capacity remains limited compared to amine-based adsorbents, particularly under low-concentration CO<sub>2</sub> conditions.<sup>79,80,214</sup> Zheng and co-workers developed moistureswing adsorbent by impregnating potassium carbonate salts on different porous supports, where activated carbon-loaded sorbents had the best performance with a higher uptake capacity than magnesium oxide and zeolite supports.<sup>214</sup> Activated carbon honeycomb monoliths functionalized with hydrated K<sub>2</sub>CO<sub>3</sub> or Na<sub>2</sub>CO<sub>3</sub> were also synthesized based on the wash coating method for DAC application. The authors reported that the moisture content in the air has the highest impact on the adsorbent's CO<sub>2</sub> capture capacity.<sup>211</sup> In addition, other commercial carbon supports, such as Ketjen Black, CA1, and SX ultra were tested for K<sub>2</sub>CO<sub>3</sub> impregnation, where Ketjen Black supported adsorbents exhibited faster CO<sub>2</sub> sorption kinetics as well as higher capture capacity in comparison to other employed supports.<sup>215,216</sup> Table 7 summarizes carbonate-based adsorbents tested under DAC-relevant conditions.

**Table 7.** Summary of Carbonate-Based Adsorbents Evaluated under DAC-Relevant Conditions

support	carbonate salt	carbonate loading	T <sub>ads</sub> (°C)	CO <sub>2</sub> concentration	q <sub>CO<sub>2</sub></sub> (dry/wet) (RH %)	T <sub>reg</sub> (°C) (regeneration atmosphere)	stability observation	refs
activated carbon honeycomb monolith	Na <sub>2</sub> CO <sub>3</sub>	0.041-0.088 gNa <sub>2</sub> CO <sub>3</sub> /g ads	20	400 ppm	0.10-0.166 (22-73%)	170 (N <sub>2</sub> )	-	210
silica aerogel	K <sub>2</sub> CO <sub>3</sub>	10-30 wt %	20	1.0%	0.4-1.32 (2.0% H <sub>2</sub> O)	200 (N <sub>2</sub> )	~6% capacity loss (10 cycles, TSA)	208
ZrO <sub>2</sub> aerogel	K <sub>2</sub> CO <sub>3</sub>	9-29 wt %	25	390-450 ppm	0.09-1.05 (25%)	200 (Ar)	stable (14 cycles, TSA)	209
γ-Al <sub>2</sub> O <sub>3</sub>	K <sub>2</sub> CO <sub>3</sub>	26.1 wt %	25	400-440 ppm	0.82 (25%)	200 (Ar)	stable (8 Cycles, TSA)	217

### 2.3. SUMMARY

Overall, DAC adsorbents are predominantly amine-based, with physically impregnated materials being the most extensively studied due to their straightforward synthesis and generally higher initial CO<sub>2</sub> capture capacities compared to grafted variants. A wide range of amine molecules and aminopolymers have been impregnated onto porous supports such as silica and alumina, whereas grafted adsorbents, most commonly based on silica, typically rely on aminosilane chemistry. Class III sorbents, prepared via in situ polymerization on the support, have also been investigated as an alternative approach. In addition, commercial amine-based polymer resins represent the current industrial benchmark for DAC applications. By contrast, carbonate-based adsorbents have received comparatively limited attention, while amine-appended MOFs and COFs are emerging as alternative DAC materials. Physisorbents generally exhibit

limited CO<sub>2</sub> uptake at ultradilute concentrations, although zeolites may be suitable for large-scale DAC in colder climates, and certain MOFs, including fluoride-based frameworks, have shown promising performance. As long-term adsorbent performance is critical for DAC viability, the following sections examine the stability of these materials under key degradation mechanisms, beginning with thermal degradation, which is often the first evaluated criterion.

### 3. THERMAL STABILITY

Most studies on DAC adsorbents have focused on testing their cyclic thermal stability and regenerability. The detailed conditions under which the experiments were carried out are summarized in Table S1 in Supporting Information and discussed in the present section. Overall, these experiments provide relevant information about the stability of the adsorbent, especially at high regeneration temperatures. However, they are often performed in the absence of oxygen, mainly in dry conditions and under an inert gas flow. Therefore, studies examining the effects of O<sub>2</sub> are discussed separately in a later section of this paper.

In general, to examine the cyclic thermal stability of an adsorbent, it is first exposed to a gas flow under adsorption conditions. This flow is typically a synthetic mixture of CO<sub>2</sub> and one or several inert gases, such as He, N<sub>2</sub>, and Ar. Some studies also utilized pure CO<sub>2</sub> instead. A few works discussed here humidify these gases to account for the effect of moisture. After sorbent saturation with CO<sub>2</sub> or after a defined adsorption period, the process is typically followed by a regeneration (desorption) step, most commonly via TSA, TCSA, or TVSA. In most cases, this stage is conducted with inert (i.e., N<sub>2</sub> or He) dry gas at a higher temperature except for some studies where both adsorption and regeneration stages are conducted at the same temperature. Steam is another regeneration option, and its effect on adsorbent stability is discussed in Section 5. After each or a certain number of adsorption + regeneration cycles, the capture capacity and occasional changes in the physicochemical properties of the material are examined. In some works, the thermal stability of adsorbents has also been examined using thermogravimetric analysis (TGA) to observe organic mass loss. Some studies coupled TGA with differential scanning calorimetry (DSC). It is important to note that although adsorbents are often tested under high temperatures up to 600-800 °C in TGA device, such extreme conditions are not directly relevant to DAC applications, where regeneration typically occurs at 60-110 °C. Nonetheless, these tests offer valuable preliminary insights into the interactions between various supports and amine materials, and several studies have shown that TGA results can serve as a good initial indicator of thermal stability under DAC conditions.<sup>147,158,169</sup> The present section begins with brief discussion on physisorbents, followed by a detailed analysis of the cyclic thermal stability of amine-based adsorbents, highlighting the key factors of influence. Then, the thermal stability of carbonate-based materials is reviewed.

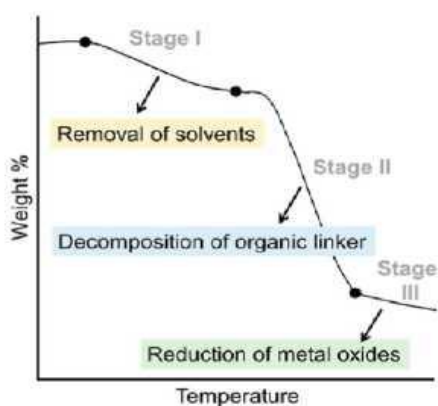
#### 3.1 PHYSISORBENTS (PHYSISORPTION MATERIALS)

Physisorbents used in DAC generally exhibit sufficient thermal robustness to tolerate the regeneration temperatures required for DAC operation; consequently, thermal degradation is typically not a limiting factor for zeolites and carbon-based adsorbents and this aspect will not be further detailed.<sup>218-220</sup> On the contrary, the thermal stability of MOFs is strongly dependent on framework structure and therefore requires thorough evaluation for thermal cyclic applications, as discussed below.

**3.1.1. Metal-Organic Frameworks (MOFs).** The thermal stability of MOFs refers to their ability to preserve structural integrity at elevated temperatures and is strongly dependent on the intended application. While catalytic and gas storage applications often require MOFs to withstand high temperatures,<sup>221</sup> carbon capture processes typically operate at relatively lower temperatures due to regeneration under moderate thermal conditions. MOF thermal stability is commonly evaluated using TGA under a given atmosphere to determine the decomposition temperature ( $T_d$ ), defined as the temperature at which significant structural changes occur within the framework. Three distinct mass-loss steps can be identified in the TGA curve (Figure 5): (i) desolvation at low temperatures, associated with the removal of residual solvent or guest molecules from the MOF pores, followed by a plateau region where the evacuated framework remains stable; (ii) decomposition of the organic linkers, during which the MOF loses its structural integrity and undergoes thermal degradation at  $T_d$ ; and (iii) reduction of metal oxides by carbonaceous species at higher temperatures.<sup>221-223</sup> In addition, certain degradation processes, such as framework collapse or amorphization, may occur without significant mass loss and are therefore not detectable by TGA. Consequently, complementary techniques such as DSC and variable-temperature powder X-ray diffraction (VT-PXRD) are often required to identify these structural transformations.<sup>222</sup>

The thermal stability of MOFs depends primarily on the strength of metal—ligand bonding, which is determined by factors such as metal charge density and the chemical nature and robustness of the organic linker. Among these, ligand stability is widely recognized as the major contributor to overall thermal stability.<sup>221,222</sup> The majority of MOFs tested for DAC exhibit sufficient thermal stability under moderate regeneration conditions. For example, MOFs featuring open metal sites and carboxylate ligands, such as HKUST-1 and Mg-MOF-74, exhibit  $T_d$  of approximately 300 and 526 °C, respectively.<sup>224,225</sup> Despite high thermal stability, both materials suffer from limited CO<sub>2</sub> uptake at 400 ppm and significant performance degradation in the presence of moisture, restricting their practical deployment. Among fluoride-based MOFs, SIFSIX-3-Cu demonstrates excellent DAC performance but possesses a comparatively low  $T_d$  of approximately 150 °C,<sup>9</sup> which can be attributed to the volatility of neutral N-donor linkers and the potential thermal decomposition of the inorganic fluoride pillaring units.<sup>226</sup> In contrast, related materials such as NbOFFIVE-1-Ni and TIFSIX-3-Ni exhibit substantially higher  $T_d$ , exceeding 340 °C, making them more promising from a thermal stability perspective.<sup>98,99</sup>

**Figure 5.** Representative TGA profile of a MOF showing three distinct mass-loss regions corresponding to solvent desorption, decomposition of organic linkers, and subsequent reduction of metal oxides by carbon. Reproduced from ref 223. Copyright 2020 American Chemical Society.



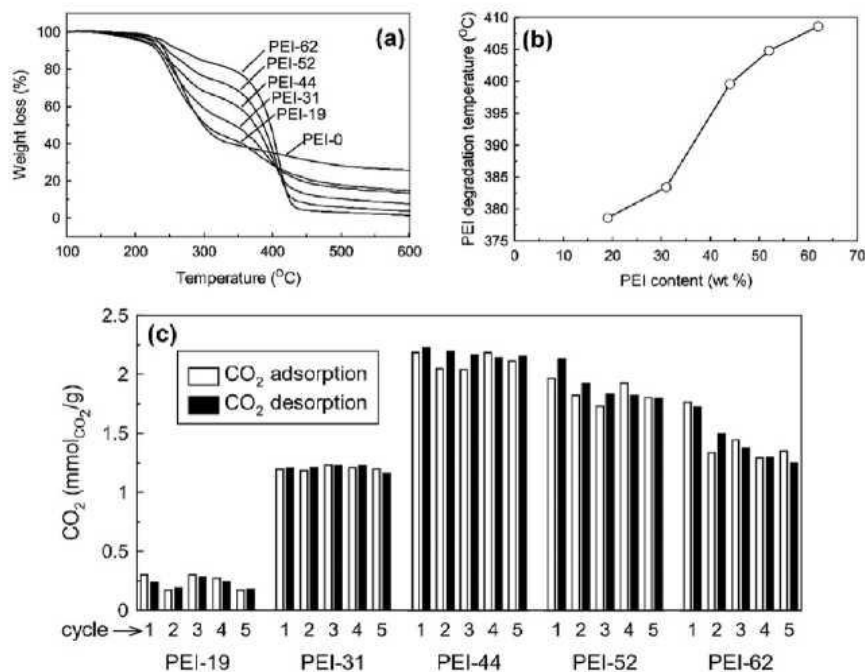
## 3.2. CHEMISORBENTS (CHEMISORPTION MATERIALS)

**3.2.1. Amine-Functionalized Adsorbents.** As previously mentioned, amine-based adsorbents are the most widely studied materials for DAC. Consequently, a relatively larger proportion of the literature has been focused on elucidating the thermal stability of these sorbents. In what follows, thermal stability of amine-functionalized materials is addressed and a comparison is made regarding the amine functionalization method: physically functionalized adsorbents (i.e., class I sorbents) vs chemically functionalized adsorbents (i.e., class II, III, and IV sorbents). Indeed, the strength of interactions between amine moieties and solid carriers can be influenced by the preparation method as well as the choice of amine and support material. Following this, the thermal degradation of available commercial adsorbents is reviewed. Finally, the formation of urea in amine-functionalized sorbents is investigated, as urea is often identified as a primary product of thermal degradation. Understanding the mechanisms underlying its formation provides a deeper understanding of the complex nature of thermal degradation in amine-based adsorbents.

**3.2.1.1. Physically Functionalized Adsorbents.** PEI-impregnated silica adsorbents are among the most popular materials in DAC studies. Therefore, the thermal cyclic stability of PEI has been examined when coating various silica supports. Nevertheless, most of these studies do not provide an in-depth analysis of deactivation mechanisms or the underlying causes of capacity loss during cyclic testing. For instance, bPEI impregnated on SBA-15,<sup>227</sup> CARiACT Q-10,<sup>228</sup> fumed silica,<sup>165</sup> HMS mesoporous silica,<sup>229</sup> silica monolith,<sup>230</sup> displayed minimal capacity loss over a limited number of cycles (typically 4–20 cycles). The temperature and conditions under which regeneration is performed significantly impact amine loss and, consequently, the decrease in CO<sub>2</sub> capture capacity, with higher temperatures leading to greater losses.<sup>167,231,232</sup> In a thermal stability test of IPEI (linear poly(ethylenimine))-impregnated adsorbents under N<sub>2</sub>, no weight loss was observed at 70 °C after 20 h of continuous exposure. However, at 100 °C, a slight mass reduction was recorded, resulting in a 5.6% capacity loss attributed to amine leaching at elevated temperatures.<sup>165</sup> Park et al.<sup>167</sup> also demonstrated that amine evaporation on SBA-15 can be partly prevented by performing the desorption step at lower temperatures (at 100 °C instead of 120 °C) leading to a better preservation of CO<sub>2</sub> capturing capacity. Variations in amine dispersion and molecular restructuring within the pore network at high temperatures have also been identified as one of the factors affecting the cyclic performance of PEI-based adsorbents. Liu et al.<sup>233</sup> prepared a DAC adsorbent by the encapsulation of PEI into organo-silica nanotubes and tested for 8 cycles, without showing any change in breakthrough time. The Fourier-transform infrared spectroscopy (FT-IR) spectra of fresh and cycled samples were similar, except for a slight change in the peaks associated with amine groups, indicating a change in the dispersion status of PEI throughout the regeneration cycle. However, the N content of the sample was only slightly decreased by about 7%, which was claimed to be insignificant. Another study showed that restructuring amine molecules can even lead to a small capacity increase over cycles. Kumar et al.<sup>234</sup> synthesized aryl-alkyl amine-rich molecules and impregnated them onto silica with various loadings. The adsorbent with a 60 wt % loading exhibited an increase in CO<sub>2</sub> uptake over 25 cycles. This small capacity increase was associated with the combined effect of slight mass loss as well as restructuring of the amine molecules at desorption temperatures that potentially increased accessibility of active sites.

**Figure 6.** (a) TGA curves for the NFC and PEI-loaded NFC sorbents: onset of NFC backbone degradation

above 200 °C followed by PEI decomposition at higher temperature; (b) variation in PEI thermal degradation temperature with increasing PEI content in the sorbents; (c) CO<sub>2</sub> adsorption performance of NFC/PEI sorbents across five DAC cycles (adsorption under air at 25 °C and regeneration under N<sub>2</sub> at 85 °C). Reproduced from ref 236. Copyright 2015 American Chemical Society.



The mobility and distribution of PEI within the pore structure during synthesis can impact the final performance of the adsorbent as well. Kwon et al.<sup>161</sup> prepared a hierarchical meso-/macroporous silica structure (H-SiO<sub>2</sub>) and impregnated PEI onto this support using two different preparation methods performing drying step under low and high vacuum. By milder vacuum during the drying step (slower drying), the performance of the adsorbent improved. Given the results, it was hypothesized that under high vacuum (i.e., at lower pressure), aminopolymers are mobile within the pores of the samples. When lower pressure is applied, this led to poor PEI distributions, such as window blockages and uneven amino-polymer film coatings on the walls, which in turn caused lower adsorption performance. Considering insignificant amine leaching during humid cyclic testing, the performance decline was associated with the rearrangement of aminopolymers in the pores, likely caused by water vapor. Nevertheless, more detailed characterization of the polymer morphology was mentioned as essential to completely understand this phenomenon.

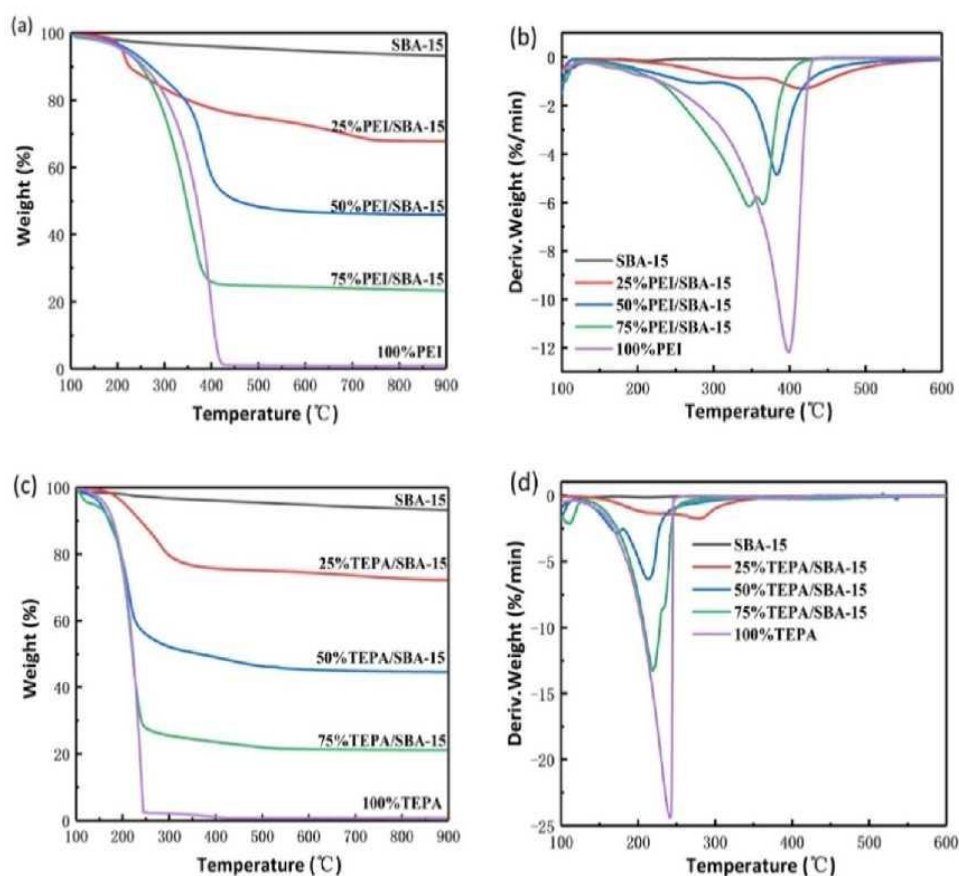
Another factor that has been identified as influencing the thermal stability of amine-impregnated adsorbents is the aminopolymer loading level. Wang et al.<sup>235</sup> found that stronger interaction between PEI and surface silanol groups of SBA-15 in lower loadings enhanced thermal stability, whereas increasing the loading up to 60 wt % resulted in weaker interactions and thus lower PEI decomposition peak temperature. Interestingly, when the loading was increased to 65 and 70%, the downward trend in the decomposition temperature reversed and increased. According to the authors, at lower loadings, PEI was dispersed and filled the pore channels of SBA-15. However, at higher loadings, PEI aggregates like pure PEI, forming a coating on the external surface of the support,

leading to agglomeration. This increases the barrier for decomposed product diffusion and heat transfer, accordingly, raising the decomposition peak temperature. Spinu et al.<sup>162</sup> reported a similar trend for bPEI-impregnated silica gel, where sorbents with 50 wt % loading exhibited superior retention of both their CO<sub>2</sub> capture capacity and aminopolymer content compared to 40 wt % samples after 26 TCSA cycles (98% vs 95% for capture capacity and 98% vs 97% for remaining aminopolymer content). The improved stability at higher loading was attributed to denser polymer packing within the pores, which strengthens hydrogen bonding among polymer chains and between amine groups and surface silanol groups, and reduces concentration gradients that cause amine leaching.

In contrast, Sehaqui et al.<sup>236</sup> reported a consistent increase in the thermal degradation onset temperature with increasing PEI loadings (0-62 wt %) when using oxidized nanofibrillated cellulose (NFC) as the support (Figure 6a,b). This suggests that the effect of amine loading on thermal stability is highly dependent on the nature of the support material. The enhanced thermal stability at higher loadings was also attributed to possible PEI agglomeration, which may have inhibited thermal degradation. However, under cyclic DAC conditions, a different trend was observed, emphasizing the importance of evaluating sorbents under relevant application environments. The adsorbents with up to 44 wt % PEI loading exhibited stable CO<sub>2</sub> capture capacity over five DAC cycles, with only minor losses. In contrast, samples with 52% and 62% PEI loading showed capacity declines of 16% and 27%, respectively (Figure 6c), without providing further explanation of this observation.

Due to their distinct physicochemical properties, different aminopolymers can exhibit varying thermal stability when supported on carrier material. In addition to PEI, several other aminopolymers have also been studied using silica as the support. Chaikittisilp et al.<sup>159</sup> impregnated low-Mw poly-(allylamine) (PAA) onto mesocellular silica foam (MCF), which had stable performance but lower capture capacity over three short cycles compared to bPEI-impregnated sample. In the study conducted by Pang et al.,<sup>164</sup> impregnated linear poly(propyleneimine) (IPPI) on SBA-15 silica showed acceptable stability with no capture capacity decrease and minimal loss of polymer mass over 50 cycles. After cyclic testing, the PPG (poly(propylene guanidine))-impregnated SBA-15 samples synthesized by Park et al.<sup>167</sup> were thermally treated under He flow at 100 and 120 °C for 6 h, during which continuous evaporation of amines in this sorbent was observed. Compared with PEI-based SBA-15, the PPG samples demonstrated larger mass loss and lower cyclic stability (56 vs 15% capacity decrease after 5 cycles).

**Figure 7.** TGA and DTG analysis of (a,b) SBA-15 with different ratios of PEI, (c,d) SBA-15 with different ratios of TEPA. Reproduced with permission from ref 169. Copyright 2021 Elsevier Publication.

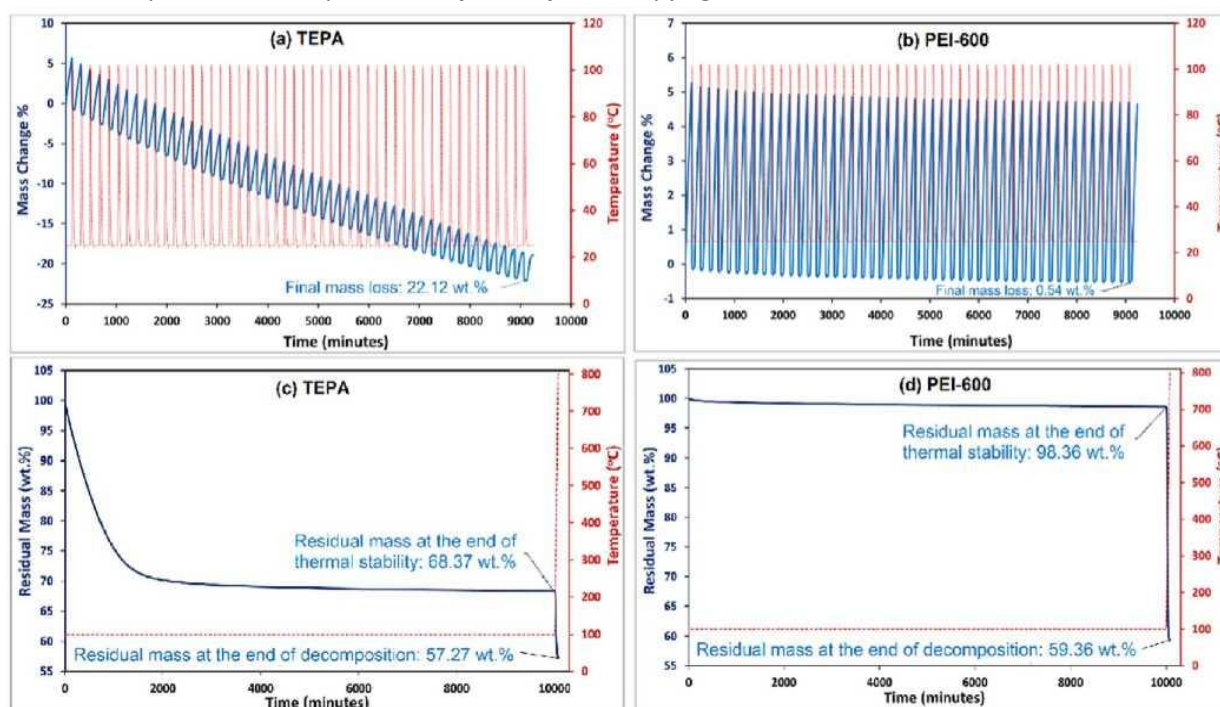


It is also suggested that the Mw of the impregnated aminopolymer may impact the thermal stability of the resulting adsorbents. Sujan et al.<sup>168</sup> impregnated poly(glycidyl amine) (PGA) with different Mws on SBA-15. After the first cycle, the capture capacity of the higher-Mw samples decreased by 1015%, while the sample containing low-Mw PGA maintained stable performance. This was attributed to the more uniform dispersion of low-Mw PGA within the pore structure, leading to better retention of the polymer and reducing its susceptibility to evaporation or degradation during heating. In contrast, Spinu et al.<sup>162</sup> observed an opposite trend for bPEI-impregnated silica gel. The sample containing higher-Mw bPEI (Mw = 1200 g/mol) exhibited stable performance over 26 TCSA cycles, whereas the lower-Mw counterpart (Mw = 800 g/mol) showed a 5% decline in CO<sub>2</sub> capture capacity. The superior cyclic stability of the higher-Mw bPEI was attributed to its bulkier structure, which reduced evaporation and leaching losses.

As discussed in the previous section, in addition to aminopolymers, amine molecules can also be impregnated onto various porous supports, including silica. Similar to bPEI, Spinu et al.<sup>162</sup> reported that higher pentaethylenhexamine (PEHA) loadings on silica gel led to improved thermal stability. While the adsorbent containing 40 wt % PEHA exhibited a 16% loss in CO<sub>2</sub> uptake, the 50 wt % counterpart showed only about 2% decline. From these findings and comparisons with previous studies, the authors suggested that overloaded samples may better preserve their cyclic capacity than those with lower amine filling ratios. In addition to tetraethylenepentamine (TEPA), Liu et al.<sup>237</sup> impregnated diethylenetriamine (DETA), ethylenediamine (ED), and PEHA onto MCM-41 mesoporous silica. The mass loss observed in TGA conditions was found to be consistent with the boiling points of amines, following the order: ED-MCM41

< DETA-MCM41 < TEPA-MCM41 < PEHA-MCM41. The longer-chain amines exhibited higher decomposition temperatures, which was attributed to their preferential accumulation on the external surface of the support rather than within the pores, leading to increased resistance to heat transfer and the diffusion of decomposition products.

**Figure 8.** Cyclic CO<sub>2</sub> capture performance of (a) TEPA- and (b) PEI-impregnated silica over 50 cycles (adsorption at 25 °C, regeneration at 100 °C under N<sub>2</sub> flow); thermal stability of (c) TEPA- and (d) PEI-impregnated silica following 10,000 min of exposure to N<sub>2</sub> at 100 °C, followed by a temperature increase to 800 °C. Reproduced with permission from ref 147. Copyright 2023 Elsevier Publication.

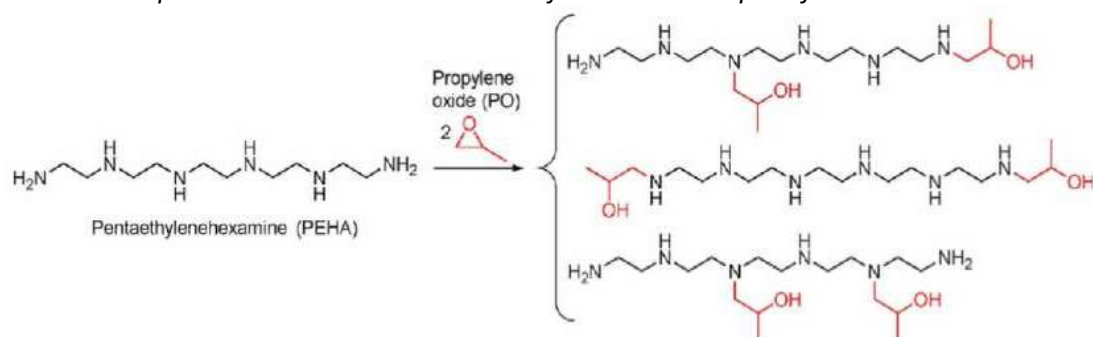


PEI and TEPA are among the most widely used amines for the synthesis of impregnated adsorbents. Several works performed a direct comparison of both amines in terms of performance and stability. Though the initial capture capacity of TEPA on silica support is greater than that of PEI,<sup>147,169</sup> both types of PEI, especially IPEI, have lower regeneration temperatures than shorter ethyleneamines.<sup>165,238</sup> More importantly, the volatility of TEPA is higher, whereas bulky amines like PEI present better cyclic thermal stability. In a limited number of cycles under dry conditions, both PEI- and TEPA-impregnated SBA-15 prepared by Miao et al.<sup>169</sup> demonstrated acceptable stability. Nonetheless, the PEI- containing SBA-15 composites demonstrated higher thermal stability in TGA measurements, as shown in Figure 7. Kumar et al.<sup>158</sup> tested the performance and cyclic thermal stability of PEI-, TEPA-, and TETA (triethylenetetramine)-impregnated SBA-15 under humid condition (relative humidity (RH) = 60%). While PEI and TEPA loaded silica experienced approximately 10% capacity decrease, TETA-based sample suffered from continuous capacity drop after each cycle with final capacity loss of 30% after 10 cycles. This loss was tentatively linked to degradation of the amine, deterioration of the CO<sub>2</sub> adsorption sites, or thermally induced changes in the amine distribution. Hosseini and Jahandar Lashaki<sup>147</sup> tested TEPA-impregnated commercial mesoporous silica, CARiACT G-10, for 50 cycles and reported 55% capacity loss (corresponding to a total mass loss of 22.12%) associated with amine evaporation (Figure 8a). In contrast, all bPEI- impregnated adsorbents, including sample containing PEI with Mw = 600 g/mol (Figure 8b), had less than 1% capacity loss over 50 cycles. Samples with a higher TEPA content experienced a higher drop in capacity. Indeed, in these cases, a larger portion of amine is more easily evaporated as it is not in contact with support. TGA tests yield qualitatively consistent results when compared with cycling testing in bed-type configuration, allowing for identification of the most thermally stable material among alternatives. In another similar study, Qi et al.<sup>239</sup> prepared a nanocomposite adsorbent by impregnating PEI or TEPA on mesoporous silica capsules (specially designed mesoporous SiO<sub>2</sub> hollow capsules) and studied its performance as well as cyclic stability. The PEI-based adsorbent lost about 22% of its initial capture capacity, while TEPA adsorbent faced about 40% capacity drop following 50 TSA cycles regenerated under N<sub>2</sub> at 100 °C. The greater thermal stability of aminopolymers over smaller amine molecules was further demonstrated in a comparative study of bPEI and PEHA.<sup>162</sup> The capacity decline followed the order: high-Mw PEI (≈0%) < low-Mw PEI (≈3%) < PEHA (≈16%).

In addition to the chemical structure of the amine, the support material and its surface chemistry significantly influence the stability of amine-impregnated adsorbents. Zhang et al.<sup>240</sup> investigated the thermal stability of TEPA impregnated on both calcined and uncalcined SBA-15. The uncalcined SBA-15-supported sample exhibited improved thermal stability, with the onset of decomposition shifting by 15 °C, which was associated with the formation of hydrogen bonds between TEPA and the oxygen atoms in the ether groups of P123 template present in the uncalcined support. A comparable trend was also reported by Ye et al.,<sup>241</sup> who found that PEI impregnated onto as-synthesized MCM-41 (i.e., without removing the template) demonstrated greater thermal stability compared to the calcined counterpart. PEI-impregnated halloysite nanotubes (HNTs) exhibited stable CO<sub>2</sub> sorption capacity over 50 cycles, attributed to the use of high-Mw PEI and strong electrostatic interactions between PEI and the HNT surface, which enhanced the overall thermal stability.<sup>242</sup> In addition, PEI also exhibited moderate cyclic stability over short cycles (3-10 cycles) when impregnated on other carriers including  $\gamma$ -alumina,<sup>133,243</sup> HP20 resin,<sup>138</sup> multiwalled carbon nanotube-based microtubes.<sup>244</sup> Nevertheless, these studies primarily report the thermal cyclic stability

without addressing the underlying degradation mechanisms or their causes, highlighting opportunities for future research in this area. While TEPA showed limited thermal stability when impregnated onto silica, its performance on alternative supports has also been explored to assess potential improvements, often without extensive investigation. TEPA impregnated on  $\gamma$ - $\text{Al}_2\text{O}_3$  exhibited stable performance over 10 subambient cycles at moderate regeneration conditions ( $T_{\text{ads}} = -25\text{ }^\circ\text{C}$  and  $T_{\text{reg}} = 60\text{--}70\text{ }^\circ\text{C}$ ).<sup>133</sup> In contrast, increasing the regeneration temperature to  $100\text{ }^\circ\text{C}$  resulted in an approximately 10% loss in  $\text{CO}_2$  capacity for alumina coimpregnated with 30% PEI and 20% TEPA,<sup>245</sup> further reflecting thermal instability of TEPA at higher regeneration temperatures. Similarly, when supported on  $\text{TiO}(\text{OH})_2$  and multiwalled carbon nanotubes, the  $\text{CO}_2$  capture capacity decreased by approximately 19% ( $T_{\text{ads}} = 60\text{ }^\circ\text{C}$  and  $T_{\text{reg}} = 100\text{ }^\circ\text{C}$ ) and 20% ( $T_{\text{ads}} = 65\text{ }^\circ\text{C}$  and  $T_{\text{reg}} = 90\text{ }^\circ\text{C}$ ) over 10 cycles, respectively. This loss is attributed to both the thermal decomposition and evaporation of TEPA, mainly due to its low Mw.<sup>246,247</sup> Overall, these studies indicate that, to date, the use of alternative supports has not led to a substantial improvement in the thermal stability of TEPA-impregnated adsorbents.

**Scheme 2.** Representative Reaction Products of PEHA with 2 Equiv of PO<sup>a</sup>



<sup>a</sup>Reproduced with permission from ref 231. Copyright 2019 Wiley-VCH.

The thermal cyclic stability of amine-impregnated adsorbents can be enhanced by improving the interaction between the active material and the support. This can be accomplished, for instance, by tuning the chemical structure of amine molecules. Goepfert et al.<sup>231</sup> impregnated propylene oxide (PO)-modified TEPA and PEHA (Scheme 2) as well as 1,2-epoxybutane (EB)-modified PEHA on Sipernat 50S silica. The resulting amines contained OH groups and exhibited higher stability than conventional TEPA and PEHA over 50 cycles. Beyond amine selection and preparation method, the nature of the support itself plays a critical role in determining interactions with the active amine phase. Tuning the surface chemistry and architecture of the carrier can significantly alter these interactions, resulting in different  $\text{CO}_2$  capture behaviors. Previous studies have demonstrated that modifying the silica support surface or incorporating additives can improve the thermal stability and performance of silica-supported amine adsorbents. Choi et al.<sup>248</sup> investigated the use of stabilizing additives to improve the thermal stability of bPEI-impregnated porous silica by incorporating APTES or titanium(IV) propoxide (tetrapropyl orthotitanate,  $\text{C}_{12}\text{H}_{28}\text{O}_4\text{Ti}$ ) during slurry preparation. The presence of these additives increased the PEI decomposition temperature and significantly reduced cyclic capacity loss (from approximately 30% to 10% after four cycles), which was attributed to stronger interactions between the amine and the modified support surface. Importantly, the introduction of these stabilizers did not reduce amine loading and resulted in only a minor decrease in initial  $\text{CO}_2$  uptake (<8%), indicating limited compromise in adsorption capacity. Moreover, the stabilized

samples exhibited enhanced adsorption kinetics and retained substantially higher final capacities after cycling (>2 mmol/g) compared to the unmodified PEI/ silica adsorbent (1.65 mmol/g), suggesting that improved thermal stability was achieved without a severe penalty in overall performance. Kuwahara et al.<sup>249</sup> enhanced the capture capacity and amine efficiency of bPEI-based silica adsorbent by modifying the acid/base properties of the oxide support through introducing Zr into the silica support before the impregnation. Although the performance of the bPEI-functionalized SBA-15 sample declined by 34% after four cycles, the Zr-containing samples exhibited only a 2% reduction. In a separate study, Kuwahara and colleagues also confirmed the positive effect of Ti incorporation on the thermal cyclic stability of modified silica.<sup>250</sup> While the capture capacity for PEI-impregnated SBA-15 was decreased after each cycle with a final 34% capacity loss after four cycles, the PEI-loaded Ti-SBA-15 and Zr-SBA-15 faced only 5% and 2% capacity decline, respectively. The higher capacity loss observed for the PEI-impregnated sample in this study, compared to the findings of Kumar et al.,<sup>158</sup> can be attributed to the higher employed regeneration temperature (110 °C vs 80 °C). The improved cyclic stability of the Ti- and Zr-modified samples was linked to limited occurrence of unfavorable aggregation/degradation of PEI as a result of improved CO<sub>2</sub> desorption kinetics and positive interactions between the PEI and the support surface.

**3.2.1.2. Chemically Functionalized Adsorbents.** Since the synthesis method primarily determines the type of bonding between the amine component and the support, it consequently influences the thermal stability of the resulting adsorbent. As discussed in the previous section, impregnated adsorbents generally exhibit poor thermal stability over multiple cycles due to amine evaporation, leaching, or degradation. To overcome this issue, several studies investigated adsorbents where chemical bonding is used to immobilize the amine molecules, i.e., class II, III and IV sorbents. For instance, Liu et al.<sup>251</sup> prepared two different TEPA-loaded adsorbents by physical impregnation and chemical grafting methods on MCF and examined their performance and stability. TEPA was grafted onto silica using a two-step chemical grafting method. First, MCF was functionalized with (3-chloropropyl)trimethoxysilane, followed by the grafting of TEPA onto the Cl-functionalized silica foam. While the impregnated sample experienced significant capture capacity loss after ten cycles, the grafted adsorbent exhibited steady performance over these cycles. The improved stability of the grafted sample was linked to alleviated leaching by creating strong chemical bonds between the TEPA and the support surface. Although grafted samples exhibited better stability than impregnated ones, the impregnated samples showed higher initial CO<sub>2</sub> capture capacity due to the higher surface density of amine groups. Similarly, Rao et al.<sup>149</sup> compared thermal stability of PEI-impregnated and APTES-grafted MCM-41 adsorbents using TGA. The PEI-based sample exhibited a 44.55% mass loss between 100 and 400 °C, whereas the APTES-loaded sample showed only an 11.59% loss over a wider temperature range of 150-600 °C. Moreover, the PEI-impregnated sample experienced a 12.65% uptake loss after the first cycle and a total loss of 14.22% after 5 cycles, whereas the APTES-grafted sample was more stable facing 5.19% capacity loss after same number of cycles. Although most grafting methods primarily consider aminosilanes tethering onto silica supports, Chen and coauthors<sup>180</sup> recently explored the feasibility of grafting N1-(3-trimethoxy-silylpropyl)diethylenetriamine (TRI) onto  $\gamma$ -alumina and assessed its performance and thermal and cyclic stability under 400 ppm of CO<sub>2</sub>. TGA results showed that TRI-grafted alumina remained stable in the 90-140 °C temperature range, exhibiting only about a 2% mass loss. However, amine loss became more significant between 140 and 220 °C, resulting in a total mass loss of 21%. In cyclic stability tests over 60 cycles ( $T_{\text{ads}} = 25$  °C and  $T_{\text{reg}} = 90$  °C), the adsorption capacity of the TRI-grafted alumina declined by approximately 17% within the first 20

cycles. As a conclusion, current studies demonstrate the use of both silica and alumina as grafted supports in class II adsorbents, though a clear performance advantage for either has not been established. A comparative study between the two supports would provide clearer insights into their thermal behavior.

Recently Al-Absi et al.<sup>183</sup> evaluated PEI-based adsorbents prepared with large-pore AlMCM-41 aluminosilicate (LPAISi) and mesoporous silica foam (MSF) using impregnation, grafting, and in situ polymerization methods. Although thermal degradation tests were conducted at 110 °C under airflow for 3 days, making it difficult to distinguish thermal from oxidative effects, the study offers valuable comparative insights into adsorbent classes and support materials using single aminopolymer. Among the tested samples, impregnated sorbents showed the most significant amine loss and decline in CO<sub>2</sub> capture capacity, while grafted and in situ polymerized sorbents demonstrated superior thermal stability due to covalent bonding between the amine and the support (Figure 9). In addition, Class III adsorbents showed better final capture capacity compared to Class II adsorbents. Furthermore, over 50 TSA cycles, impregnated samples showed poor stability with ≈6% capacity decline, whereas chemically functionalized sorbents maintained their performance, with showing only 0.3% loss.

The thermal stability of class IV adsorbents has also been investigated. Jung et al.<sup>252</sup> evaluated a series of doublefunctionalized materials prepared by grafting 3-(aminopropyl)- trimethoxysilane (APTMS) or TRI onto silica gel, followed by impregnation with TEPA or PEI. Among the TEPA- impregnated samples, silica gel impregnated without prior grafting demonstrated the highest thermal stability at 160 °C. This behavior was attributed to stronger interactions between

TEPA and silica surface compared to those between TEPA and grafted amine groups, leading to reduced amine loss. Furthermore, stronger interactions were observed when aminosilanes with longer hydrocarbon chains were employed (TRI versus APTMS). The authors further proposed that the thermal stability of double-functionalized sorbents could be enhanced by incorporating functional groups with higher affinity for the grafted amines into the impregnated species. In contrast, Zhang et al.<sup>253</sup> reported thermal stability enhancement in the case of APTES grafting onto uncalcined SBA-15 prior to TEPA impregnation. The immobilized APTES provides hydrogen-bonding/anchoring sites that promote a more uniform TEPA distribution and stronger amine-support interactions, thereby reducing TEPA mobility and loss (e.g., volatilization) during thermal cycling. This result indicates that, depending on the nature of the support and grafted functionalities, the combined grafting-impregnation approach may either enhance or fail to improve thermal stability.

In summary, impregnated sorbents are typically more prone to capacity loss during thermal cycling caused by the weaker physical interactions between the amine and the support. In contrast, grafted and in situ polymerized sorbents form chemical bonds with the support and therefore generally display improved thermal stability, with the latter also achieving higher CO<sub>2</sub> uptake owing to the formation of long aminopolymer chains. Although grafted sorbents exhibit notable thermal stability, improving their CO<sub>2</sub> adsorption capacity remains challenging, as strategies such as increasing grafting density or tailoring the support surface to promote higher amine uptake can reduce pore accessibility, increase diffusional (mass-transfer) resistance, raise hydrophilicity, and thereby accelerate performance loss during thermal cycling.

**Amine-Functionalized MOFs.** Analysis of existing studies on amine-functionalized MOFs indicates that their thermal stability is strongly influenced by the functionalization strategy. For DAC-relevant amine-functionalized MOFs synthesized via amine-bearing linkers, comprehensive TGA- based stability analyses are often not reported, such as IRMOF-74-III series and MIL-101(Cr)-SO<sub>3</sub>H-TAEA.<sup>143,198</sup> However, studies on

the UiO-66 series, which has also been investigated for CO<sub>2</sub> adsorption,<sup>254</sup> demonstrated that incorporating amine-containing linkers such as 2-amino-terephthalic acid leads to a noticeable reduction in  $T_d$ , from approximately 500 °C to around 400 °C.<sup>255, 256</sup> This decrease in thermal stability has been attributed to the inductive electron-withdrawing effect of nitrogen atoms, which weakens adjacent carbon—carbon bonds within the linker framework.<sup>256</sup> In contrast, amine-functionalized MOFs prepared via postsynthetic modification, including Mg-MOF-74 and Mg<sub>2</sub>(dobpdc), generally retain the original  $T_d$  of the framework, although additional low-temperature mass loss related to the decomposition of the appended amine functionalities are observed.<sup>85,141,257,258</sup> Moreover, increasing the alkyl chain length on secondary amines has been shown to suppress diamine volatilization, thereby improving overall thermal stability.<sup>258</sup>

**Figure 9.** Impact of preparation method on CO<sub>2</sub> uptake of fresh and thermally degraded (TD) samples (measured at 400 ppm, 20 °C). Reproduced from ref 183. Copyright 2024 American Chemical Society.

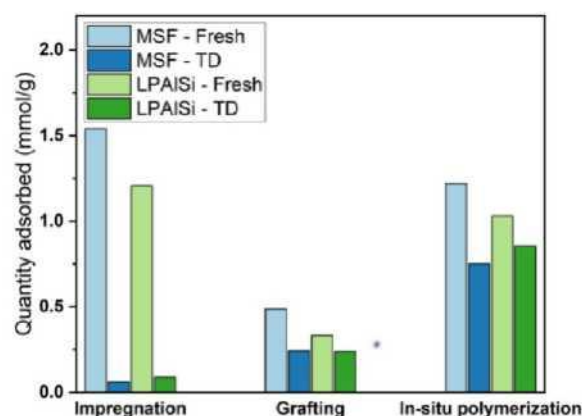
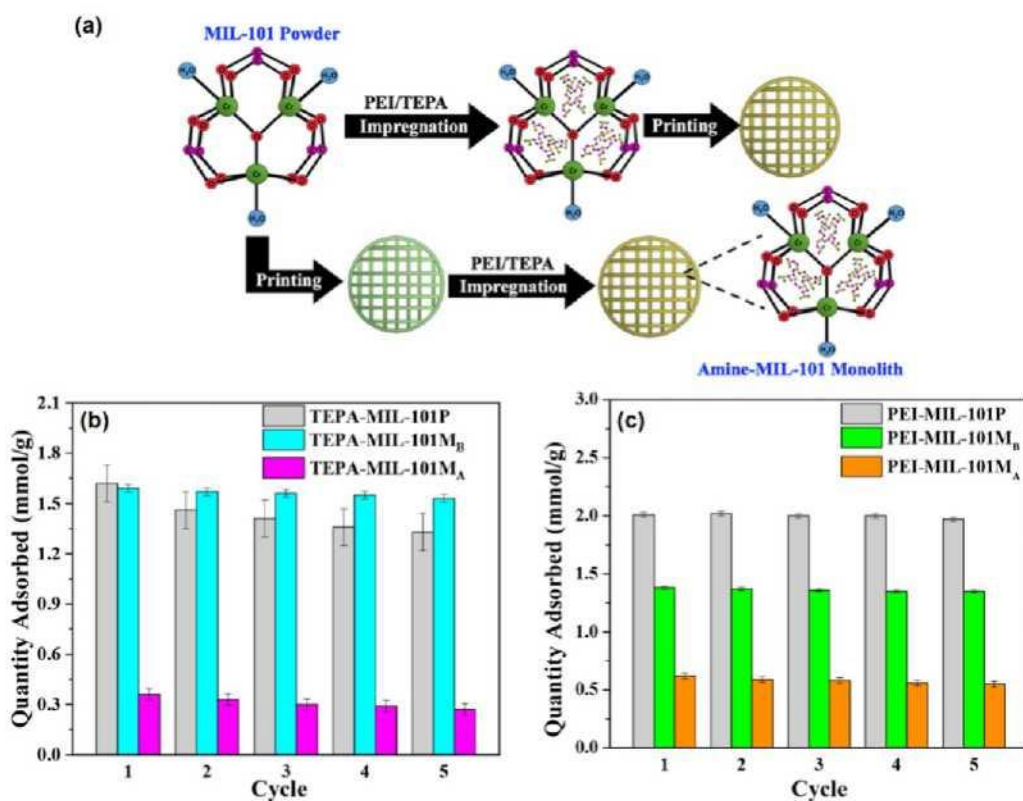


**Figure 10.** (a) Pre- and postimpregnation of TEPA on MIL-101 monoliths and CO<sub>2</sub> uptake capacity of (b) TEPA- and (c) PEI-based adsorbents;  $M_A$  and  $M_B$  denote postimpregnated and preimpregnated samples, respectively, while  $P$  refers to samples in powder form. Reproduced from ref 261. Copyright 2019 American Chemical Society.



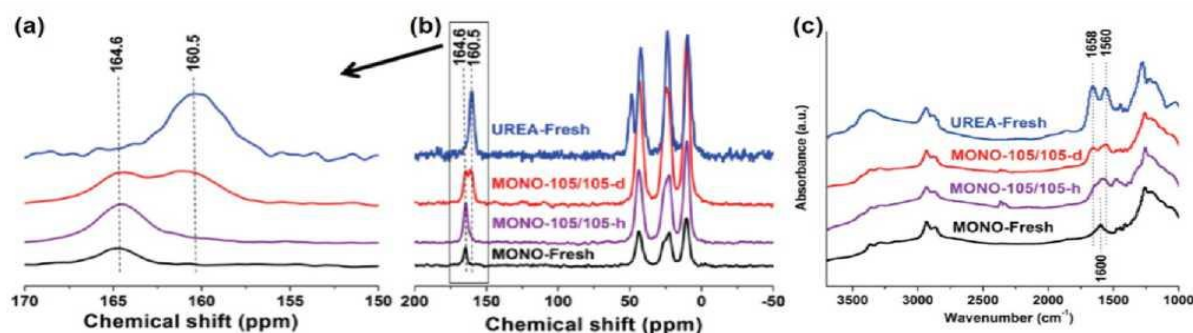
Darunte et al.<sup>186</sup> compared TREN (tris(2-aminoethyl)-amine)-grafted and TREN-impregnated MIL-101(Cr) and observed that grafting improved thermal cyclic stability but resulted in much lower initial CO<sub>2</sub> uptake (0.35 vs 2.8 mmol/g) due to limited amine loading, as grafting typically allows only one amine molecule per available Cr coordination site. In comparisons of impregnated sorbents, PEI-loaded MIL-101(Cr) exhibited superior thermal stability (<5% capacity loss over three cycles) relative to TREN-impregnated samples (~13%), which was attributed to the higher volatility of TREN. Rim et al.<sup>259</sup> studied TEPA- and PEI-impregnated MIL-101(Cr) under ambient (25 °C) and subambient (−20 °C) conditions. PEI-loaded samples showed stable performance over 15 cycles at a regeneration temperature of 60 °C, with final capacities of 1.64 and 1.11 mmol/g under ambient and subambient adsorption, respectively. Owing to the higher volatility of TEPA, regeneration was conducted at 25 °C, resulting in a final working capacity of 0.73 mmol/g after 15 cycles; following an initial ~20% capacity loss, stable performance was maintained in subsequent cycles.

The stability and performance of MOFs in various shapes have also been examined in the literature.<sup>260-262</sup> Wang et al.<sup>260</sup> reported stable performance over 14 TSA cycles for 3D-printed cellulose acetate monoliths incorporating MIL-101(Cr) and bPEI under dry, subambient conditions with regeneration at 60 °C. Lawson et al.<sup>261</sup> prepared 3D-printed MIL-101 monoliths impregnated with bPEI or TEPA using either preimpregnation (amine loading before printing) or postimpregnation (amine loading after printing) and compared them with impregnated powders (Figure 10a). While TEPA-impregnated powders showed higher initial CO<sub>2</sub> uptake but experienced capacity loss upon cycling, PEI-based materials consistently performed better in powder form than in monoliths (Figure 10b,c). Among structured adsorbents, preimpregnated monoliths exhibited superior cyclic stability over five cycles. These results indicate that

adsorbent structure can significantly influence stability, underscoring the importance of evaluating materials in both powder and structured forms.

**Amine-Functionalized COFs.** The thermal stability of COFs is commonly assessed by TGA. In this context, COF-609 exhibits thermal degradation at temperatures above 200 °C, which has been attributed to the decomposition of tetrahydroquinoline linkages formed via postsynthetic transformation of the original imine bonds.<sup>144</sup> COF-999 undergoes framework decomposition between 250 and 800 °C with a mass loss of 75.2% in this range.<sup>145</sup> Compared with its precursor frameworks, this polyamine-bearing COF exhibits a more rapid thermal degradation, which is attributed to steric repulsion introduced by the polyamine groups that weakens interlayer interactions and promotes layer separation at elevated temperatures.<sup>145,263</sup> Similarly, COF-709 shows framework decomposition in the same temperature range, accompanied by a mass loss of 53.5%.<sup>196</sup>

**Figure 11.** (a,b) <sup>13</sup>C CP/MAS NMR and (c) DRIFT spectra of APTMS monoamine samples cycled at 105 °C under dry (MONO-105/105-d) and humid (MONO-105/105-h) conditions, compared with a fresh MONO sample and a urea-functionalized reference (UREA-Fresh). The <sup>13</sup>C NMR spectrum shows a 164.6 ppm peak from carbamates (atmospheric CO<sub>2</sub> adsorption) and a distinct 160.5 ppm signal in MONO-105/105-d attributed to urea formation. DRIFT spectra reveal the disappearance of the NH<sub>2</sub> scissoring band (1600 cm<sup>-1</sup>) and appearance of urea-related bands at 1658 and 1560 cm<sup>-1</sup>, consistent with the UREA reference. Reproduced from ref 274. Copyright 2010 American Chemical Society.



**3.2.1.3. Amine-Functionalized Carbon Fibers.** These materials have recently been explored as sorbents for ETSA in DAC applications. In this approach, heat is generated directly within electrically conductive sorbent structures via Joule heating, enabling rapid and localized temperature swings without the need for steam or external heat-transfer media.<sup>28</sup> Moreover, the absence of steam during regeneration largely eliminates hydrothermal stress, while the rapid adsorption—desorption cycles can minimize oxidative degradation. At the same time, ETSA introduces new durability considerations, such as the potential for localized hot spots, and electrical fatigue of conductive supports. Understanding how these factors influence long-term sorbent stability will be critical for the deployment of ETSA-enabled DAC systems.

Compared with conventional indirect regeneration approaches, ETSA enables shorter residence times at elevated temperatures; however, the limited number of stability studies available to date prevents definitive conclusions regarding its ability to mitigate thermally induced degradation. For instance, Jang et al.<sup>28</sup> evaluated bPEI-impregnated carbon fibers under ETSA conditions for 10 cycles, employing adsorption,

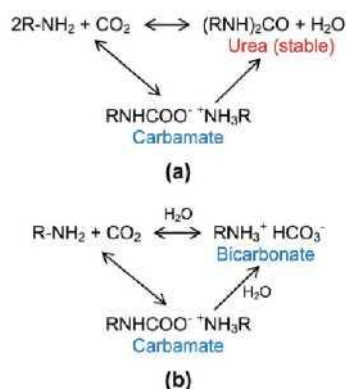
vacuum, and regeneration steps of 20, 5, and 10 min, respectively. During regeneration, an applied voltage of 5.9 V across a bundle of 80 fibers increased the sorbent surface temperature to approximately 100–120 °C. Over these 10 cycles, a CO<sub>2</sub> capture capacity loss of about 6.5% was reported. As oxidative degradation was not examined, part of the observed performance decline may be associated with unintended oxygen ingress during high-temperature regeneration. To date, stability assessments of ETSA-based carbon—fiber sorbents have been largely limited to short-term thermal cycling, underscoring the need for extended lifetime studies over significantly higher cycle numbers. Future research should focus on strengthening interactions between conductive supports and active amine phases, while simultaneously improving oxidative resistance without compromising capture performance. In addition, evaluating long-term stability under varying humidity levels will be essential for assessing the practical viability of these materials in large-scale.

**3.2.1.4. Commercial Adsorbents.** The thermal stability of Lewatit, a benchmark DAC adsorbent, has been studied in several works. Alesi and Kitchin<sup>264</sup> evaluated thermal cyclic performance of this adsorbent, reporting stable capacity over 18 cycles. Under 275 adsorption—desorption cycles conducted by Parvazinia et al.,<sup>205</sup> Lewatit exhibited acceptable cyclic performance though with 4.84% capacity loss. In another similar work, Lewatit lost 5.47% capacity over 180 cycles.<sup>265</sup> This also highlights the importance of evaluating the stability of adsorbents over a relatively high number of cycles, as the loss of capacity is greater with prolonged applications. Parvazinia and colleagues<sup>205</sup> also examined the cyclic stability of Purolite A109 over 40 cycles, observing an 11.24% capacity decline compared with a 1.42% decrease for Lewatit. The capacity loss in both adsorbents was attributed to urea formation during cyclic operation. In the Lewatit thermal stability study conducted by Yu et al.,<sup>266</sup> 50 h of continuous exposure to N<sub>2</sub> resulted in 40% decrease in capture capacity, with degradation initiating only at 200 °C, which is substantially higher than typical regeneration temperature. However, repeated cycling at lower temperatures can still lead to adsorbent degradation, underscoring the importance of long-term stability assessments. Elfving et al.<sup>267</sup> developed a proprietary aminoresin adsorbent, consisting of polystyrene resin functionalized with primary amine groups, which exhibited a CO<sub>2</sub> capture capacity of 0.44 mmol/g under DAC conditions. The material was tested for 19 TCSA cycles with regeneration at 100 °C and showed a 7% loss in adsorption capacity, which exhibited a gradual, steady decline instead of a sharp loss in the initial cycles.<sup>268</sup>

**3.2.1.5. Urea Formation: A Cyclic Deactivation Mechanism.** Urea formation, also referred to as CO<sub>2</sub>-induced degradation, was considered to be one of the main deactivation mechanisms of amine-based carbon capture adsorbents. This phenomenon appears to be more pronounced for conventional carbon capture adsorbents with higher CO<sub>2</sub> content (flue gas) and less concern has been reported for ultradilute DAC application.<sup>147,269</sup> Moreover, the CO<sub>2</sub>-induced degradation can happen in desorption when using CO<sub>2</sub> as purge gas to increase the purity of the recovered CO<sub>2</sub>.<sup>266,270</sup> Nevertheless, continuous removal of CO<sub>2</sub> during regeneration, either by vacuum, sweeping gas, or steam, limits its accumulation, thereby reducing the likelihood of this mechanism occurring. In general, urea formation is accompanied by a gradual increase in the mass of the adsorbent as well as a capacity diminution.<sup>252,271</sup> In the works carried out by Guta et al.<sup>272</sup> and Li et al.<sup>273</sup> on the impact of CO<sub>2</sub> on oxidative degradation, PEI-impregnated  $\gamma$ -Al<sub>2</sub>O<sub>3</sub> was exposed to both CO<sub>2</sub>-free and a 400 ppm of CO<sub>2</sub> conditions, where no urea formation was reported in the presence of CO<sub>2</sub>. Nonetheless, some DAC studies have suggested the potential for urea formation, albeit without thorough characterization evidence,<sup>265</sup> particularly when desorption was conducted under pure and high-concentration CO<sub>2</sub> streams.<sup>266</sup> Therefore, this mechanism is shortly discussed in this review.

The formation of urea and the associated capacity decrease can vary depending on the chemical structure of the implemented amine. Furthermore, adsorption conditions and gas composition, such as the presence of water, can influence the extent of this degradation mechanism. In the study performed by Sayari and Belmabkhout,<sup>274</sup> three different adsorbents were prepared using a pore-expanded MCM-41 (PE-MCM-41) mesoporous silica support: one by impregnating bPEI, and the other two by grafting a monoamine, APTMS, and a triamine, TRI. All adsorbents exhibited an approximately 40% reduction in capture capacity during adsorption with pure CO<sub>2</sub> at 105 °C, followed by regeneration under N<sub>2</sub> at the same temperature. Based on carbon-13 crosspolarization magic angle spinning nuclear magnetic resonance (<sup>13</sup>C CP/MAS NMR) analysis and in situ diffuse reflectance infrared Fourier transform (DRIFT) shown in Figure 11, which revealed peaks comparable to those of urea, the authors proposed urea formation as the main degradation mechanism under dry, oxygen-free conditions. The role of water in preventing CO<sub>2</sub> uptake decline was also examined, and no capacity loss was observed under humid conditions, confirming that urea compound formation occurs in dry environments. Scheme 3 shows the dehydration mechanism leading to urea and the inhibiting effect of waters.

**Scheme 3.** (a) Mechanism of Urea Formation in Absence of Moisture, and (b) Inhibition in the Presence of Water Vapor<sup>a</sup>



<sup>a</sup>Reproduced from ref 274. Copyright 2010 American Chemical Society.

Different amine groups, particularly primary and secondary amines, are believed to exhibit varying stability under CO<sub>2</sub> exposure, which influences the extent of urea formation. In a work from Sayari's group, APTMS and trimethoxy[3-(methylamino)propyl]silane (TMMAPS), which have respectively single primary and secondary amines, were grafted on PE-MCM-41.<sup>275</sup> Secondary amines demonstrated thermal stability up to 200 °C in TGA analysis and maintained performance over 60 cycles, with no evidence of urea formation. In contrast, primary amines exhibited a 21% reduction in CO<sub>2</sub> capture capacity, attributed to urea formation, as confirmed by DRIFT and <sup>13</sup>C CP/MAS NMR results. Liu et al.<sup>251</sup> evaluated TEPA-grafted MCF under 15% CO<sub>2</sub>, observing a performance decline after 50 cycles. This reduction was attributed to urea formation, as the primary amine groups in TEPA are particularly susceptible to CO<sub>2</sub>-induced degradation. The susceptibility of secondary amines to urea formation was further investigated in a subsequent study by Sayari et al.,<sup>276</sup> who showed that secondary amines can be involved in urea formation when located adjacent to primary amines within the same ethylenediamine chain (as in 3-(2-aminoethylamino)propyltrimethoxysilane (DI) or TRI grafted on SBA-15), or in the presence of other

secondary amines (as observed with IPEI-impregnated SBA-15). Though urea formation due to adsorbent degradation is typically expected under high CO<sub>2</sub> concentrations, the decline in capture capacity of previously mentioned TRI-grafted alumina tested under 400 ppm of CO<sub>2</sub> in N<sub>2</sub> during adsorption and N<sub>2</sub> during regeneration was attributed to urea formation.<sup>180</sup> This conclusion was supported by the presence of C=O and C-N bond peaks in the FT-IR spectra, which resembled those reported for urea formation during the degradation of TRI-grafted PE-MCM-41 in the study by Sayari et al.<sup>276</sup> However, Sayari and colleagues investigated TRI-grafted silica under pure CO<sub>2</sub> for both adsorption and regeneration, making a direct comparison difficult.

The influence of support material on the stability of amine-functionalized adsorbents is also reflected in the emergence of urea when exposed to pure CO<sub>2</sub>. TEPA-impregnated silica sorbents exhibited an 84.58% loss in initial uptake after 10 cycles, whereas TEPA-impregnated  $\gamma$ -Al<sub>2</sub>O<sub>3</sub> samples showed a capacity decrease of less than 20%.<sup>277</sup> The lower stability of silica-based sorbents was attributed to urea formation, as confirmed by FT-IR spectra, while alumina-based supports effectively inhibited urea-induced degradation. This difference was linked to the high density of Lewis acid sites on the alumina surface, which promotes cross-linking with TEPA molecules and alters the charge density of primary amines. X-ray photoelectron spectroscopy (XPS) analysis further revealed that primary amines were converted into secondary amines, which exhibit greater resistance to urea formation. The CO<sub>2</sub>-induced degradation of Lewatit was also investigated by Yu et al.,<sup>266</sup> who observed more severe degradation at higher CO<sub>2</sub> partial pressures and temperatures (1 atm CO<sub>2</sub> at 150 °C vs 0.8 atm at 120 °C). After 72 h of exposure to 80% CO<sub>2</sub>, Lewatit exhibited 8% and 21% reduction in uptake capacity at 120 and 150 °C, respectively. FT-IR spectra of the degraded samples revealed a peak at 1670 cm<sup>-1</sup>, characteristic of urea, with increasing intensity corresponding to the degree of degradation.

**3.2.2. Carbonate-Based Adsorbents.** Alkali carbonates are intrinsically thermally stable and the main thermal limitations reported for these sorbents are therefore not carbonate decomposition, but rather performance losses caused by temperature-enabled phenomena such as support-carbonate reactions (e.g., formation of mixed hydroxycarbonates),<sup>213,278</sup> salt redistribution,<sup>279</sup> and humidity-related phase changes affecting regenerability.<sup>209</sup> Although fewer studies have addressed carbonate-based adsorbents for DAC, some works have explored their application and evaluated cyclic stability. Guo et al.<sup>208</sup> reported an approximately 5% capacity loss over 10 cycles for a silica aerogel-supported K<sub>2</sub>CO<sub>3</sub> adsorbent, with potassium carbonate utilization efficiency decreasing from 88.62% to 83.74%. Rodriguez-Mosqueda et al.<sup>207</sup> showed that K<sub>2</sub>CO<sub>3</sub>-impregnated activated carbon honeycombs achieved higher CO<sub>2</sub> capacity than Na<sub>2</sub>CO<sub>3</sub> samples, with both exhibiting stable performance over 10 cycles. Bali et al.<sup>213</sup> synthesized a potassium-based sorbent by calcining potassium acetate impregnated on an alumina support and reported stable performance over 5 cycles regenerated at 250 and 350 °C. However, a decline in capacity was observed at 110 °C, attributed to the formation of KAl(CO<sub>3</sub>)(OH)<sub>2</sub> (a support-derived phase), which requires temperatures above 200 °C for effective regeneration.<sup>278</sup> Derevschikov and co-workers<sup>279</sup> investigated a potassium carbonate-containing mesoporous zirconia aerogel (K<sub>2</sub>CO<sub>3</sub>/ZrO<sub>2</sub>) over 4 in situ TSA cycles using macro attenuated total reflectance—Fourier transform infrared (ATR-FTIR). They observed migration of carbonate species during the heating step, which could influence subsequent adsorption behavior. Such redistribution may modify the structure—property relationship (e.g., by inducing pore blockage and altering mass-transfer behavior), ultimately reducing CO<sub>2</sub> capture capacity over time. Despite the stable cyclic performance of K<sub>2</sub>CO<sub>3</sub>/ZrO<sub>2</sub> over 14 cycles reported by Veselovskaya et al.,<sup>209</sup> the authors noted that

carbonate-loaded materials can be affected by leaching under humid conditions over multiple cycles. This is further expanded in the hydro(thermal) stability section of this paper.

### 3.3. SUMMARY

In summary, physisorbents generally exhibit high thermal stability within the temperature range relevant to DAC, although their CO<sub>2</sub> adsorption capacities vary across different material classes. Among these materials, MOF frameworks may undergo structural degradation at elevated temperatures, with fluoride-based MOFs being particularly vulnerable. Among amine-functionalized chemisorbents, amine-grafted and in situ polymerized adsorbents exhibit better thermal stability at elevated temperatures due to the chemical bonds between amine groups and the support material. In contrast, impregnated samples exhibit lower stability, with capacity losses and alterations in surface functional groups, resulting from weak amine-support interactions that facilitate amine leaching, degradation, evaporation, or structural rearrangement. Aminosilanes are typically grafted onto silica supports, whereas various aminopolymers and amine molecules have been impregnated onto different porous materials. Among impregnated amines, PEI and TEPA are widely used; PEI generally exhibits higher thermal stability due to its bulkier structure, although this depends on the loading level, whereas TEPA often shows capacity loss on various supports because of its volatility. In addition to amine structure, the nature of the support strongly influences amine-support interactions and the resulting thermal stability. Existing studies suggest that modifying both amine chemistry and support properties can strengthen these interactions and enhance adsorbent stability. However, despite numerous investigations into the thermal cyclic stability of different amine components on various supports, systematic evaluations of the support's role in long-term stability and direct comparisons across support materials remain limited. The thermal stability of amine-functionalized MOFs has been explored only to a limited extent, primarily through cyclic testing. Although the MOF frameworks generally remain structurally stable at regeneration temperatures, their cyclic thermal performance strongly depends on the amine employed. Nevertheless, the practical application of MOFs as supports for amine-based sorbents remains challenging due to their high cost, scalability limitations, and sensitivity to moisture, as discussed in detail in Section 5. Similarly, the thermal stability of amine-loaded COFs, an emerging class of DAC adsorbents, has not been examined in depth; nevertheless, available studies indicate stable performance during long-term cyclic operation.

For carbon—fiber sorbents developed for ETSA, stability evaluations have so far been limited to short-term thermal cycling, highlighting the need for long-duration lifetime studies over greater numbers of cycles, as well as assessment of additional degradation mechanisms such as localized hot spots and electrical fatigue of conductive supports. Commercial adsorbents generally exhibit robust thermal stability while retaining relatively high CO<sub>2</sub> capture capacities, highlighting their potential for practical DAC deployment. However, extended cyclic testing is still required to reliably assess long-term stability and lifetime, as well as to define KPIs such as replacement intervals, adsorbent costs, and associated operational expenses. Finally, urea formation is generally considered a minor degradation pathway under DAC conditions and has been reported to primarily affect primary amines, particularly at high CO<sub>2</sub> concentrations.

Carbonate-based sorbents are intrinsically thermally robust. However, as summarized in Section 2 (Table 7), their DAC-relevant working capacities are often modest. Moreover, desorption can become more energy-intensive when carbonate—support interactions, particularly on alumina, lead to the

formation of thermally stable phases (e.g.,  $\text{KAl}(\text{CO}_3)(\text{OH})_2$ ) that require high regeneration temperatures. To address these limitations, further work is needed to enhance  $\text{CO}_2$  capture capacity under DAC conditions and to investigate how cycling-induced structural changes translate into performance losses for carbonate-based adsorbents.

## 4. OXIDATIVE DEGRADATION

High oxygen concentration in air is expected to have a negative impact on the long-term performance and regenerability of adsorbents in real-world DAC applications. Inorganic-based and physisorbent materials, such as carbonates and unfunctionalized MOFs, are generally more resistant to oxidative degradation owing to the absence of readily oxidizable organic moieties; however, studies specifically investigating their stability under oxidative conditions remain scarce. While oxidative gas streams can, in principle, induce framework degradation through organic linker cleavage, systematic evaluations of the oxidative stability of physisorbent MOFs are rare.<sup>223</sup> In contrast, amine-based adsorbents are well-known to be highly susceptible to this type of deactivation. This degradation mechanism becomes a significant issue in the presence of  $\text{O}_2$  and at high temperatures. To prevent this, it is vital to run the regeneration step in the absence of oxygen.<sup>266</sup> Even when the adsorption media is purged to eliminate molecular oxygen before conducting regeneration, the presence of  $\text{O}_2$  traces can lead to progressive adsorbent oxidation.<sup>181</sup> Moreover, after the regeneration phase, the adsorbent bed is usually quenched with air. This short step is characterized by a higher  $\text{O}_2$  concentration and moderate temperatures which can also be problematic.<sup>272,280</sup> Despite the importance of studying oxidative degradation of adsorbents, assessing oxidative stability is often overlooked due to the utilization of ultrahigh purity gas cylinders in laboratories.<sup>177</sup> This section examines the oxidative stability of amine-impregnated and grafted adsorbents, followed by oxidative degradation in amine-functionalized MOFs and COFs, and concludes with a discussion of commercial adsorbents.

### 4.1 AMINE-FUNCTIONALIZED ADSORBENTS

The lower  $\text{CO}_2$  concentration in the air results in a reduced reactivity of these adsorbents in DAC systems compared to conventional point source capture technologies. Under such conditions, the accessibility of “free” amine groups exposed to  $\text{O}_2$  accelerates the oxygen-induced degradation mechanisms.<sup>281</sup> This degradation leads to reduced  $\text{CO}_2$  capture capacity, changes in physicochemical properties, and the formation of both solid and volatile byproducts. The thermal and oxidative stability of amine solutions used as chemical solvents for postcombustion carbon capture has been widely characterized,<sup>282-284</sup> whereas their stability when immobilized on solid supports has received far less attention. Generalizing the findings from amine-based solvents to amine-based adsorbents is not straightforward. Amine species attached to solid supports differ from those used in liquid solvents, and the presence of water plays a critical role in certain oxidative pathways. Additionally, the strength of amine bonding to the support surface may affect their susceptibility to decomposition. Also, based on experiments on amine solutions, amines can decompose into smaller, very volatile components; however, the collection and characterization of these species in solidbased sorbents remain challenging.<sup>177</sup> Although the oxidative stability of DAC adsorbents has been examined in only a limited number of studies, this issue is becoming

increasingly relevant as adsorption-based DAC systems gain attention. This section reviews the oxidative degradation of amine-based DAC adsorbents, which are the most susceptible to this form of degradation. It summarizes key findings from the literature, comparing the oxidative stability of various amine-impregnated and grafted materials. In addition, it examines the parameters influencing oxidative stability, the underlying degradation mechanisms, and the formation of oxidative byproducts.

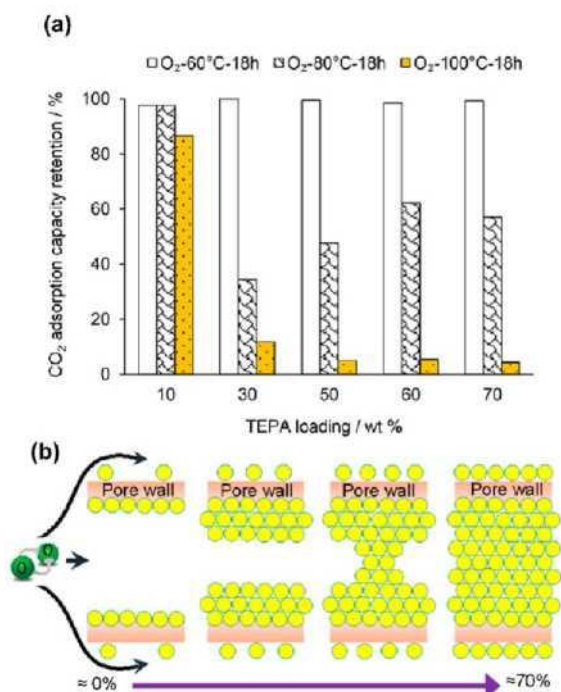
**4.1.1. Impregnation.** The current section analyzes the oxidative stability of amine-impregnated adsorbents, focusing on the influence of key parameters such as temperature, amine loading, and Mw on this degradation mechanism. It then identifies and categorizes the solid and gaseous oxidative byproducts, exploring how the chemical structure of the amine influences both oxidative stability and the formation of these byproducts. The radical-induced oxidation mechanism is discussed in detail, along with the role of water and CO<sub>2</sub> in accelerating or modifying this process. Finally, mitigation strategies to reduce oxidative degradation are evaluated. A summary of experimental conditions is provided in Table S2 of the Supporting Information.

The oxidative stability of various amine-impregnated adsorbents has been assessed by measuring the amine loss and/or reductions in capacity or amine efficiency after exposure to an O<sub>2</sub>-containing stream, with susceptibility to oxidative degradation strongly dependent on exposure temperature. While bPEI impregnated on fumed silica tested by Goeppert et al.<sup>160</sup> was stable under airflow at 85 °C for only 4 cycles, bPEI impregnated on SBA-15 in the work of Heydari- Gorji and Sayari<sup>281</sup> was completely deactivated, losing 100% of its capacity and changing color from white to brownish yellow after 20 h of exposure at 120 °C. Similarly, Meng et al.<sup>285</sup> evaluated the ability of bPEI-impregnated silica to capture CO<sub>2</sub> from oxygen-containing streams. The adsorbent only displayed a significant capacity loss above 75 °C, being more than 90% for treatments at and above 120 °C. Moreover, the decline in CO<sub>2</sub> uptake was significantly higher in the presence of oxygen compared to an oxygen-free stream (88.5% vs 32.9%). Besides a color change, the oxidation of samples above 75 °C was evidenced in DRIFT spectra by the breakage of the polyamine backbone.

Vu et al.<sup>286</sup> studied the oxidative degradation of TEPA- impregnated MCF under accelerated conditions and observed that, in addition to treatment temperature, both the duration of treatment and the amine loading had an amplifying effect on degradation (Figure 12a). In contrast, decreasing oxygen concentration positively influenced stability of the adsorbent loaded with a higher amine content (30-70%). Vu and colleagues suggested that the oxidation rate appears to be primarily controlled by the rate of O<sub>2</sub> diffusion to the amine molecules. Thus, stability is dependent on the loading and distribution (surface or in-pore) of the impregnated amine. Increasing loading from 30 wt % to 60 wt % reduced O<sub>2</sub> diffusion and degradation due to amine agglomeration in the pores. However, at 70 wt %, surface amines facilitated oxygen reactions, generating more free radicals and accelerating degradation (Figure 12b). Moreover, increasing the treatment temperature not only increased the reaction rate but also O<sub>2</sub> diffusion. Although Vu and coauthors did not explicitly identify the dominant O<sub>2</sub> diffusion regime at each amine loading, diffusion in mesoporous media is generally influenced by both molecule—molecule and molecule—pore wall interactions.<sup>287</sup> Accordingly, at lower amine loadings, O<sub>2</sub> diffusion is likely dominated by molecule—molecule collisions, whereas increasing amine loading enhances confinement and reduces pore diameter, shifting diffusion toward molecule—wall collisions. At the highest loading, where amines partially cover the external surface, increased O<sub>2</sub> accessibility can promote surface oxidation, thereby accelerating TEPA degradation. Sarazen et al.<sup>166</sup> similarly reported a trade-off between capture capacity and oxidative

stability with increasing aminopolymer loading. The decrease in stability at higher loading was attributed to the formation of polymer aggregate, resulting in reduced constraining interactions with the walls that increased the diffusion of gas molecules.

**Figure 12.** (a) Retention of CO<sub>2</sub> adsorption capacity as influenced by oxidation temperature and (b) illustration of amine molecule distribution and clustering in silica pores and surface for amine loadings of 10 to 70 wt %. Reproduced from ref 286. Copyright 2019 American Chemical Society.



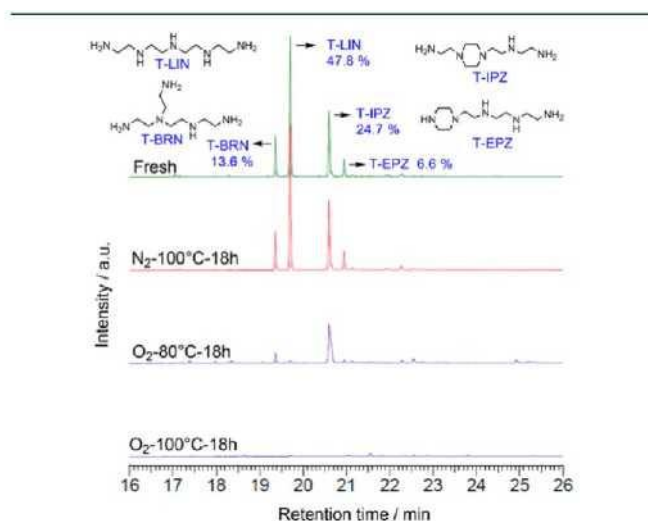
Since the degradation rate of amine solutions is largely governed by the oxidation rate during the induction phase,<sup>288,289</sup> the high viscosity of amines was also believed to retard the onset of degradation by controlling the diffusion rate of O<sub>2</sub> to the amine sites. Vu et al.<sup>290</sup> examined the effect of alkyl linker length between amine functional groups and aminopolymer Mw on the oxidative stability of impregnated adsorbents. The CO<sub>2</sub> capture capacity retained by bPEI-based samples after oxidative degradation was in the following order: bPEI300 < bPEI600 < bPEI1200 < bPEI25000. The greater oxidative stability of high-Mw PEI was associated with the higher viscosity of this aminopolymer, which reduced oxygen diffusion. The remaining CO<sub>2</sub> uptake of amine-loaded samples after oxidative degradation followed the trend TETA < TEPA < PEHA, with increasing amine chain length leading to higher viscosity and improved oxidative stability. The authors further compared TETA- and SPER (spermine)-impregnated sorbents and found that, despite comparable CO<sub>2</sub> capture capacities, the TETA-based material exhibited inferior oxidative stability, which was attributed to its lower-Mw, lower viscosity, reduced thermal stability, and shorter carbon linker length. Consistently, a separate study reported enhanced oxidative stability for sorbents impregnated with higher-Mw IPPI or IPEI relative to those containing lower-Mw amines.<sup>164</sup>

Under oxidative conditions, the degradation of amine- functionalized adsorbents leads to the formation of both solid and volatile degradation byproducts. The first category is more readily studied by analyzing the sorbent after a given assay. For instance, in the work carried out by Heydari-Gorji and

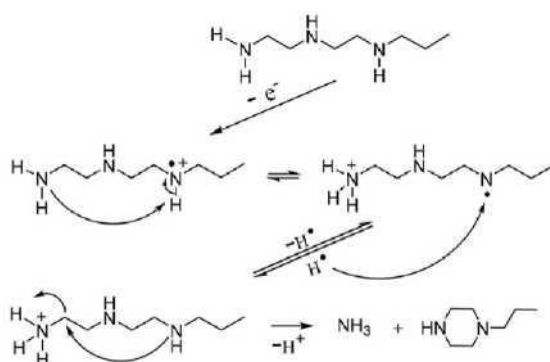
Sayari<sup>281</sup> DRIFT and <sup>13</sup>C NMR spectra indicated the formation of carbonyl (C=O) from species such as carboxylic acids and/or amides. To further investigate the oxidatively emerged compounds, Ahmadlinezhad and Sayari<sup>291</sup> applied a solvent-extraction method to separate oxidatively degraded components and examined them using several 1D and 2D NMR techniques. The findings revealed that the oxidatively produced materials primarily consisted of imine (C=N) and carbonyl groups, and a range of structural units containing C=O and —CH=N— species were identified in degraded IPEI- and bPEI-loaded samples. Similar findings were reported by Meng et al.<sup>285</sup> in the DRIFT spectra of oxidized samples, where characteristic stretching vibrations of C=O and C=N bonds were observed. Miao et al.<sup>292</sup> compared the oxidative stability of SBA-15 supported adsorbents impregnated with bPEI and TEPA, where both samples displayed bands assignable to C=O and C=N bonds in FT-IR spectra at 100 °C. These oxidatively formed solid products, such as amides, acids, and imides, exhibit lower basicity, resulting in reduced affinity for acidic CO<sub>2</sub> and, consequently, a decrease in 293 capture capacity.

The oxidative degradation of amine-based adsorbents results not only in the formation of solid residues but also in the release of volatile compounds. Similar to amine solutions, where ammonia (NH<sub>3</sub>) generation following oxidation has been reported,<sup>294</sup> Nezam et al.<sup>295</sup> observed an increase in the C/N ratio during oxidation of bPEI-impregnated  $\gamma$ -Al<sub>2</sub>O<sub>3</sub>, indicating a disproportionate loss of nitrogen-containing species relative to the polymer backbone. This finding suggested complex degradation pathways and the formation of volatile reaction products such as ammonia and hydroxylamine, rather than the evaporation of decomposed low-Mw polymer components. The volatile autoxidation products of alumina-supported bPEI were identified and quantified by Racicot et al.<sup>296</sup> using TGA/DSC coupled with FT-IR. Besides CO<sub>2</sub> and H<sub>2</sub>O, NH<sub>3</sub> was determined to be the main volatile compound, and formation rate of these components was consistent with the overall oxidation rate. H<sub>2</sub>O had the highest amount produced, followed by NH<sub>3</sub> and CO<sub>2</sub>. The quantity of formed ammonia corresponded to the cleavage of the C—N bond in primary amine end groups in the aminopolymer chain. In addition to the C/N ratio being a useful indicator of oxidative degradation, the normalized rate of NH<sub>3</sub> formation also showed a strong correlation with the oxidation rate determined by DSC, suggesting its potential as a complementary analytical measure. Similarly, Vu et al.<sup>286</sup> attributed the capacity loss in TEPA-impregnated silica foam to the formation of solid byproducts with reduced basicity and CO<sub>2</sub> affinity, as well as the release of ammonia. A solvent extraction and GC analysis revealed that while the main components of TEPA (T-BRN, T-LIN, T-IPZ, and T-EPZ, as defined in Figure 13) remained unchanged under nitrogen, exposure to O<sub>2</sub> caused significant degradation and the formation of new low-Mw species prone to evaporation. For instance, T-LIN underwent electron abstraction from a secondary amine, followed by H migration and dissociation, leading to ammonia release and six-membered ring formation (Scheme 4). These rings have lower CO<sub>2</sub> affinity, contributing to reduced capture 286 capacity.

**Figure 13.** Structures of the four primary ethyleneamine components in technical-grade TEPA: 1,4,7,10,13-pentaazatridecane (T-LIN), 4-(2-aminoethyl)-N-(2-aminoethyl)-N'-[2-[(2-aminoethyl)amino]ethyl]-1,2-ethanediamine (T-BRN), 1-(2-aminoethyl)-4-[[2-(2-aminoethyl)amino]ethyl]piperazine (T-IPZ), and 1-[2-[[2-[(2-aminoethyl)amino]ethyl]amino]ethyl]-piperazine (T-EPZ); and GC analysis of TEPA-impregnated silica foam samples before and after exposure to oxidative conditions. Reproduced from ref 286. Copyright 2019 American Chemical Society.



**Scheme 4.** Proposed Radical Pathway for the Formation of Six-Membered Rings during Oxidative degradation of T-LIN<sup>a</sup>



<sup>a</sup>Reproduced from ref 286. Copyright 2019 American Chemical Society.

Apart from characterizing degradation products, the effect of amine chemical structure on the resilience to oxidative degradation has been also assessed. Early works in the literature ascribed the oxidative degradation of amine components to the presence of secondary amine groups or absence of primary amines, highlighting their increased susceptibility to oxidative degradation. Bali et al.<sup>293</sup> examined the stability of bPEI and PAA impregnated on  $\gamma$ -alumina under oxidative conditions. Secondary-amine-rich bPEI samples displayed a higher decrease in CO<sub>2</sub> uptake capacity and the appearance of C=O bands in FT-Raman and <sup>13</sup>C CP/MAS NMR spectra, suggesting a higher oxidative resistance of primary amines compared to secondary amines. Zhang et al.<sup>165</sup> studied oxidative stability of IPEI-based fumed silica by exposing the material to airflow for 15 h at 100 °C, resulting in a significant 92.8% reduction in adsorption capacity. This pronounced degradation was attributed to the chemical structure of IPEI, which contains only secondary amines that are considered to be more susceptible to oxidative degradation. In a later study, Potter et al.<sup>173</sup> reported a reduction in organic content for both bPEI- and methylated bPEI-impregnated SBA-15 following oxidative treatment at around 100 °C; however, an increase in organic content was observed at 130 °C. At lower temperatures, the capacity loss of the samples was linked to evaporation and partial degradation of PEI, while at higher temperatures, the mass increase was

associated with oxygen addition to aminopolymers or their fragments, forming amides and other oxidized compounds, as confirmed by  $^{13}\text{C}$  NMR. The lower stability and greater organic content loss of methylated PEI solid adsorbent was also observed and attributed to the absence of primary amines. Pang et al.<sup>172</sup> conducted a more in-depth investigation into the hypothesis that secondary amines contribute to reduced oxidative stability

**Figure 14.** (a) FT-IR spectra, (b) ESI mass, (c)  $^1\text{H}$  NMR, and (d)  $^{13}\text{C}$  NMR spectra of fresh (black) and oxidatively treated (red) IPEI and IPPI aminopolymers studied by Pang et al. Reproduced from ref 172. Copyright 2017 American Chemical Society.

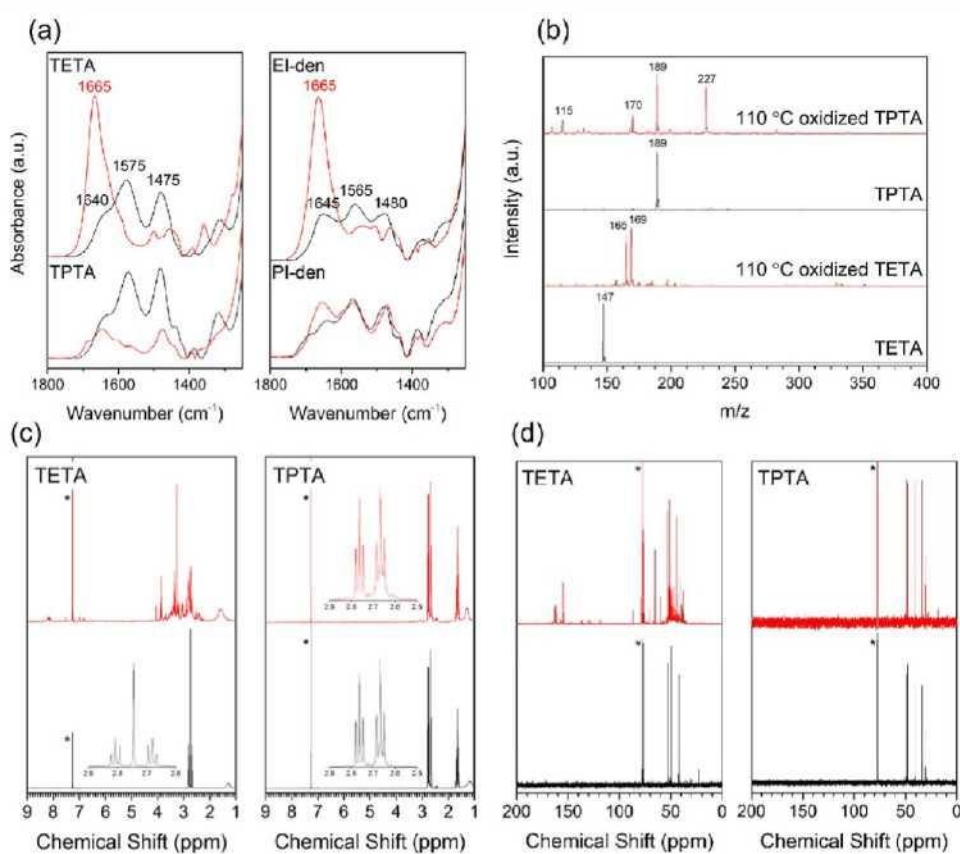
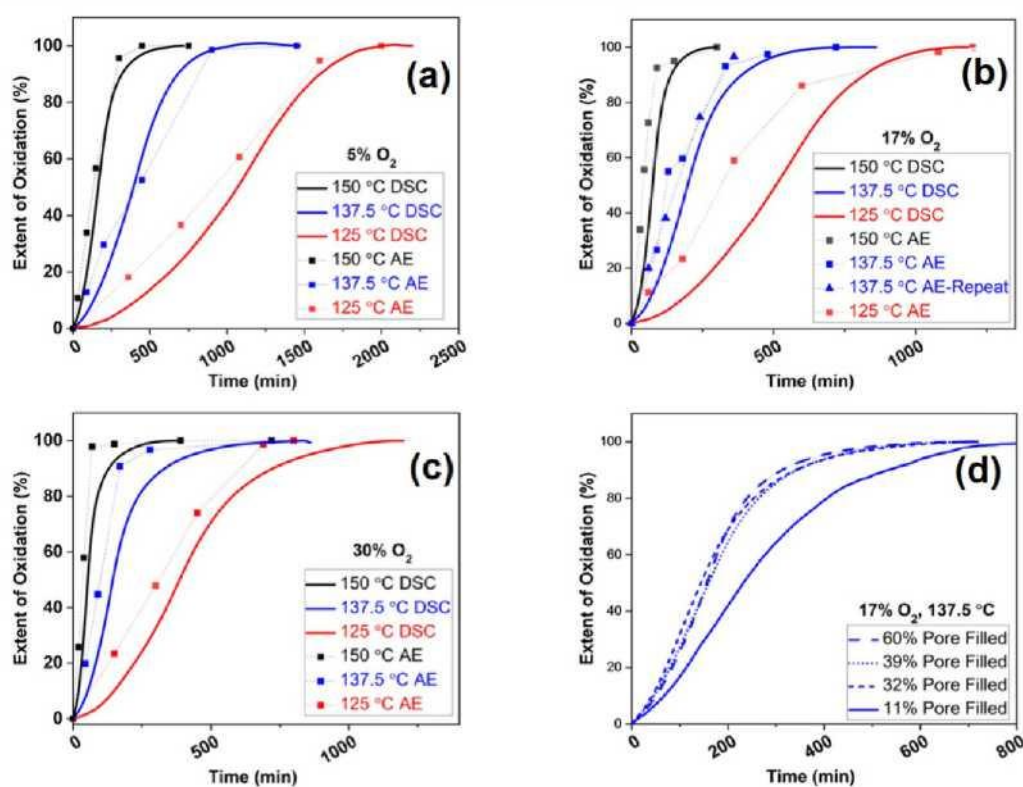


**Figure 15.** Oxidation extent of PEI over time measured through DSC and amine efficiency loss across (A-C) varying oxygen levels and (D) differing pore filling ratios. Reproduced from ref 295. Copyright 2021 American Chemical Society.



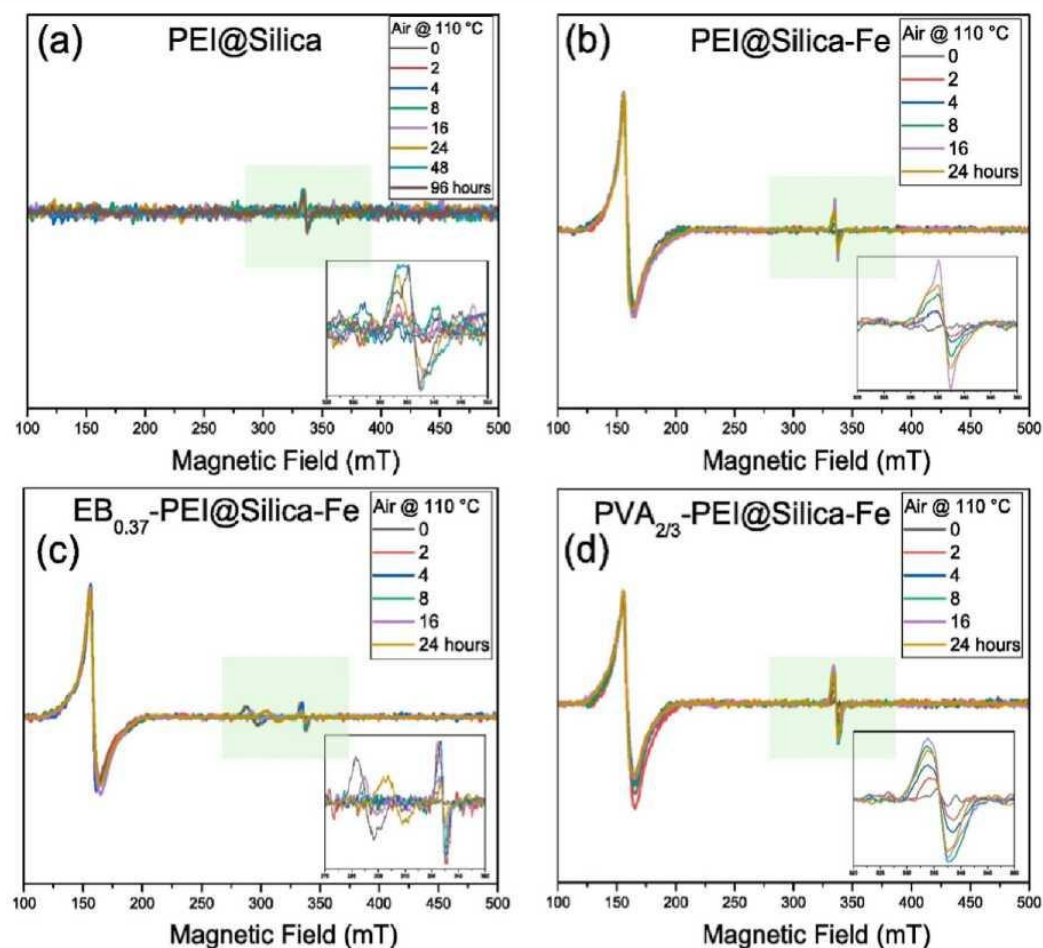
They synthesized dendritic PPI (PI-den) and TETA- impregnated SBA-15 sorbents and evaluated their performance and oxidative stability in comparison to dendritic PEI (EI-den) and tripropylenetetramine (TPTA)-impregnated adsorbents. The order of stability was TPTA > PI-den > TETA ≈ EI-den, corresponding to amine efficiency reductions of 20%, 50% and 90%, respectively. Secondary amines were not the sole cause of the oxidative degradation, as dendritic materials without secondary amines also underwent degradation. Instead, the higher stability of propylene linkers compared to ethylene linkers has been identified as a key factor, highlighting the significant impact of molecular structure on oxidative durability. Based on electrospray ionization mass spectrometry (ESI-MS), the authors proposed the occurrence of similar types of oxygen-assisted thermal rearrangement reactions for all molecules that result in intramolecular cyclization and/or alkylamine chain transfer reactions (Figure 14). Such reactions could generate secondary amines from dendritic species, leading to the observed oxidation of EI-den. They further suggested that thermal rearrangements are facilitated by the higher density of primary amines in dendritic structures, which are more prone to forming degradation products, thereby explaining the greater loss of amine efficiency and CO<sub>2</sub> capture capacity observed for PI-den relative to TPTA.

Given that the chemical structure of amines influences oxidative stability, several studies have focused on synthesizing various amines and evaluating their oxidative stability when impregnated onto silica supports. In a separate study by Pang et al.,<sup>164</sup> IPPIs with different Mws were impregnated on SBA-15 and oxidative stability was compared with IPEI-impregnated samples. While IPEI-loaded adsorbents lost 60-80% of their initial capacity and showed formation of C=N and/or C=O groups, IPPI supported sorbent experienced capacity loss of 17-35%, confirming the higher stability of propylene linkers over ethylene ones. Investigating alternative amine structures for oxidative resilience, Suján et al.<sup>168</sup> developed a PGA-

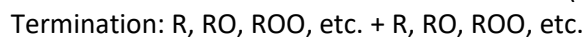
impregnated SBA-15 adsorbent and reported an approximately 50% decrease in capacity and negligible mass loss in TGA after accelerated oxidative treatment at 110 °C for 24 h. IR spectra indicated degradation of the polymeric backbone and loss of NH<sub>2</sub> groups, accompanied by the formation of amide and imide species. PGA, which contains only primary amines, exhibited greater oxidative stability compared to IPEI, bPEI, and branched poly(propyleneimine) (bPPI), while it was less stable than IPPI. Although PGA is structurally similar to PAA, which has been reported to have satisfactory oxidative stability,<sup>293</sup> the former has a carbon in the polymer backbone that is substituted with oxygen. This structural difference demonstrated that a carbon in polymeric backbone prevents oxidation, while oxygen accelerates this degradation mechanism. However, the effect of heteroatoms in the polymeric backbone on oxidative degradation has been rarely addressed in the literature.

Further exploring how structure impacts oxidative degradation, Kumar et al.<sup>234</sup> impregnated synthesized aryl-alkyl amine rich molecules onto SBA-15. In contrast to previous studies reporting higher oxidative stability for PPI-based adsorbents with propyl linkers compared to ethyl linkers,<sup>164,166,172</sup> the sample incorporating ED exhibited greater stability than that containing propylenediamine (PD), retaining 35% and 22% of its initial capacity, respectively, after 24 h exposure to 21% O<sub>2</sub> in He at 90 °C. In addition to the physical effects associated with differences in oligomeric alkylamine chain spacing, this contradictory trend was attributed to electronic modifications of the amine groups induced by the aromatic core, which alters the relative oxidative stability of ethyl- and propyl-linked amines. Accordingly, in phenyl-core-based structures, ethyl and propyl spacers exhibit comparable oxidative stability, indicating that the relative stability of these linkers is strongly influenced by neighboring alkyl and aryl functionalities.

**Figure 16.** EPR spectra recorded during air oxidation at 110 °C revealed a characteristic radical signal at 336.3 mT. In undoped PEI impregnated onto silica (PEI@Silica), this peak appeared after 24 h, whereas in Fe-doped PEI@Silica (PEI@Silica-Fe), the signal emerged after only 2 h and was significantly more intense, indicating accelerated radical formation due to Fe. The addition of EB and poly(vinyl alcohol) (PVA) (EB<sub>0.37</sub>-PEI@Silica-Fe and PVA<sub>2/3</sub>-PEI@Silica-Fe) did not noticeably reduce radical intensity, suggesting that their contribution to oxidative stability is not related to radical scavenging mechanisms. Reproduced with permission from ref 299. Copyright 2024 Elsevier Publication.



Oxidative degradation in liquid amine systems is mainly caused by the formation of free radicals, which is a well-established mechanism.<sup>289,297,298</sup> Based on this, Vu et al.<sup>286</sup> proposed a similar degradation mechanism for solid adsorbents, highlighting the role of free radical chain reactions in amine degradation. In this mechanism, thermal fluctuations or similar triggers initiate free radical chain reactions by abstracting a hydrogen atom, resulting in a free radical. The process continues with propagation reactions and the production of hydroperoxides, which break down to yield additional radicals. Termination occurs when two radicals react with each other to form a nonreactive molecule. These reactions are depicted below



The oxidative degradation kinetics of bPEI-impregnated adsorbents are found to be consistent with a radical-induced oxidation mechanism. Nezam et al.<sup>295</sup> established the oxidation kinetics of bPEI-

impregnated  $\gamma$ -Al<sub>2</sub>O<sub>3</sub> adsorbent using DSC and TGA. The initial curvature in DSC curves in their study indicated the presence of oxidative induction period, suggesting that bPEI oxidation would be analogous to common carbon-based polymers (Figure 15). A similar trend has been observed in other studies, often described as an S-shaped curve (or sigmoidal profile), characteristic of oxidation under dry aerobic conditions, showing a radical-induced autoxidation process.<sup>280,286,290,295</sup> Nezam and colleagues also hypothesized that changing the oxidative treatment conditions (i.e., O<sub>2</sub> concentration or temperature) would affect the relative rates of reactions within the mechanism. For instance, changing the rates of the propagation and chain branching reactions could affect the total heat generated, yet the reaction products would remain constant since the termination steps are unaffected. The formation of radical species was recently evidenced by Yan and Sayari<sup>299</sup> using electron paramagnetic resonance (EPR) technique in the oxidation study of PEI-impregnated silica. Moreover, oxidation was found to be exacerbated when the silica support was doped with transition metals such as Fe or Cu (Figure 16), demonstrating the detrimental effect of metal contaminants on oxidative degradation.

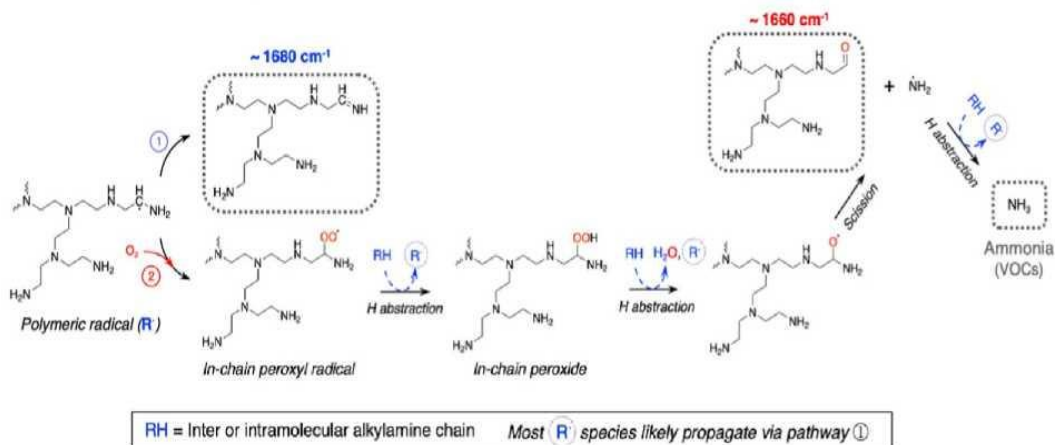
The autoxidation process involves both free radical formation and chain scission reactions that occur at the same time in different parts of the polymer backbone. In addition to the formation of C-centered radicals, the reaction between metals and O<sub>2</sub> can lead to the formation of reactive oxygen species (ROS), such as O<sub>2</sub><sup>•-</sup> and <sup>•</sup>OH, which react with amine-loaded adsorbent and cause oxidative degradation. Considering the results obtained regarding the nature of bond cleavage, oxidative products, and autocatalytic oxidation mechanisms, Carneiro and colleagues<sup>280</sup> proposed key reaction pathways for the oxidative degradation of the bPEI-based adsorbent in Scheme 5. The radical-mediated autoxidation mechanism under dry and humid aerobic conditions initiates with hydrogen abstraction from C-H bonds, leading to the formation of imine and carbonyl species, particularly at primary amine sites. The terminal C-N bond cleavage, especially near primary amines, was found to be a critical pathway for sorbent deactivation due to loss of highly reactive primary amine sites.

Despite the potentially important role of water in oxidative degradation, the influence of moisture on DAC sorbent deterioration has received limited attention in the literature. In a study conducted by Vu et al.,<sup>286</sup> it has been shown that the presence of water vapor in an oxygen-containing environment can either mitigate or accelerate oxidative degradation, depending on the amine structure. While water reduced oxidative degradation in TETA-, TEPA-, PEHA-, and bPEI-impregnated silica samples, this effect was not observed for SPER. Carneiro et al.<sup>280</sup> elaborated the oxidative degradation mechanism of bPEI-impregnated on  $\gamma$ -Al<sub>2</sub>O<sub>3</sub> and investigated the effect of humidity on this mechanism. Contrary to previous works,<sup>270,281,300</sup> this study showed the accelerating effect of moisture on oxidative degradation. Under humid stream, the induction phase, during which carbon-centered radicals are progressively formed and accumulated, was shortened and the degradation rate was doubled (Figure 17). In humid conditions, oxidative degradation of bPEI was accelerated due to the enhanced mobility of ROS and their interaction with the polymer matrix. Water disrupts hydrogen bonds within the polymer, increasing the mobility of oligomer chains and facilitating the diffusion of O<sub>2</sub> and ROS into the bulk material. Additionally, water-induced imine hydrolysis generates secondary carbonyl species, further degrading the sorbent. The oxidative degradation of different supports in humid conditions is also evaluated in Carneiro's work,<sup>280</sup> in which  $\gamma$ -Al<sub>2</sub>O<sub>3</sub> were found to exhibit higher ROS activity and oxidative degradation compared to hydrophobic silica supports like SBA-15. This difference was attributed to the hydrophilic nature of alumina, promoting water penetration and enhancing chain mobility within the polymer. In contrast,

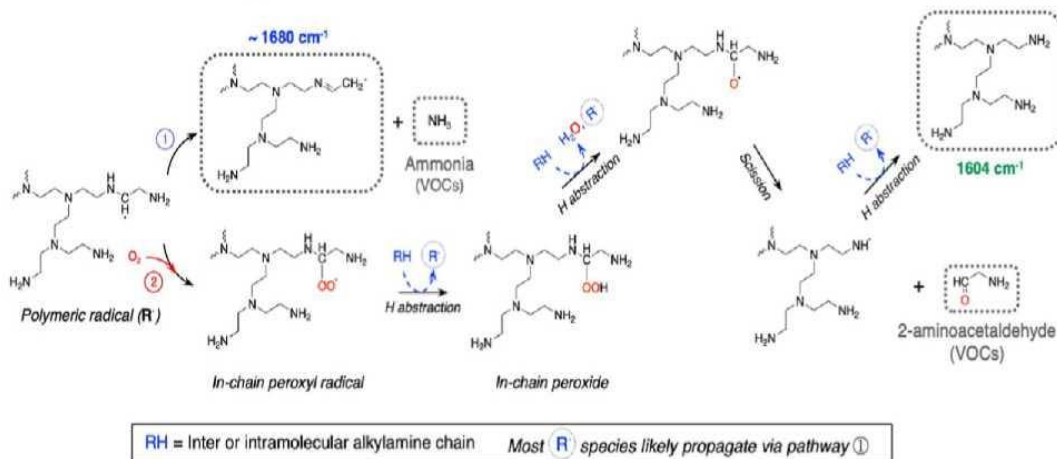
hydrophobic silica supports reduce water clustering and ROS diffusion, mitigating oxidative damage. To improve the oxidative stability of amine-based sorbents, the authors proposed increasing the hydrophobicity of the support material and strengthening CH bonds within the aminopolymer backbone. For instance, using longer alkyl spacers appeared to enhance resistance to oxidative degradation.

**Scheme 5.** Representation of the Oxidative Cleavage Mechanism for C-N Bonds in bPEI Backbones as Proposed by Carneiro et al<sup>a</sup>

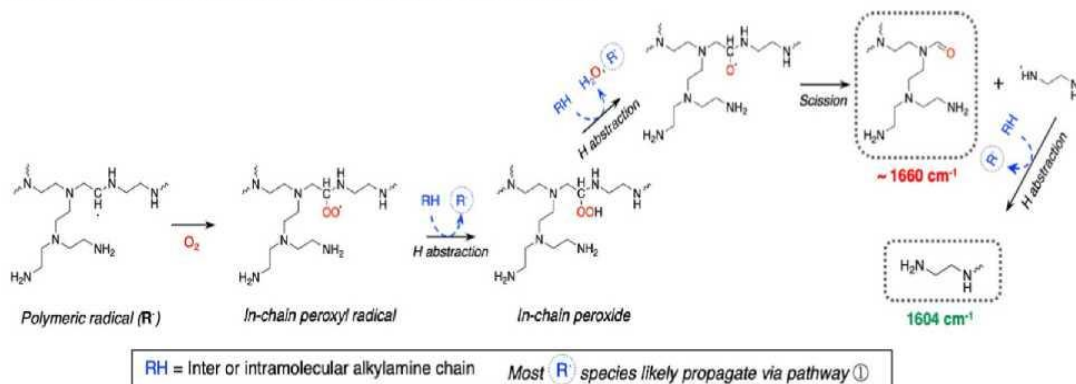
**Mechanism A: C-N cleavage at terminal 1° amines**



**Mechanism B: C-N cleavage at terminal 2° amines**

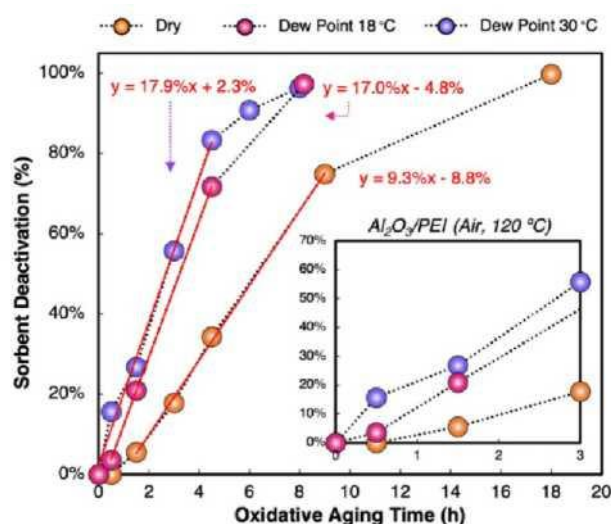


**Mechanism C: C-N cleavage at 2° amines along the polymer chain**



Reproduced with permission from ref 280. Copyright 2023 Wiley-VCH.

**Figure 17.** Oxidative deactivation profiles of PEI-based adsorbents under dry and humid conditions at 120 °C. Reproduced with permission from ref 280. Copyright 2023 Wiley-VCH.



Research on the oxidative degradation of amine-based adsorbents is evolving, and several recent studies have highlighted the potentially significant impact of CO<sub>2</sub> on this mechanism. These studies have shown that even low concentrations of CO<sub>2</sub> can have a substantial effect on degradation pathways and kinetics. Rosu et al.<sup>301</sup> evaluated the impact of extended aging on IPPI-impregnated SBA-15 adsorbents. Minimal performance and amine efficiency decline was observed for samples aged in air for 1.5 years or prepared with IPPI stored in sealed vials for 2 years, tested under 400 ppm of CO<sub>2</sub>/He conditions. Aged IPPI impregnated onto fresh SBA-15 was also tested under an accelerated oxidative test with 21% O<sub>2</sub>/He for 24 h at 110 °C, followed by 6 TSA cycles. In these experiments, the capacity and amine efficiency loss for the samples was significantly more pronounced under 400 ppm of CO<sub>2</sub> adsorption than under 10% CO<sub>2</sub> conditions. The effect of CO<sub>2</sub> concentration (400 pm vs 10%) on kinetic behavior was explored before and after accelerated oxidation. Under 10% CO<sub>2</sub>, the initial linear segments of the kinetic curves remained similar for both samples. In contrast, under 400 ppm of CO<sub>2</sub>, both curves quickly deviated in the linear region (Figure 18). Guta et al.<sup>272</sup> conducted a more detailed investigation into the influence of CO<sub>2</sub> on the oxidative degradation of PEI-impregnated  $\gamma$ -Al<sub>2</sub>O<sub>3</sub> under both continuous and cyclic operation modes and found that 0.04% CO<sub>2</sub> in air caused an 80% capacity loss after 7 days, compared to only 19% loss in CO<sub>2</sub>-free air (Figure 19). The presence of CO<sub>2</sub> eliminated the induction phase of degradation. Interestingly, the detrimental effect of humidity was reduced under CO<sub>2</sub>. Metadynamics simulations suggested that carbamic acids formed during CO<sub>2</sub> adsorption catalyze C-N bond cleavage via facilitating proton transfer, lowering the activation energy for degradation (Scheme 6).

Li et al.<sup>273</sup> further explored the impact of CO<sub>2</sub> on the oxidative degradation of PEI-impregnated alumina using experimental and modeling approaches. They observed that under 400 ppm of CO<sub>2</sub> in air, capacity reduction was accompanied by appearance of carbonyl/imine peaks and new primary amines. Even though the presence of CO<sub>2</sub> accelerated oxidative degradation compared to a CO<sub>2</sub>-free environment, higher CO<sub>2</sub> concentrations delayed the onset of deactivation and shifted it to higher temperatures. At higher CO<sub>2</sub> concentrations, enhanced acid-base interactions restricted polymer side chain mobility, reducing radical propagation and slowing oxidation, as confirmed by <sup>1</sup>H NMR relaxometry data. Regarding the effect of CO<sub>2</sub> in the degradation mechanisms, it was suggested that the oxidation mechanism involves radical formation leading to amides, with chemisorbed CO<sub>2</sub>, such as carbamic acid or carbamate/

ammonium pairs, catalyzing C-N bond cleavage in the presence of alkyl radicals, producing ammonia and imine species (Scheme 7).

**Figure 18.** Kinetic curves before and after accelerated oxidation treatment for the 45% IPPI composite prepared by blending two IPPI with number-average molecular weight ( $M_n$ ) = 6700 and 700 followed by adsorption under 90 mL/min of (A) 10% and (B) 400 ppm of  $\text{CO}_2$  conditions. Reproduced from ref 301. Copyright 2020 American Chemical Society.

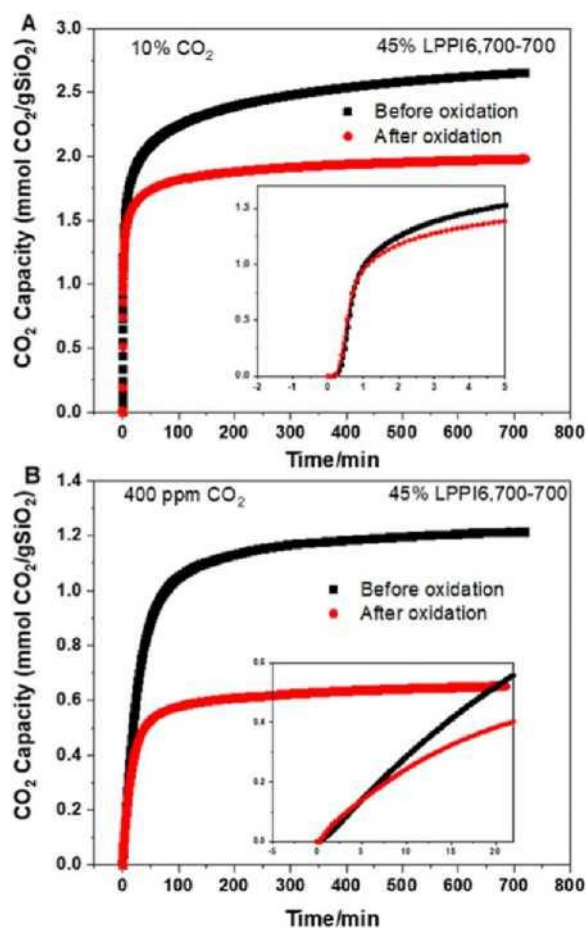
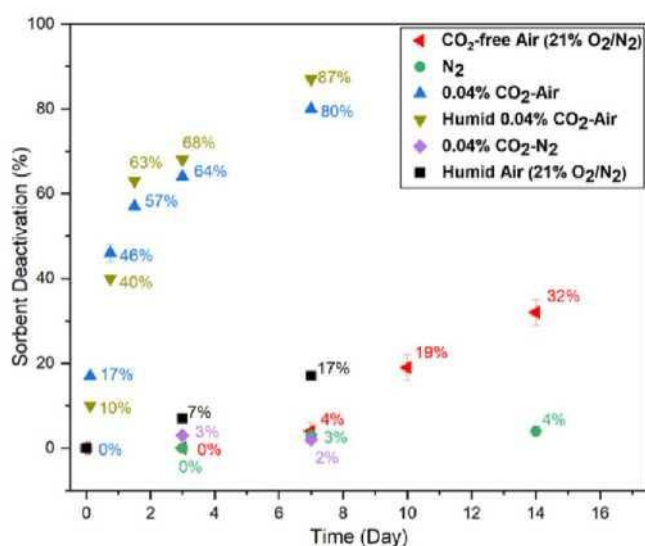


**Figure 19.** Deactivation behavior of 45% PEI/ $\gamma\text{-Al}_2\text{O}_3$  sorbent exposed to  $\text{CO}_2$ -free air,  $\text{N}_2$ , 0.04%  $\text{CO}_2$ -air, and 0.04%  $\text{CO}_2$  in  $\text{N}_2$  at 70 °C over varying durations. Reproduced from ref 272. Available under a CC-BY 4.0 license. Copyright 2023 Guta et al.



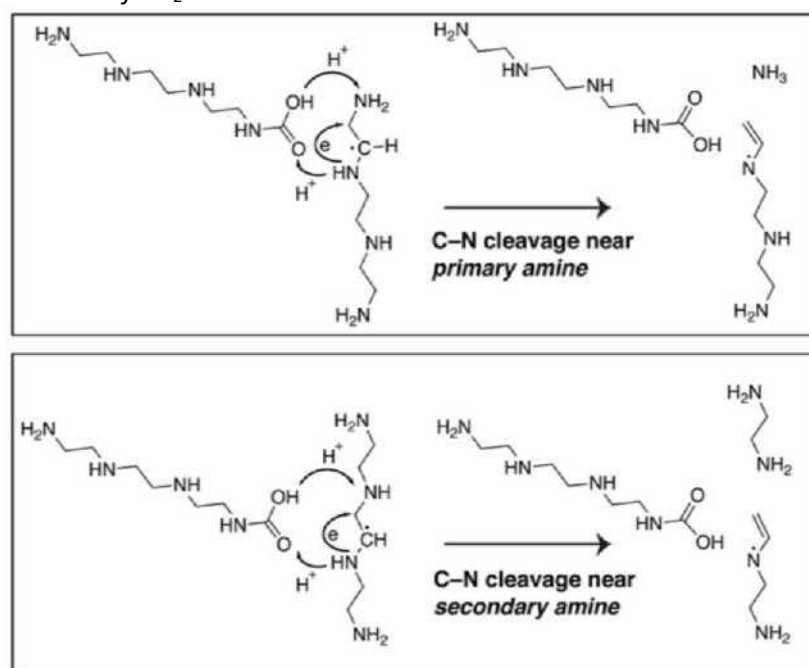
Various strategies have been proposed to mitigate oxidative degradation in amine-based adsorbents, including the use of amines with different proportions of primary, secondary, tertiary, and sterically hindered groups; the introduction of oxidation inhibitors, radical scavengers, or chelating agents; the incorporation of hydrogen-bonding polymers; and the chemical modification of amine functionalities. Srikanth and Chuang<sup>132</sup> observed enhanced oxidative stability of silica-supported TEPA by impregnating polyethylene glycol (PEG) into this adsorbent. The trend of capacity decrease caused by oxidative degradation was reported as TEPA-impregnated silica with PEG (Mw = 200) < TEPA-impregnated silica with PEG (Mw = 600) < TEPA-impregnated silica. The lower-Mw PEG contained more OH groups, which formed hydrogen bonds with TEPA amine functionalities, enhancing their dispersion on the silica support and improving oxidative resistance. Goepfert et al.<sup>231</sup> evaluated the oxidative performance of samples impregnated with epoxide-modified TEPA and PEHA. After exposure to an air stream at 100 °C, epoxide-enhanced sorbents were more stable, reducing capacity loss from 90% to less than 20%. In addition, PO-modified adsorbents retained their performance even after 3 years of shelf storing and exhibited constant capacity for 15 cycles under DAC conditions.

As metal impurities facilitate the oxidative degradation of amine-based adsorbents, the addition of chelators can reduce oxidative deactivation in solid sorbents. For example, Min et al.<sup>270</sup> developed an oxidatively stable solid sorbent by integrating two methods: modifying PEI with EB to form tethered 2-hydroxybutyl groups before impregnation, and incorporating chelators into macroporous silica to neutralize (poison) metal ions in the PEI solution (Figure 20a). After an accelerated oxidation test, the capture capacity of PEI/SiO<sub>2</sub> decreased by 52%, while EB-functionalized samples experienced a smaller loss of 23%. The enhanced stability of the latter adsorbent was associated with the conversion of a large proportion of the primary amines to secondary amines through alkylation with 2-hydroxybutyl groups, as confirmed by <sup>13</sup>C NMR studies. Furthermore, considering the FT-IR spectra, EB-functionalization led to the generation of a substantial number of hydroxyl groups, which facilitated hydrogen bonding with adjacent amine groups, thereby improving stability. Regarding the use of chelating agents, although all impregnated chelators were successful in promoting oxidative stability, phosphate or phosphonate sodium salts performed more effectively. Trisodiumphosphate (TSP) was identified as a promising chelator, thanks to its inorganic nature and inability to undergo oxidative degradation. Combining both strategies provided a

significant synergy in stability (Figure 20b,c).

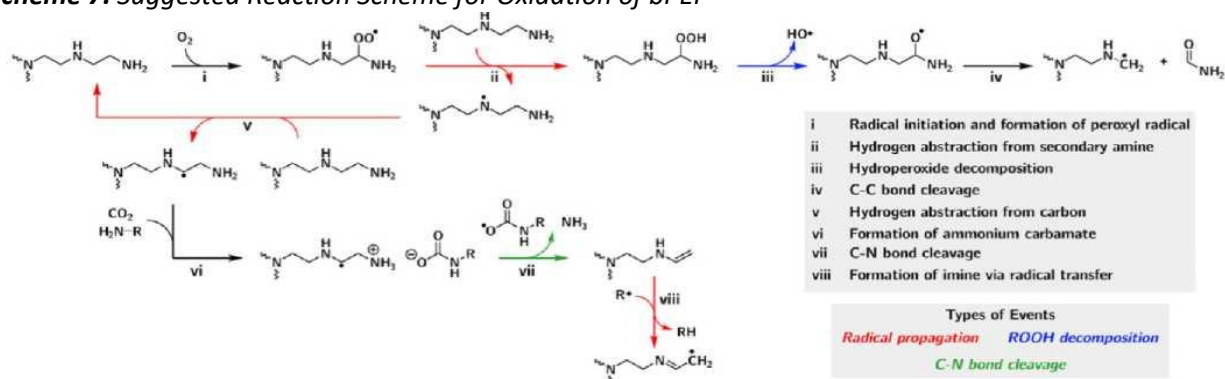
Building upon earlier strategies involving EB functionalization, Yan and Sayari<sup>299</sup> enhanced the oxidative stability of bPEI-impregnated silica by EB functionalization and addition of poly(vinyl alcohol) (PVA). The NMR and MS data demonstrated that oxidation occurred mainly in PEI, with partial involvement of the EB moiety, whereas PVA remained unchanged. While these strategies did not completely prevent radical formation, the slower oxidation observed in the presence of additives was attributed to stronger C-H bonds as demonstrated by DFT theoretical calculations. Additionally, EB and PVA served as radical trapping agents, temporarily stabilizing radical centers without neutralizing them, or as barriers, inhibiting PEI oxidation by slowing radical propagation. The hydrogen bonding between these agents and PEI further enhanced protection against oxidation of the aminopolymer.

**Scheme 6.** Reaction Mechanisms for C-N Bond Cleavage Adjacent to Primary and Secondary amines in the Presence of CO<sub>2</sub><sup>o</sup>



<sup>o</sup>Reproduced from ref 272. Available under a CC-BY 4.0 license. Copyright 2023 Guta et al.

**Scheme 7.** Suggested Reaction Scheme for Oxidation of bPEI<sup>o</sup>



<sup>a</sup>Reproduced from ref 273. Available under a CC-BY 4.0 license. Copyright 2024 Li et al.

Guta et al.<sup>302</sup> evaluated a series of hydrocarbon polymer stabilizers as radical scavengers to mitigate oxidative degradation of PEI-impregnated  $\gamma$ -Al<sub>2</sub>O<sub>3</sub>. Among the additives tested, 4,4'-bis( $\alpha,\alpha$ -dimethylbenzyl)diphenylamine (BDDPA) provided the highest oxidative stability, which was attributed to a regenerative radical-trapping cycle that neutralizes radical intermediates generated during oxidation (e.g., alkyl, hydroxyl, aminyl, and alkoxy radicals) while enabling repeated antioxidant regeneration. Incorporation of 2 mol % stabilizer led to an initial CO<sub>2</sub> capacity reduction of 10-18%, ascribed to diffusion limitations and partial blockage of amine sites.

Nevertheless, the reduced oxidative degradation can compensate for the initial capacity loss over long-term operation.

Complementary to chemical modification of the amine phase, altering the support material itself has also proven beneficial. Kuwahara et al.<sup>250</sup> modified the acid/base properties of the SBA-15 through incorporating various heteroatoms (Al, Ti, Zr, and Ce) and impregnated PEI on these supports. It was demonstrated that incorporating heteroatoms into the silica matrix not only enhanced the CO<sub>2</sub> capture performance but also improved oxidative stability (Zr > Ce > Ti > Al > unmodified). Based on FT-IR peak shift, it was concluded that the PEI amine groups displayed different interactions with the surface compared to the unmodified support. These results underscore that the support is not a passive structural support: its chemistry alters the amine microenvironment and, in turn, impacts amine accessibility and susceptibility to oxidative degradation. Accordingly, improving durability should include rational support selection/design and surface-chemistry modification to minimize degradation-promoting interactions. Furthermore, long-term aging studies should track changes in both the amine phase and the support to assess overall stability.

**Figure 20.** (a) Process for synthesizing oxidation-resistant CO<sub>2</sub> adsorbents by functionalizing PEI with EB and incorporation of small amounts of chelators into silica support. (Right) Oxidative stability results: (b) CO<sub>2</sub> working capacity retention (%) of PEI/SiO<sub>2</sub> and EB-PEI/SiO<sub>2</sub> with and without 2 wt % TSP after exposure to 3% O<sub>2</sub>, 15% CO<sub>2</sub>, 10% H<sub>2</sub>O in N<sub>2</sub> at 110 °C for 30 days; (c) FT-IR spectra comparing PEI/SiO<sub>2</sub> without TSP and EB-PEI/SiO<sub>2</sub> with 2 wt % TSP before and after aging. Reproduced with permission from ref 270. Copyright 2018 Nature Publishing Group.

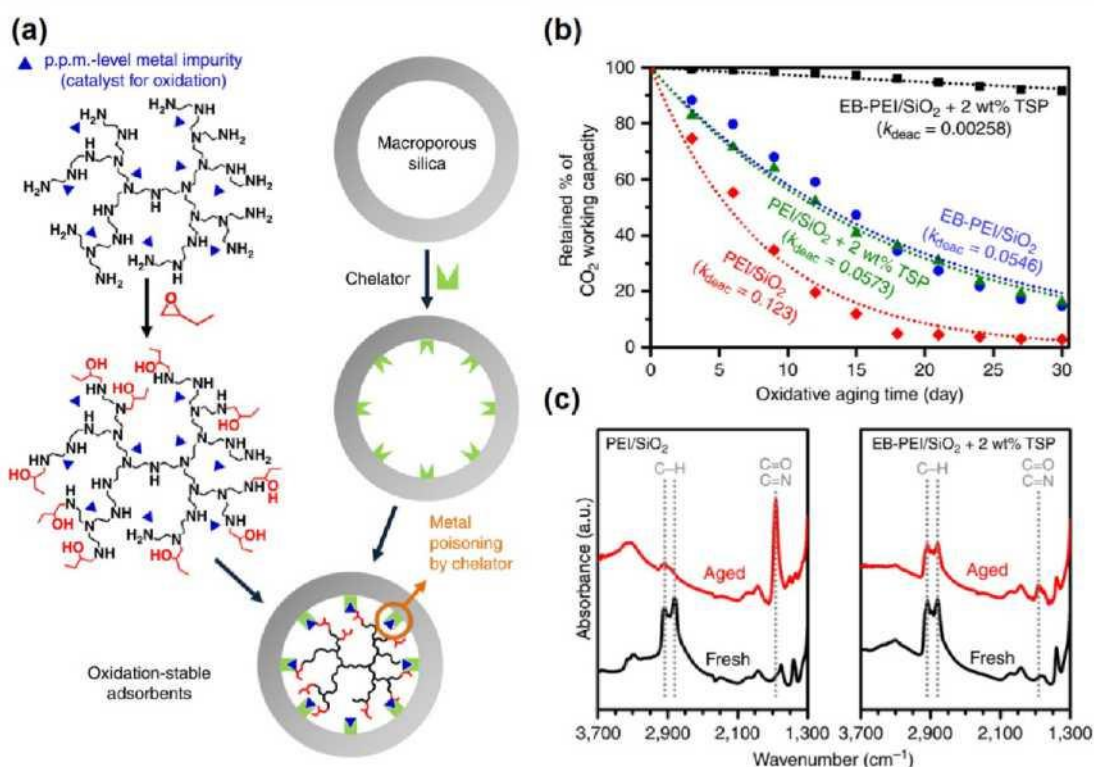
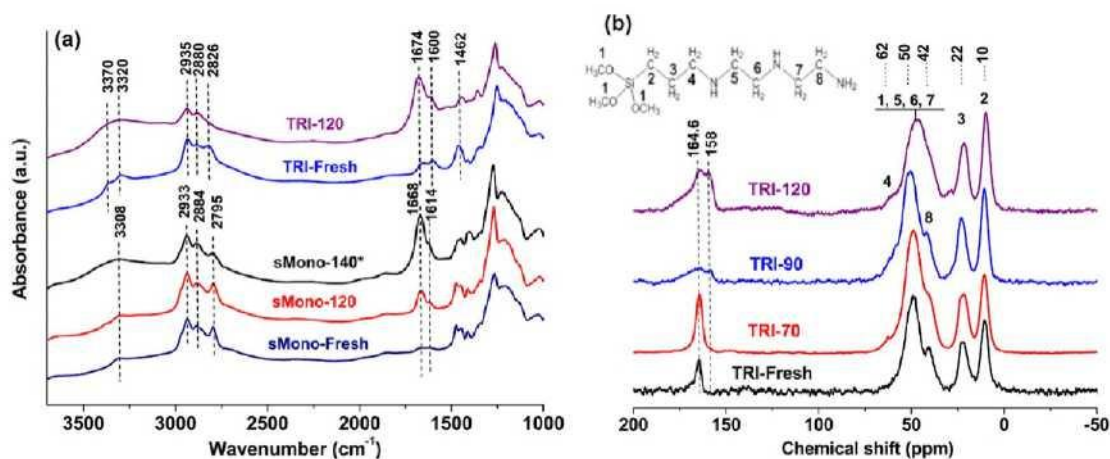


**Figure 21.** (a) DRIFT spectra of fresh and degraded grafted samples: single secondary amine at 120 and 140 °C (sMono-120, sMono-140) and triamine at 120 °C (TRI-120); (b) <sup>13</sup>C CP/MAS NMR spectra of fresh and degraded triamine-grafted samples at 70, 90, and 120 °C (TRI-70, TRI-90, TRI-120). Reproduced with permission from ref 304. Copyright 2011 Elsevier Publication.



**4.1.2. Grafting.** As with impregnated sorbents, the oxidative stability of various amine-grafted adsorbents has been examined in a number of studies, with the chemical structure and type of amine functionality identified as one of the key factors influencing oxidative degradation. Calleja et al.<sup>303</sup> identified oxidative degradation compounds while studying the effect of the drying step on the synthesis of APTMS-, DI-, and TRI-grafted SBA-15. Extending the drying time at 110 °C under air led to the formation

of C=N bonds in DI- and TRI-grafted samples, whereas no imine development was observed in the APTMS-loaded adsorbent. In addition, since reaction intermediates are more readily formed via an electron donor—acceptor mechanism with secondary amine groups than with primary amines, oxidative degradation was considered less likely in the absence of secondary amines. To better understand how the type of amine functionality influences oxidative degradation in amine-grafted adsorbents, Heydari-Gorji and colleagues<sup>304</sup> examined the oxidative stability of four different adsorbents grafted with single primary, secondary, and tertiary monoamines and a triamine material (TRI) with both primary and secondary amines onto PE-MCM-41 silica. The authors reported important differences in the oxidative degradation (measured as drop of CO<sub>2</sub> uptake) depending on the grafted amine chemical structure following the order: primary < secondary ≪ TRI. The lower stability of the secondary amines was also confirmed by the significant changes observed in their DRIFT spectra (Figure 21a). In agreement with the DRIFT results, for the case of TRI, <sup>13</sup>C CP/MAS NMR analysis (Figure 21b) suggested the formation of C=O or C=N species, such as carboxylic acids and imines. Using multiple 1D and 2D NMR spectroscopy techniques, Ahmadalinezhad et al.<sup>305</sup> determined the chemical structure of surface species resulting from the oxidative degradation of TMMAPS and TRI grafted onto pore-expanded mesoporous MCM-41 silica. In this study, secondary amines were shown to have a strong influence on oxidative stability, and functional groups such as imine, amide, and carboxyl groups were identified as oxidation products. In addition, several structural units bearing C=O and -N=C- species have been identified.

Similarly, Bollini et al.<sup>306</sup> demonstrated that oxidative degradation is significantly affected by both the types of amines and their proximity by investigating the stability of APTMS-, MAPS ((3-methylaminopropyl)trimethoxysilane)-, DMAPS ((*N,N*-dimethylaminopropyl)trimethoxysilane)-, DI-grafted MCF silica under accelerated oxidative tests. These aminosilanes contain single primary, secondary, tertiary amines at the end of a propyl surface linker, and primary and secondary diamines separated by an ethyl linker, respectively. In addition, while primary and tertiary amines were stable under the conditions tested, secondary amines were subjected to oxidative degradation at high temperatures. Additionally, in the NMR results of the MAPS- and DI-functionalized samples, peaks attributed to C=O of an acid/amide group could be observed. The coexistence of primary and secondary amines in the aminosilane suggests a cooperative intramolecular degradation pathway, with the secondary amine contributing significantly to the degradation process.

Didas et al.<sup>307</sup> further investigated the oxidative stability of single primary amine aminosilanes, focusing on the influence of linker length on stability by grafting aminomethyltriethoxysilane, 2-aminoethyltrimethoxysilane, and APTMS onto SBA-15. While the sample with methyl amine functionality was thermally unstable, adsorbents grafted with aminosilanes bearing ethyl and propyl linker showed a great oxidative stability. To elucidate the effect of aminosilane structure and spacer length between amine groups on CO<sub>2</sub> capture and oxidative stability, Yoo et al.<sup>177</sup> prepared a series of adsorbents by grafting different linear and branched aminosilanes composed of primary, secondary, and tertiary amine groups onto SBA-15. The stability of the adsorbents was defined to be as follows: APTMS > L-propyl (3-(2-aminopropylamino)-propyltrimethoxysilane) > B-propyl (*N*<sup>1</sup>-(3-aminopropyl)-*N*<sup>1</sup>-(3-(triethoxysilyl)propyl)propane-1,3-diamine) > B-ethyl (*N*<sup>1</sup>-(2-aminoethyl)-*N*<sup>1</sup>-(3-(triethoxysilyl)propyl)ethane-1,2-diamine) > DI (referred to as L-ethyl in their article). The authors showed that the  $\alpha$ C-H bond dissociation energy (BDE) near primary amines increases with the alkyl chain length, resulting in a stronger  $\alpha$ C-H bond on the propyl linker compared to the ethyl linker. Conversely, the  $\alpha$ C-H BDE of

secondary and tertiary amines was lower than that of primary amines. As the alkyl chain increased near the secondary amines, the  $\alpha$ C-H BDE also increased slightly, whereas the opposite trend was observed for  $\alpha$ C-H BDE near the tertiary amine. This explained the greater oxidation resistance of the L-propyl material compared to the B-propyl, while the B-ethyl was more stable than the L-ethyl under the selected oxidation conditions.

The majority of studies on oxidative stability have employed continuous exposure to elevated temperatures in the presence of O<sub>2</sub> or TSA cyclic tests. In contrast, Gebald et al.<sup>181</sup> investigated AEAPDMS (*N*-(2-aminoethyl)-3-aminopropylmethyl-dimethoxysilane)-functionalized NFC over 100 TVSA cycles, which exhibited only a slight decline in capacity. The formation of amide/imide species was observed in XPS and FT-IR results. Residual oxygen in the desorption chamber after evacuation or minor leaks were believed to contribute to the formation of these components. On the other hand, no nitrile/imine formation occurred. Furthermore, in this study, consistent with observations for impregnated adsorbents, a more pronounced capacity decline was observed under humid conditions, which was attributed to the cleavage of aminosilane moieties and the formation of amide/imide and nitrile/imine groups.

**4.1.3. Amine-Functionalized MOFs.** In contrast to other amine-loaded porous adsorbents, the oxidative stability of amine-functionalized MOFs has not been extensively studied. Siegelman et al.<sup>200</sup> investigated the oxidative stability of the cyclic diamine-functionalized framework 2-(aminomethyl)-piperidine-Mg<sub>2</sub>(dobpdc) (2-ampd-Mg<sub>2</sub>(dobpdc)), and observed negligible loss in CO<sub>2</sub> adsorption capacity after exposure to a gas stream containing 21% O<sub>2</sub> at 100 °C for 5 h. Spectroscopic analysis using <sup>1</sup>H NMR and IR revealed no detectable oxidation-derived degradation products. The observed oxidative resistance is related to the spatial distribution of amine functionalities within the structure. Metal centers are separated by approximately 7 Å along the pore channels, which prevents oxidative interactions between adjacent amine groups. Furthermore, postsynthetically grafted Mg<sub>2</sub>(dobpdc) frameworks functionalized with 1,1-dimethylethylenediamine (den) and *N*-ethylethylenediamine (een) (branched primary and primary-secondary diamines, respectively) exhibited high oxidative stability, maintaining more than 95% of their initial CO<sub>2</sub> uptake after 20 cycles under a gas stream containing 5% O<sub>2</sub> (15/5/80% CO<sub>2</sub>/O<sub>2</sub>/N<sub>2</sub>).<sup>189,190</sup>

Recently, Xiong et al.<sup>308</sup> investigated the oxidative degradation behavior of een-functionalized Mg<sub>2</sub>(dobpdc) (referred to as e-2-Mg<sub>2</sub>(dobpdc) in their study). The material exhibited CO<sub>2</sub> capacity loss under both prolonged oxidative exposure (dry air at 25 °C for 60 days) and accelerated oxidation conditions (dry O<sub>2</sub> at atmospheric pressure and 100 °C for 5-15 days). Comprehensive characterization demonstrated that oxidative degradation predominantly affects the appended diamine rather than the host framework: while significant diamine decomposition was observed, the Mg<sub>2</sub>(dobpdc) framework retained its structural integrity, as evidenced by unchanged powder X-ray diffraction (PXRD) patterns, preserved surface areas, consistent high-angle annular dark-field scanning transmission electron microscopy (HAADF-STEM) morphology, and identical aromatic resonances in the <sup>13</sup>C solid-state NMR spectra of pristine and oxidized samples. <sup>1</sup>H NMR analysis of acid-digested materials further confirmed diamine degradation. To elucidate the role of amine structure, additional diamines were examined, identifying *N,N*-dimethylethylenediamine (mm-2) as the most oxidatively robust. It exhibited minimal capacity loss and the lowest degree of amine degradation under accelerated oxidative conditions. This enhanced stability was attributed to the suppression of N-centered radical formation at the tertiary amine site of mm-2. Mechanistic investigations established that diamine oxidation proceeds via radical-mediated C-N bond cleavage, with computational analysis supporting initiation by hydroxyl radicals, likely generated

from trace metal impurities, followed by formation of C-centered radicals, O<sub>2</sub> addition, and rate-limiting O-O bond cleavage. Oxidative byproducts, including acetaldehyde, ethylamine, and other aldehyde- and imine-containing species, were identified using gas chromatography—mass spectrometry (GC-MS) and <sup>13</sup>C solid-state NMR. These findings provide valuable molecular-level design principles for improving oxidative resistance in amine-appended MOFs; however, further systematic oxidative stability investigations across diverse amine chemistries are needed to fully elucidate degradation mechanisms. In parallel, continued efforts are required to enhance CO<sub>2</sub> adsorption capacity and working efficiency of MOFs under the dilute conditions relevant to DAC. Finally, given the simultaneous presence of moisture and oxygen in ambient air, future studies must address their combined impact on both framework robustness and amine stability in amine-appended MOFs.

**4.1.4. Amine-Functionalized COFs.** The cyclic stability of COF-999 was evaluated under a synthetic air stream containing O<sub>2</sub> and 400 ppm of CO<sub>2</sub> at 25 °C and 50% RH, followed by regeneration under N<sub>2</sub> at 60 °C. In these conditions, COF-999 exhibited stable CO<sub>2</sub> uptake over 10 adsorption—desorption cycles.<sup>145</sup> Similarly, COF-709 was subjected to the same cycling protocol, except that a higher RH of 75% was employed during the adsorption step, and demonstrated stable performance over 10 cycles.<sup>196</sup> To further assess long-term stability, COF-999 was evaluated under outdoor air conditions in Berkeley (United States) over a 20 day period, 100 adsorption—desorption cycles, with ambient CO<sub>2</sub> concentrations ranging from 410 to 517 ppm. Throughout this extended cycling test, COF-999 maintained stable capture performance, exhibiting productivity between 1.03 and 1.48 mmol/g. No significant changes were observed in the CO<sub>2</sub> adsorption isotherms following the cyclic testing, and characterization by FT-IR and scanning electron microscope (SEM) confirmed retention of the framework structure.<sup>145</sup> While these results demonstrate excellent oxidative stability over 100 cycles, practical DAC deployment requires materials to withstand thousands of cycles; therefore, accelerated oxidative aging and longer-term cycling tests are essential to comprehensively evaluate the durability of this material.

**4.1.5. Commercial Adsorbents.** The oxidative stability of Lewatit has been evaluated by Yu et al.,<sup>266</sup> who investigated the impact of temperature and oxygen concentration. A continuous dry air exposure over 72 h resulted in a 30% to 80% reduction in CO<sub>2</sub> capture capacity as temperature increased from 50 to 120 °C, with the most significant degradation occurring above 80 °C. Reducing the O<sub>2</sub> concentration from 21 to 12% improved the oxidative stability. For the degraded sample at 120 °C, EA showed a 23% reduction in nitrogen, and the FT-IR spectra of the treated material exhibited formation of amide species. In addition to chemical degradation, the authors reported slight morphological changes, evidenced by variations in surface area, pore volume, and pore size as determined by Brunauer-Emmett-Teller (BET) and Barrett-Joyner—Halenda (BJH) analyses, which contributed to the observed reduction in adsorbent capacity. By contrast, a slight improvement in adsorbent stability under humid conditions relative to dry conditions was observed, which was attributed to the rapid formation of carbamate and bicarbonate species that partially suppressed oxidative degradation of the amine functionalities. Moreover, the adsorbent did not undergo any substantial oxidative degradation when stored in ambient air for three months. Hunt et al.<sup>265</sup> developed an in-house system comprised of automated reaction cells to test the cyclic oxidative stability of Lewatit over multiple cycles under air flow. The adsorbent experienced a 31.2% capacity loss after 180 cycles, which was linked to both oxidative and CO<sub>2</sub>-induced degradation mechanisms. However, the individual contributions of these mechanisms to the capacity loss and stability analysis were not determined.

Elfving et al.<sup>268</sup> also evaluated a proprietary aminoresin under TVSA cycles to assess the influence of

regeneration conditions on adsorbent stability. Cyclic TVSA tests with regeneration at 100 °C under compressed air resulted in a 13% capacity loss over 22 cycles, whereas regeneration at 60 °C led to a smaller 6% decrease over the same number of cycles. However, the working capacity was less than 10% lower than that achieved at a higher temperature due to incomplete desorption. In 23 closed TVSA cycles at 100 °C (without air flow), an 8% decline in CO<sub>2</sub> uptake was observed. Nevertheless, similar to the study of Gebald et al.,<sup>181</sup> it remained unclear whether the capacity loss was caused by oxidative degradation from residual O<sub>2</sub> in the bed or by thermal degradation. In addition, Elfving and coauthors noted that the trend of capacity decline in their study could not be clearly established, whether it was linear, plateaued after a certain number of cycles, or accelerated over time, and highlighted the complexity of degradation under inert or vacuum conditions, where factors such as vacuum pressure and regeneration temperature may also contribute to capacity loss.

## 4.2 SUMMARY

Inorganic materials and physisorbents, which do not contain organic amine groups, generally exhibit high oxidative stability, whereas amine-functionalized adsorbents are far more prone to oxidative degradation. The oxidative stability of amine-based adsorbents is significantly influenced by operational parameters such as temperature and oxygen concentration. For amine-appended MOFs, oxidative stability has similarly been shown to depend strongly on the incorporated amine, whereas COFs have demonstrated encouraging resistance to oxidative degradation in the limited number of studies reported to date. Among impregnated systems, increasing the amine loading beyond a certain level has been found to negatively affect oxidative stability. While higher amine loading initially increases O<sub>2</sub> diffusion resistance and enhances oxidative stability, exceeding a certain limit can ease the availability of amine sites to react with oxygen. Aminopolymers with a greater Mw have been shown to enhance oxidative stability, primarily due to increased polymer viscosity, which hinders oxygen diffusion. Similarly, longer amine chain lengths of amine molecules contribute to higher viscosity and improved resistance to oxidative degradation.

Based on the available literature, no clear conclusion can yet be drawn regarding the impact of different synthesis methods

on the oxidative stability of amine-based adsorbents. However, it is evident that the chemical structure of the amine plays a key role in determining oxidative resistance, with different amines exhibiting varying degrees of stability. While earlier works suggested that secondary amines were inherently more susceptible to degradation, more recent findings suggest that the oxidative behavior is highly dependent on the combined effects of amine type, molecular architecture, and proximity of functional groups. For example, although propylene linkers have generally shown better oxidative stability than ethylene linkers, this trend does not hold in phenyl-based structures, where spacer type has minimal impact.

Oxidative degradation typically leads to a decline in CO<sub>2</sub> uptake capacity due to the formation of less basic degradation products, such as amides, imides, nitriles, and imines, as well as volatile byproducts like ammonia. The oxidation mechanism generally follows a radical-induced autoxidation pathway and is exacerbated by the presence of metal impurities in the adsorbent. Notably, cleavage of terminal C-N bonds near primary amines has been identified as a key pathway for sorbent deactivation. Water can further accelerate oxidation, particularly in alumina-supported systems due to their greater hydrophilicity, while low concentrations of CO<sub>2</sub> also promote degradation. To mitigate oxidative degradation, several strategies have been explored, including the use of oxidation inhibitors, radical scavengers, and chelating agents,

along with heteroatom modification of the support material, the incorporation of hydrogen-bonding polymers, and chemical alteration of amine groups. Nevertheless, important gaps remain in the literature, particularly concerning the oxidative stability of in situ polymerized adsorbents and systematic comparisons across different support materials bearing amine functionalities.

## 5. HYDRO(THERMAL) STABILITY

The presence of water vapor in ambient air is unavoidable and can play a critical role in determining both the adsorption performance and stability of solid adsorbents. While humidity has been shown to enhance the CO<sub>2</sub> adsorption capacity of amine-based adsorbents,<sup>128,309</sup> it can adversely impact the capture performance of physisorbents and induce degradation in certain zeolites and MOFs.<sup>310</sup> To evaluate hydro stability, adsorbents are typically subjected to humidified gas flow under adsorption conditions, followed by regeneration, usually under dry conditions, and structural changes as well as capacity loss are assessed over multiple adsorption—desorption cycles. Alternatively, sorbents can be exposed to a humidified gas stream for a predetermined duration to monitor structural and performance changes. Complementary to hydro stability, hydrothermal stability is assessed either by directly exposing the adsorbent to steam or by placing it in a vessel (e.g., autoclave) containing water and applying elevated temperatures. This is followed by an analysis of changes in the physicochemical properties of the adsorbent after treatment. The experimental conditions are presented in detail in Table S3 of the Supporting Information.

It should be noted that not all adsorbent classes have been systematically evaluated under both hydro and hydrothermal conditions, as water sensitivity can limit their suitability for steam-assisted regeneration. This section begins with the hydro stability of physisorbents, particularly zeolites and MOFs, for which hydrothermal stability under direct steam exposure has not been reported. For conventional amine-based adsorbents, studies have focused primarily on hydrothermal stability, while hydro stability under humid air has not been comprehensively examined, as degradation is often dominated by amine leaching and support degradation during steam exposure. The section then addresses the hydro stability of amine-functionalized MOFs and COFs, for which hydrothermal data are currently lacking, followed by a brief overview of commercial adsorbents. Finally, carbonate-based materials are discussed under humid conditions due to the lack of hydrothermal stability data.

### 4.2 PHYSISORBENTS (PHYSISORPTION MATERIALS)

**4.1.6. Zeolites.** Humidity negatively impacts CO<sub>2</sub> capture by zeolites as water competes with CO<sub>2</sub> for the same adsorption sites. Moreover, zeolites typically used for carbon capture have low Si/Al ratios and are prone to hydrolysis under moist conditions,<sup>56</sup> necessitating upstream drying of the gas stream, including in DAC systems.<sup>57,58,63</sup> Nevertheless, incomplete drying may allow trace moisture to accumulate in the adsorbent over successive cycles, potentially leading to a gradual decline in CO<sub>2</sub> uptake; however, the extent of this effect and its reversibility require further experimental investigation. Lyadov and Lusardi<sup>64</sup> investigated water coadsorption in zeolite 13X and potassium-exchanged merlinoite (K-MER, Si/Al = 3.6) under 400 ppm of CO<sub>2</sub>. After five cycles at 5% RH, K-MER exhibited a 27% reduction relative to its dry CO<sub>2</sub> capacity, whereas zeolite 13X experienced a substantially larger loss of 53%. The superior moisture tolerance of K-MER was attributed to weaker interactions with adsorbed species and

predominantly physisorbed CO<sub>2</sub> and H<sub>2</sub>O, as evidenced by DRIFTS analysis. These weaker interactions were associated with differences in framework Si/Al ratio and charge-balancing cations (Na<sup>+</sup> vs K<sup>+</sup>), with zeolite topology identified as the dominant factor.

**4.1.7. Carbonaceous Adsorbents.** As mentioned in Section 2, humidity has a negative effect on the performance of carbonaceous adsorbents, primarily due to their low CO<sub>2</sub> selectivity relative to N<sub>2</sub> and H<sub>2</sub>O. In addition, their low adsorption capacity at dilute CO<sub>2</sub> concentrations further limits their DAC applicability. For instance, a carbon monolith developed by Lee et al.<sup>311</sup> exhibited a CO<sub>2</sub> uptake of only 0.00137 mmol/g at 3000 ppm, while unfunctionalized activated carbon fibers evaluated by Korah et al.<sup>312</sup> showed no measurable CO<sub>2</sub> capacity under DAC-relevant conditions.

**4.1.8. Metal-Organic Frameworks (MOFs).** In the presence of humidity, MOFs with open metal sites commonly experience a decline in CO<sub>2</sub> adsorption capacity as water molecules competitively coordinate to the unsaturated metal centers.<sup>313</sup> Furthermore, water can also coordinate with metal ions in the framework, breaking metal—ligand bonds and leading to reduced crystallinity and porosity.<sup>79</sup> The susceptibility of these exposed sites to H<sub>2</sub>O adsorption further limits the use of such materials in DAC applications. Mg-MOF-74 evaluated under humid conditions showed a significant decrease in capacity, losing approximately 50% of its CO<sub>2</sub> uptake by the second cycle.<sup>142</sup> In another study, Mg-MOF-74 was exposed to 40 °C and 75% RH, which exhibited pronounced capacity loss of 68% after 14 days.<sup>83</sup> The mechanistic aspects of hydro stability and degradation in the MOF-74 series have been widely reported in the liter- 314,315 ature.<sup>34,35</sup>

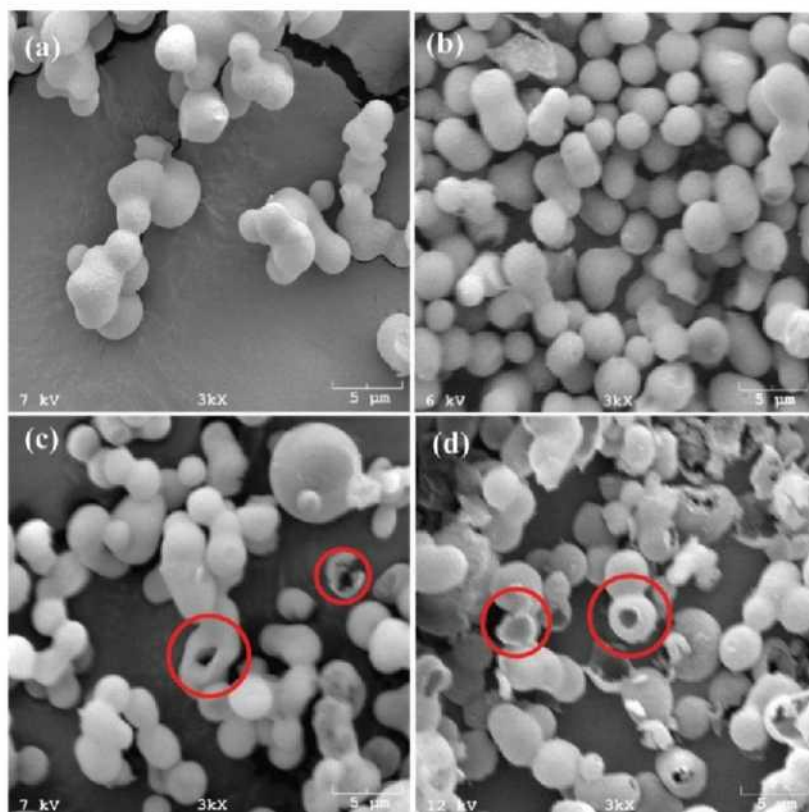
Recent studies indicate that the hydro stability of MOFs can be enhanced through thermodynamic strategies, such as strengthening metal—ligand coordination and increasing

framework rigidity, and kinetic approaches, including hydrophobic ligand incorporation, postsynthetic hydrophobic modification (e.g., introduction of hydrophobic groups within the pores or application of hydrophobic surface coatings), and increased steric hindrance around metal nodes, all of which suppress water diffusion and hydrolysis.<sup>313,316</sup> In addition to these approaches, core-shell MOF architectures based on Zr- based frameworks such as UiO-66 and UiO-67 have been reported for DAC applications. In these materials, the core has strong affinity for CO<sub>2</sub>, while the hydrophobic shell protects 317,318 the core from water exposure.

Despite their high CO<sub>2</sub> uptake under dry conditions, the performance of SIFSIX and TIFSIX materials declines in humid environments. Barsoum et al.<sup>100</sup> employed single-crystal X-ray diffraction (SCXRD) to define the symmetry of SIFSIX-3-Ni crystals and examined how H<sub>2</sub>O and CO<sub>2</sub> molecules occupy the crystal framework during competitive gas adsorption. The authors reported that, over time, SiF<sub>6</sub><sup>2-</sup> units move into the material pores, blocking CO<sub>2</sub> adsorption sites and lowering the capture efficiency. As water forms hydrogen bonds with SiF<sub>6</sub><sup>2-</sup> and coordinates strongly to the metal sites, its removal is challenging, necessitating prolonged heating to nearly fully restore the material. In addition, following accelerated humid tests, the adsorbent could not be fully regenerated due to partial degradation of the porous structure, leading to the formation of small, single-layer nanosheets of edge-sharing nickel oxide octahedra. TIFSIX-3-Ni, characterized by Low et al.,<sup>99</sup> exhibited relatively good stability under humid conditions at 25 °C. However, reduced stability was observed at 45 °C, and in a separate long-term test involving 50 cycles in ambient air with varying humidity, the material underwent significant degradation, with losses in porosity, crystallinity, and CO<sub>2</sub> uptake accompanied by visible color changes.

By contrast, NbOFFIVE-1-Ni exhibits remarkable resistance to humidity, as demonstrated by variable-humidity PXRD, water adsorption measurements, prolonged immersion in liquid water, and dynamic breakthrough experiments under humid conditions, all of which confirm the preservation of crystallinity and CO<sub>2</sub> capture performance. The superior water stability of NbOFFIVE-1-Ni relative to other fluoride-based MOFs has been attributed to the nucleophilic character of the (NbOF<sub>5</sub>)<sup>2-</sup> inorganic pillar.<sup>98</sup> Consequently, this class of MOFs is a promising design basis for developing nextgeneration DAC adsorbents through further structural and chemical optimization.

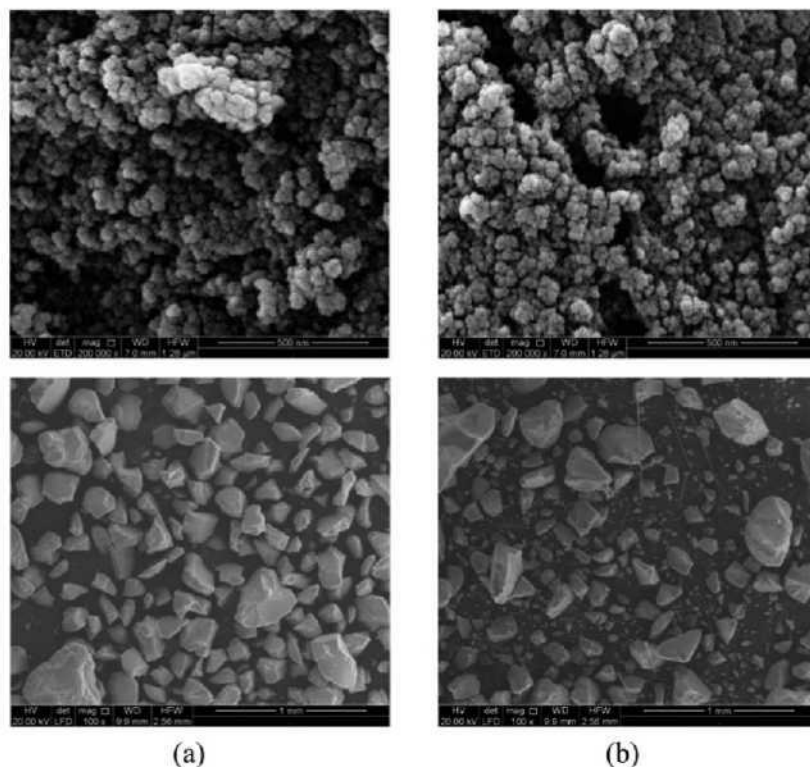
**Figure 22.** Scanning electron microscope (SEM) images of MCF support particles: (a) before treatment and after steam/air exposure at (b) 106 °C, (c) 120 °C, and (d) 180 °C. Reproduced from ref 320. Copyright 2010 American Chemical Society.



## 5.2 CHEMISORBENTS (CHEMISORPTION MATERIALS)

**5.2.1. Amine-Functionalized Adsorbents.** Despite the beneficial effect of humidity on CO<sub>2</sub> capture in amine-based adsorbents, their use, particularly impregnated samples, for DAC from humid air may lead to material degradation due to amine hydrolysis or leaching. However, to the best of the authors' knowledge, no detailed studies have specifically investigated this issue, with most research instead focusing on hydrothermal stability under steam exposure. As noted previously, steam-assisted regeneration methods, such as S-TSA and S-TVSA, have been implemented because steam provides an efficient heat source, serves as an effective purge gas, and enables straightforward separation of H<sub>2</sub>O and CO<sub>2</sub> after regeneration.<sup>30</sup> Nevertheless, since exposure to steam can cause adsorbent degradation, evaluating material stability under these conditions is essential. In the following, steam-treated amine-based adsorbents are compared, emphasizing the critical impact of the choice of support materials on hydrothermal stability. In addition, despite the limited number of published studies, the hydro stability of Lewatit under humidified conditions is briefly reviewed.

**Figure 23.** SEM images of SiO<sub>2</sub>: (a) fresh, (b) steam-treated. Top row: magnification 200,000×; bottom row: magnification 100×. Reproduced with permission from ref 324. Copyright 2013 American Chemical Society.



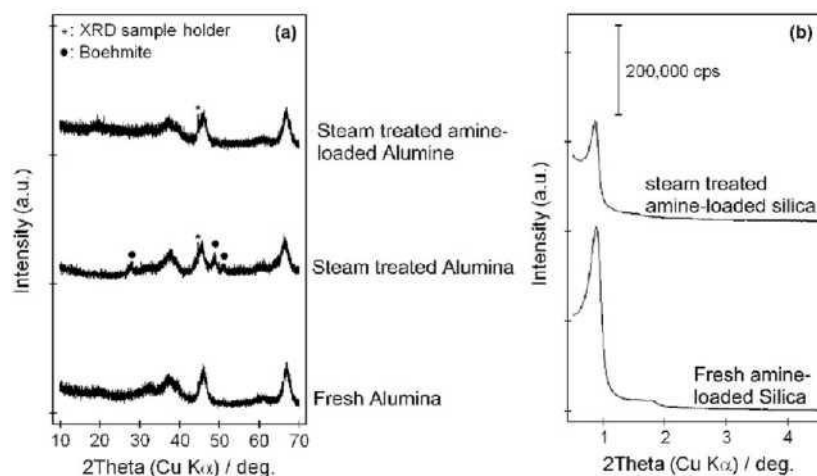
**5.2.1.1. Impregnation.** The high temperature and reactive nature of steam can affect porous materials differently, potentially causing structural changes based on the properties of material. Therefore, this section separately examines silica and alumina supports, which are the most commonly used carrier materials for amine-based adsorbents. Furthermore, it is important to note that the hydrothermal stability of an aminebased adsorbent might be influenced by two key factors: (1) the steam resistance of the bare support and (2) the stability of the amine-loaded material when exposed to steam.

From a structural standpoint, pore-wall thickness plays a key role in the hydrothermal stability of silica supports. Mesoporous silicas with thin pore walls, such as MSF and MCM-41, are therefore more susceptible to hydrothermal degradation.<sup>319</sup> Li et al.<sup>320</sup> investigated the hydrothermal stability of bare MCF, another thin-walled mesoporous silica, under air/steam and N<sub>2</sub>/steam gas mixtures at 106-180 °C in an autoclave for 24 h. The mesoporous structure of the steam- treated MCF collapsed, showing an increase in pore and window size, along with a reduction in BET surface area and pore volume. The instability of the material intensified with exposure to higher temperatures, resulting in complete structural collapse at 180 °C under steam/air conditions, as shown in the SEM images (Figure 22). The silica material exhibited similar structural collapse regardless of the presence or absence of oxygen, indicating that oxygen does not affect its stability under steam. Al-Absi et al.<sup>183</sup> assessed the hydrothermal stability of MSF by exposing the material to water at 110 °C for 3 days in an autoclave. BET surface area and pore volume decreased by about 50% and 25%, respectively, and SEM images revealed a structural collapse of the MSF support, attributed to the hydrolysis of siloxane bridges. Mechanistically, structural collapse of silica can occur upon exposure to liquids, either during direct contact or during the subsequent drying phase. Collapse during liquid exposure is influenced by the nature of both the liquid and the solid, as well as their interactions, while collapse during drying is primarily attributed to capillary forces within the porous structure. In the constant-rate drying phase, high liquid tension, especially due to the high surface tension of water, can

generate internal pressures of several hundred bars. These stresses compress the silica framework, leading to pore shrinkage and structural degradation.<sup>321</sup> MCM-41 synthesized by Tompkins and Mokaya<sup>319</sup> exhibited a substantial reduction in surface area, approximately 93% (from 958 to 69 m<sup>2</sup>/g), after undergoing steam treatment, which involved heating the samples at 900 °C for 4 h in a tube furnace under an N<sub>2</sub> flow saturated with water vapor at room temperature. By contrast, large-pore MCM-41 examined by Jahandar Lashaki et al.<sup>322</sup> experienced about a 5% loss in surface area after 24 h of steam exposure at 120 °C, which can be attributed to the milder experimental conditions used in this study.

On the other hand, silica supports with thicker pore walls, such as SBA-15, exhibit improved tolerance to steam exposure. Bare SBA-15 tested by Chaikittisilp et al.<sup>243</sup> maintained its structural integrity after exposure to steam at 105 °C for 24 h, showing a 27.9% reduction in BET surface area but no observable morphological changes in SEM images. Similarly, Jahandar Lashaki et al.<sup>323</sup> reported acceptable hydrothermal stability of bare SBA-15 under steam treatment at 120 °C for 24 h, with only a 7% decrease in BET surface area. Some commercial silica supports have also demonstrated stability under hydrothermal treatment. For example, CARiACT G-10 was exposed to a 90 vol % H<sub>2</sub>O/He mixture at 105 °C for 5 h, and no significant morphological changes were observed in SEM images (Figure 23).<sup>324</sup> Furthermore, the BET surface areas of the steam-treated and fresh samples remained comparable. This superior hydrothermal stability was attributed to the thicker pore walls of the silica material.

**Figure 24.** PXRD patterns of (left) fresh, steam-treated, and steam treated amine-loaded alumina; (right) fresh and steam treated amine loaded silica that shows a decline in peak intensity due to mesostructure collapse following steam treatment. Reproduced from ref 243. Copyright 2011 American Chemical Society.



Nevertheless, extended exposure to steam can lead to structural destruction even in silica supports with comparatively thick pore walls. Min et al.<sup>325</sup> investigated the hydrothermal stability of macroporous silica (MacS) and three types of mesoporous silica (MCF, SBA-15, and MCM-41) under prolonged steam exposure at an elevated temperature of 120 °C for 14 days. While the BET surface area of MacS decreased only modestly, by 13% after treatment, the mesoporous silicas exhibited a substantial decline, with surface area reductions exceeding 70% over the same period. The greater stability of MacS was attributed to its thicker pore walls compared to those of the mesoporous silicas. Although the fresh MacS initially exhibited lower surface area and pore volume, it retained the highest value among the tested materials after 14

days of steam treatment, underscoring its potential suitability for steam-assisted applications. Moreover, these findings suggest that the process conditions employed during regeneration (such as temperature of steam) are critical in determining the appropriate support material for ensuring long-term adsorbent stability.

The hydrothermal stability of silica supports can be improved through two main strategies: (i) the addition of different salts to the synthesis gel prior to hydrothermal synthesis,<sup>326,327</sup> and (ii) extending the hydrothermal synthesis duration or crystallization time and/or increasing the temperature,<sup>328,329</sup> with the latter method increasing the thickness of the pore walls.<sup>319,330</sup> Tompkins and Mokaya<sup>319</sup> enhanced the hydrothermal stability of MCM-41 by introducing trace amounts of aluminum through dry grafting method. Resulted Al-incorporated MCM-41 aluminosilicate materials exhibited similar X-ray diffraction (XRD) patterns before and after hydrothermal treatment at 900 °C for 4 h, suggesting enhanced structural stability compared to the undoped support. Using a one-pot synthesis method, Jahandar Lashaki et al.<sup>322</sup> incorporated aluminum into large pore MCM-41 silica

(Al-MCM-41) and observed only a  $\approx$ 5% decrease in surface area and a  $\approx$ 3% reduction in pore volume after 24 h of steam exposure at 120 °C. Similarly, Al-Absi et al.<sup>183</sup> reported that the LPAlSi support exhibited less than a 15% decrease in surface area and pore volume after 3 days of exposure to hot water at 110 °C. This enhanced stability was attributed to the incorporation of aluminum atoms into the silica framework in tetrahedral coordination, which remained intact following hot water treatment.

In contrast to studies linking capacity loss to the poor hydrothermal stability of silica supports,<sup>320</sup> other works have explored the underlying reasons for uptake decline in systems utilizing more stable silica materials. Chaikittisilp et al.<sup>243</sup> examined the effect of steam on PEI-impregnated SBA-15, observing a 67.1% reduction in CO<sub>2</sub> capacity and over 80% loss in pore volume. Based on SEM images and the diminished XRD peaks of the steam-treated support, these losses were attributed to partial restructuring of the silica framework and surface coverage by amines leached from the pores, making the material nonporous. In a previously cited study, Min et al.<sup>325</sup> also assessed the hydrothermal stability of PEI-impregnated macroporous and mesoporous silica supports. After 14 days of steam exposure at 120 °C, the PEI-impregnated MacS exhibited only a 10% reduction in CO<sub>2</sub> uptake, attributed to the thick pore walls of the support. In contrast, the capture capacities of PEI-loaded MCM-41, SBA-15, and MCF decreased by 61%, 50%, and 42%, respectively. This decline was primarily associated with increased PEI leaching, as degradation of the silica pore structure allowed the aminopolymer to migrate out of the pores, increasing its susceptibility to removal.

Hammache et al.<sup>324</sup> prepared PEI-impregnated CARiACT silica adsorbents and a silanated variant by mixing PEI with APTES. After 6 steam-assisted cycles at 105 °C, the PEI-impregnated and silane-functionalized materials exhibited CO<sub>2</sub> capacity losses of 12% and 10%, respectively. Although the incorporation of aminosilane did not improve hydrothermal stability, the silanated adsorbent exhibited a slightly higher cyclic capture capacity, which was attributed to a more uniform distribution of PEI facilitated by silane incorporation. Subjecting the samples to the same number of cycles with steam alone, in the absence of CO<sub>2</sub> adsorption, resulted in

comparable capacity losses. By contrast, continuous exposure to steam at 105 °C for 5 h led to only a 3% decrease in CO<sub>2</sub> uptake. The authors therefore hypothesized that much of the degradation observed during cyclic operation originates from the drying step, in which residual steam is purged from the bed with He at 105 °C. The reduced capacity observed in the cyclic experiment of the PEI-impregnated sample was

attributed to reaggregation of amine groups, which partially blocked the support pores. In contrast, the capacity loss of the silanated adsorbent was ascribed to steam-induced reactions between PEI and the silane additive, leading to the loss of active CO<sub>2</sub> adsorption sites. Sandhu et al.<sup>228</sup> (2016) reported less than a 10% decrease in capture capacity for PEI-impregnated CARIACT after 20 steam-assisted cycles at 110 °C, corresponding to a total steam contact time of 3.3 h, compared with only a 5% loss under continuous steam exposure for 5 h. The authors proposed that the greater capacity decline observed in the cyclic test primarily resulted from thermal degradation during the drying step, in which N<sub>2</sub> stripping followed steam regeneration. Furthermore, EA and DRIFTS measurements of steam-treated samples showed no evidence of amine leaching or chemical degradation.

As previously discussed, the reduced stability of amine-based adsorbents under steam exposure is often linked to the choice of support material. Unlike silica,  $\gamma$ -alumina demonstrates greater stability during steam treatment. In fact, steam-treated alumina showed an increase in both BET surface area and mesoporous diameter.<sup>243</sup> This increase was attributed to the formation of boehmite particles on the  $\gamma$ -alumina surface through hydration, as confirmed by XRD analysis (Figure 24). Based on the observed hydrothermal stability of alumina, Chaikittisilp et al.<sup>243</sup> investigated the performance of PEI-impregnated  $\gamma$ -Al<sub>2</sub>O<sub>3</sub> and SBA-15 under direct steam exposure. Following steam treatment, the adsorption capacity decreased by about 16% at 400 ppm and 20% at 10% CO<sub>2</sub>, which was attributed to porosity loss during steam exposure and potential oxidative degradation of the amines due to residual oxygen in the N<sub>2</sub>-purged autoclave.

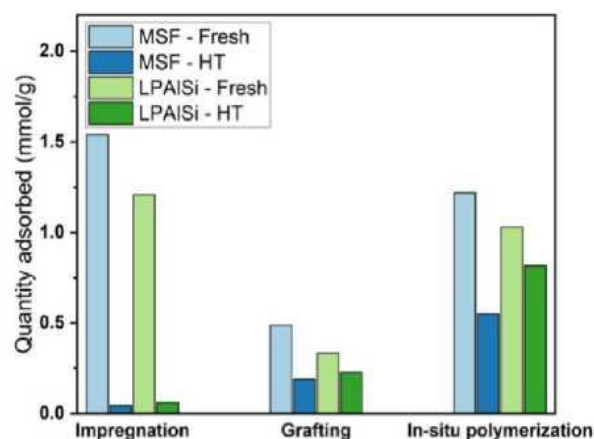
The effect of boehmite, formed by the hydrolysis of  $\gamma$ -alumina, on the CO<sub>2</sub> uptake of the PEI-impregnated sample was also investigated. Sakwa-Novak and Jones<sup>331</sup> evaluated bPEI-impregnated  $\gamma$ -Al<sub>2</sub>O<sub>3</sub> under 400 ppm of CO<sub>2</sub> following a 5 min steam treatment and observed a 15% increase in capture capacity. This enhancement was attributed to the formation of a boehmite phase through surface hydration during steam exposure, accompanied by a reduction in surface acidity that promoted the reagglomeration of PEI within the pores. Overall, no capacity loss was noted during cyclic testing or short-term steam exposure, indicating that boehmite formation has a negligible adverse effect on the CO<sub>2</sub> uptake of the steam-treated adsorbent.

**5.2.1.2. Grafting.** In addition to studies on impregnated sorbents, researchers have also explored the hydrothermal stability of silica-based grafted adsorbents, stressing the similarly important role of the support material. Jahandar Lashaki et al.<sup>323</sup> grafted TRI onto SBA-15 and tested the material over two steam-assisted cycles of 3 h each. The treatment led to a slight decrease in CO<sub>2</sub> uptake, amine efficiency, and adsorption kinetics, while the BET surface area of the grafted samples declined significantly (21-37%). Based on changes in the pore size distribution of the calcined grafted samples before and after single steam stripping cycle, the performance decline was attributed to amine restructuring within the pores, which introduced diffusional limitations in the adsorbent. In a separate study, Jahandar Lashaki et al.<sup>322</sup> reported that TRI grafted onto large pore Al-MCM-41 exhibited higher CO<sub>2</sub> capture capacity and faster adsorption kinetics at 25 °C, along with improved hydrothermal stability under steam exposure compared with large-pore undoped MCM-41-supported samples. Additionally, while the BET surface area of grafted MCM-41 silica declined by 36-49% after steam exposure, the triamine-grafted aluminosilicate exhibited a smaller reduction of 31-35%, highlighting the beneficial effect of aluminum incorporation on both the performance and stability of silica-supported amine adsorbents.

Li et al.<sup>320</sup> investigated the hydrothermal stability of a series of amine-functionalized MCF adsorbents exposed to steam at different temperatures in an autoclave under both steam/air and steam/N<sub>2</sub>

atmospheres. All amine-functionalized adsorbents experienced capacity and apparent mass loss due to the deterioration of silica support and amine degradation. Greater mass loss was observed under steam/air conditions, indicating that oxidative degradation occurred in parallel to hydrothermal degradation. Among the materials examined, the adsorbent prepared via in situ polymerization of aziridine showed the highest stability, followed by the IPEI-impregnated sample, whereas the APTMS- and AEAPTMS-grafted sorbents were the least stable. Since the amine functionalities employed differ substantially in chemical structure, direct comparison of hydrothermal stability across the different adsorbent classes is challenging. The superior stability of the in situ polymerized material was attributed by the authors to the presence of covalently attached aminopolymers, which were proposed to partially stabilize and protect the silica support against steam-induced collapse. Although not explicitly discussed by Li and coauthors, the relatively higher stability of the impregnated sorbent compared with grafted analogues may be attributed to a uniform distribution of IPEI within the pore network, which could partially prevent the silica surface from water. In contrast, grafted amines do not necessarily provide homogeneous surface coverage, potentially leaving the silica framework more exposed to hydrothermal attack. Furthermore, the diamine AEAPTMS is more hydrophilic than the monoamine APTMS, which may also contribute to the lower stability of the AEAPTMS-grafted material under steam exposure. Unlike the previous study, Al-Absi et al.<sup>183</sup> adopted a more controlled comparative approach by maintaining similar PEI-based amine chemistries across different adsorbent classes, enabling a systematic evaluation of the hydrothermal stability of adsorbents supported on MSF and LPAISi. All MSF-supported samples experienced significant capacity loss due to structural collapse, as previously discussed. PEI-impregnated sorbents on LPAISi also performed poorly after 3 days of hydrothermal treatment at 110 °C in an autoclave, as shown in Figure 25, primarily due to polymer leaching caused by weak physical interactions between the support and the aminopolymer. In contrast, grafted and in situ polymerized adsorbents on LPAISi exhibited improved hydrothermal stability, with the latter variant showing the most robust performance. The enhanced stability of the PEI-grafted adsorbent relative to impregnated samples observed by Al-Absi et al.<sup>183</sup> contrasts with the trend reported earlier by Li et al.,<sup>320</sup> suggesting the critical role of amine chemistry rather than grafting versus impregnation alone. In particular, the highly branched structure of PEI may enable more uniform surface coverage and improved protection of the silica framework compared with amino-silanes, thereby enhancing resistance to hydrothermal degradation.

**Figure 25.** Impact of preparation method on CO<sub>2</sub> uptake of fresh and hydrothermally treated (HT) samples (measured at 400 ppm, 20 °C). Reproduced from ref 183. Copyright 2024 American Chemical Society.



**5.2.1.3. Amine-Functionalized MOFs.** Although IRMOF-74-III-CH<sub>2</sub>NH<sub>2</sub> does not exhibit high CO<sub>2</sub> uptake at atmospheric concentrations, it demonstrates excellent framework stability and sustained CO<sub>2</sub> capture performance, as confirmed by PXRD analysis and breakthrough experiments conducted at 65% RH. These findings highlight the potential of this class of adsorbents for further investigation as promising candidates for DAC applications to increase their capture capacity. ED-loaded Mg-MOF-74, assessed by Mahajan et al.,<sup>199</sup> exhibited only a 2.7% capacity decrease over 18 cycles in dry conditions. However, the same adsorbent experienced a significant 74% capacity loss in the presence of 2 vol % humidity. PXRD and EA results revealed a reduction in crystallinity and nitrogen content of the ED-loaded sample after both dry and humid cyclic runs. In addition, FT-IR spectra showed a decline in peak intensities corresponding to the amine groups, indicating amine volatilization at temperatures above 120 °C, which was further confirmed by TGA analysis. Amine loss in dry conditions was attributed to the removal of free amines during consecutive cycles, whereas in humid conditions, stripping of ED from grafted sites by water molecules during cycling was identified as the primary cause. The substantial H<sub>2</sub>O uptake of this material further suggested that ED can dissolve in water and be removed as droplets during regeneration. Consequently, the primary limitations of ED-loaded Mg-MOF-74 for DAC include considerable water adsorption, slow CO<sub>2</sub> uptake at low temperatures, rapid capacity loss under humid conditions, and structural degradation.

The hydro stability of amine-functionalized Mg<sub>2</sub>(dobpdc) series has been assessed in multiple studies. Lee et al.<sup>142</sup> indicated that ED-Mg<sub>2</sub>(dobpdc) (referred to as en- Mg<sub>2</sub>(dobpdc) in their study) exhibited only minor reductions in CO<sub>2</sub> uptake after 5 cycles, approximately 6% under dry and 4% under humid conditions. Furthermore, comparative experiments involving exposure to saturated air at RH = 100% for 6 min, followed by regeneration at 130 °C for 4 h, demonstrated that unfunctionalized Mg-MOF-74 and Mg<sub>2</sub>(dobpdc) faced substantial capacity losses of approximately 50% and 80%, respectively. In contrast, both DMEDA- (denoted as mmen in the original work) and ED-functionalized Mg<sub>2</sub>(dobpdc) retained their CO<sub>2</sub> capture capacities, underscoring the beneficial role of amine functionalization in preserving framework integrity and adsorption performance in the presence of moisture. Similarly, McDonald et al.<sup>185</sup> reported CO<sub>2</sub> adsorption isotherms for mmen-Mg<sub>2</sub>(dobpdc) measured after exposure to water vapor at both 40 and 100 °C, observing no noticeable differences between moisture-exposed and dry samples. A similar trend has been observed for amine- encapsulated MOFs. For instance, Darunte et al.<sup>186</sup> observed that PEI-loaded MIL-101(Cr) maintained its capacity after being saturated in He flow at 32% RH, suggesting resistance to humid conditions.

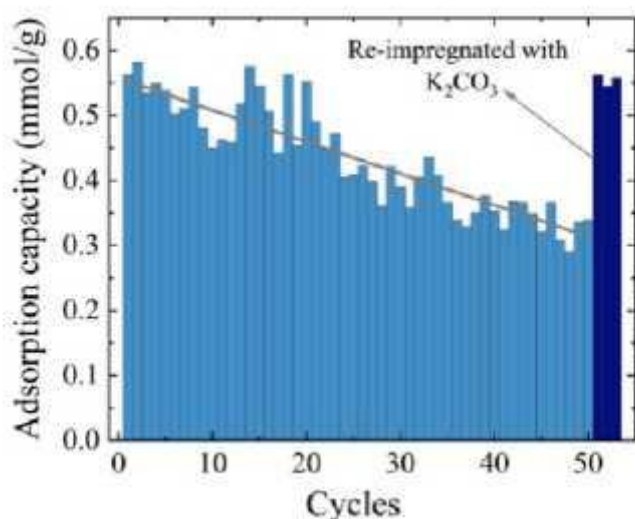
**5.2.1.4. Amine-Functionalized COFs.** In the presence of humidity, the capture performance of amine-functionalized COFs does not decline but instead increases noticeably. The CO<sub>2</sub> uptake of COF-999 more than doubled when the RH was increased to 50%, rising from 0.85 to 2.05 mmol/g.<sup>145</sup> This enhancement is attributed to the presence of amine functionalities within the framework, which promoted the formation of carbamate and bicarbonate species. Similarly, the CO<sub>2</sub> capture capacity of COF-709 increased by more than 2.5- fold upon increasing the RH to 70%, from 0.48 to 1.24 mmol/ g.<sup>196</sup> In addition, relatively low water uptake was observed, with values of 0.09 g<sub>water</sub>/g<sub>COF</sub> for COF-999 at 50% RH and 0.13 g<sub>water</sub>/g<sub>COF</sub> for COF-709 at 75% RH. This behavior is associated with the employment of hydrophobic building units that limit water adsorption.<sup>145,196</sup> In the case of COF-709, the polyamine bPEI is covalently attached to the framework through C-S bonds formed via aromatic nucleophilic substitution, further contributing to its stability.<sup>196</sup> The hydro stability of both COFs is also supported by stable performance during repeated humid cycling tests, as discussed previously. Taken together, the high CO<sub>2</sub>

capture capacity under atmospheric conditions, combined with favorable thermal, oxidative, and hydro stability and low-temperature regeneration, highlights this class of COFs as promising candidates for DAC. Nevertheless, challenges related to large-scale synthesis and efficient integration into air-contactor systems remain to be addressed. Moreover, evaluation of the hydrothermal stability of these COFs is required to enable broader implementation of steam-assisted regeneration strategies in DAC applications.

5.2.1.5. **Commercial Adsorbents.** The influence of steam on the stability of Lewatit adsorbent was also studied by Yu et al.<sup>266</sup> The adsorbent was exposed to steam for 48 h, and no substantial capacity decrease was observed, which is linked to adsorbent synthesis method and strong bonds between support and active amine compound. Nonetheless, comprehensive assessments of the hydro(thermal) stability of these materials remain limited, underscoring the need for further studies to clarify the impact of humidity and steam on adsorbent lifetime.

5.2.2. **Carbonate-Based Adsorbents.** The hydro stability of activated carbon impregnated with  $K_2CO_3$  was examined by Zheng and colleagues<sup>214</sup> under MSA cycles. The adsorbent lost 40% of its capacity over 50 cycles, which was attributed to active component leaching resulting from dissolution of  $K_2CO_3$  in water under humid conditions and subsequent removal over multiple cycles. The initial capture capacity was recovered through reimpregnation of potassium carbonate on the support material (Figure 26). These results show the susceptibility of carbonate-based adsorbents to moisture cycling and underline the need for material modifications or stabilization strategies to enable their reliable application in MSA processes.

**Figure 26.**  $CO_2$  capture capacity drop of  $K_2CO_3$  impregnated on activated carbon across 50 tested MSA cycles and retrieved uptake in 3 cycles after reimpregnation. Reproduced with permission from ref 214. Copyright 2024 Wiley-VCH.



### 5.3. SUMMARY

Hydro stability is critical for physisorbents due to competition between  $H_2O$  and  $CO_2$  for adsorption sites, making upstream drying essential for zeolite-based DAC systems. Among MOFs, materials with open metal sites are particularly susceptible to capacity loss in the presence of moisture, whereas certain fluoride-based frameworks, such as NbOFFIVE-1-Ni, exhibit notable water resistance. Amine-functionalized MOFs show more diverse behavior. MOFs with amine-decorated linkers generally display high hydro stability

despite low CO<sub>2</sub> uptake at atmospheric concentrations, while MOFs with amines appended to metal nodes exhibit stability that appears to depend on the parent framework and amine-framework interactions. Overall, further investigations are needed to elucidate how support structure, amine chemistry, and their interactions govern the hydro stability of this class of sorbents under DAC-relevant conditions.

Amine-functionalized COFs exhibit high hydro stability under humid conditions but require hydrothermal stability assessment for steam-assisted regeneration approaches. For other amine-functionalized porous adsorbents, no detailed studies have been reported examining hydro stability across a wide range of relative humidity levels, whereas hydrothermal stability has received greater attention due to the frequent use of steam during DAC regeneration. Available literature highlights a strong dependence of steam resistance on the choice of support material. Mesoporous silicas with thin pore walls are particularly susceptible to steam-induced structural collapse, while supports with thicker pore walls or incorporated heteroatoms (e.g., Al) demonstrate improved stability. In addition to structural degradation, pore restructuring and surface coverage by leached amines have been identified as key contributors to capacity loss. By contrast,  $\gamma$ -alumina exhibits high hydrothermal stability under steam exposure. Moreover, in situ polymerized and grafted adsorbents generally outperform impregnated samples due to the presence of covalent amine-support bonds. Notably, a systematic comparison of different amine functionalities on a single support, across both impregnation and grafting strategies, remains lacking and is essential for establishing clear structure-stability relationships.

## 6. CHALLENGES AND FUTURE PERSPECTIVES

Despite recent progress, the development of optimal DAC adsorbents for efficient CO<sub>2</sub> capture remains a major challenge.

In particular, long-term stability under realistic operating conditions, including repeated regeneration at high temperatures, exposure to oxygen, humidity, and steam, requires more comprehensive investigation, as degradation under these conditions negatively impacts performance and increases capture costs. The choice of regeneration strategy strongly influences the dominant degradation pathways. While thermal degradation is a major concern in TSA, it may be mitigated in TVSA by employing vacuum or alternative regeneration approaches that limit the maximum regeneration temperature required for CO<sub>2</sub> desorption. However, despite the growing use of vacuum-assisted regeneration, the impact of vacuum level on adsorbent degradation and lifetime has not yet been systematically examined and remains an important area for future study.

Another key deactivation pathway that adversely affects the performance and stability of DAC sorbents, particularly aminebased materials, is oxidative degradation. Although this process is more pronounced at elevated temperatures, it can also occur under moderate operating conditions, albeit to a lesser extent, for example during cooling or adsorption steps. However, because most cyclic stability tests are conducted over a limited number of cycles and often under accelerated conditions, they may not accurately reflect long-term behavior under realistic DAC operation. Moreover, the existing literature does not provide a clear understanding on the influence of synthesis methods or adsorbent class on oxidative stability. While various strategies have been explored to enhance oxidative resistance (including structural modification of amine functionalities, the use of radical scavengers and chelating agents, and the incorporation of hydrogen-bonding polymers) many of which have shown measurable improvements,

oxidative degradation remains a significant challenge. Addressing this issue will require further studies to elucidate degradation mechanisms and to develop robust, scalable mitigation strategies.

Furthermore, improvements in adsorbent stability should not come at the cost of reduced CO<sub>2</sub> capture capacity. Accordingly, future research should focus on strategies that enhance both stability and uptake, particularly for adsorbent classes with comparatively low initial capacities, such as grafted materials. Although numerous studies have examined the thermal cyclic stability of amine-functionalized adsorbents on various supports, a comprehensive understanding of how support properties influence long-term durability is not yet fully established. In particular, the role of support materials in oxidative degradation pathways has received limited attention. Moreover, potential interactions and beneficial or detrimental effects among different stabilization strategies remain poorly understood. For example, while the incorporation of heteroatoms into silica supports is known to enhance thermal stability, its influence on the oxidative stability of amine-based adsorbents has yet to be clarified. An additional gap in the literature is the oxidative stability of adsorbents synthesized via in situ polymerization.

Hydro stability is particularly critical for MSA processes and for systems employing moisture-sensitive physisorbents, whereas hydrothermal stability is especially relevant for steam-assisted regeneration strategies. Although carbonate-based adsorbents exhibit high thermal and oxidative stability, their practical deployment is constrained by low CO<sub>2</sub> uptake, slow reaction kinetics, and high regeneration energy demands. In addition, K<sub>2</sub>CO<sub>3</sub>-based DAC materials have shown active-phase leaching during extended humidity swing operation, highlighting the need for further research to address these limitations. Given that DAC systems operate continuously under fluctuating humidity conditions, studies on the hydro stability of amine-based adsorbents across a wide range of relative humidities remain insufficient. Likewise, long-term performance degradation of MOFs under humid air represents a key challenge that must be addressed. Beyond stability, issues related to scalable production, greener synthesis routes, and cost reduction remain critical for MOF-based adsorbents. By contrast, amine-functionalized COFs have emerged as promising DAC candidates, demonstrating favorable performance even under humid conditions; however, their large-scale synthesis and practical deployment also require further investigation.

Conducting stability evaluations prior to DAC system development is crucial, either to determine the most suitable regeneration method for a given adsorbent or to select an adsorbent that is inherently compatible with the intended regeneration approach. Such stability assessments enable effective screening of materials for specific regeneration scenarios, informing not only the choice of active phase but also the selection of appropriate porous support. Furthermore, stability testing provides system designers and process engineers with the data needed to optimize operational sequences and key steps, such as cooling, drying and evacuation, thereby minimizing degradation, extending adsorbent lifetime, and ultimately reducing operational expenses and CO<sub>2</sub> capture costs associated with adsorbent replacement.

In the fuel-cell field, catalyst and cell durability is commonly evaluated using accelerated degradation tests, often termed accelerated stress tests (ASTs).<sup>332-334</sup> For proton-exchange membrane (PEM) fuel cells, the U.S. Department of Energy Hydrogen and Fuel Cell Technologies Office has issued standardized AST protocols to probe catalyst degradation, carbon-support corrosion, and membrane chemical and mechanical stability.<sup>335</sup> A similar approach could be adopted in DAC by developing DAC-relevant ASTs, applicable to both physisorbents and chemisorbents, particularly amine-based materials, and ultimately moving toward standardized protocols for stability assessment. Nevertheless, limitations recognized in fuel-cell ASTs also apply to solid sorbents. Accelerated methods typically isolate individual stressors (e.g.,

temperature, O<sub>2</sub>, humidity), which can overlook coupled effects that occur under realistic cyclic operation. Moreover, intensified conditions used to accelerate degradation (e.g., elevated temperature or oxygen concentration) can induce pathways that differ from those in practical DAC, potentially under- or over-estimating the dominant mechanisms. Establishing a quantitative link between continuous accelerated exposure and cyclic DAC operation is particularly challenging. In addition, real carbon capture systems introduce further sources of variability (e.g., oxygen ingress, insulation/vacuum defects, and control-system upsets) that complicate direct translation of AST outcomes to field lifetimes. Therefore, ASTs are most valuable for rapid screening, comparative ranking, and identifying likely degradation modes; however, predicting sorbent lifetime generally requires coupling ASTs with long-duration cyclic tests and validated lifetime models. Once a reliable relationship between accelerated and cyclic conditions is established, ASTs could become a powerful and standardized tool for DAC sorbent durability assessment.

To address existing gaps in the field, modeling and computer-aided approaches should be employed alongside experimental investigations and used in a complementary manner. In particular, multiscale modeling frameworks that link molecular-, pore-, and process-level phenomena offer a powerful means to rationally design DAC adsorbents and to optimize both their performance and long-term stability.<sup>336,337</sup> In parallel, broader use of high-throughput machine learning workflows has strong potential to accelerate the discovery and optimization of DAC adsorbents with enhanced capture efficiency and durability.<sup>338-341</sup> Molecular-level modeling can further contribute by elucidating degradation pathways, thereby informing the design of more robust materials suitable for realistic DAC operating conditions. Moreover, coupling process-level modeling with cyclic performance data and life cycle assessment is critical for establishing effective maintenance strategies, including optimal adsorbent replacement intervals. This ensures efficient and net-removal DAC operation with stable performance and controlled maintenance costs over the system lifetime. Ultimately, advancing the stability and efficiency of adsorbents is essential to enable large-scale deployment of DAC technologies, which will play a pivotal role in global climate change mitigation efforts.

## 7. CONCLUSIONS

Essential properties of an ideal DAC adsorbent include high CO<sub>2</sub> uptake with low H<sub>2</sub>O coadsorption, strong CO<sub>2</sub> selectivity, rapid adsorption-desorption kinetics, low regeneration energy, and long-term stability. The latter is a critical requirement for practical, large-scale world deployment. Poor stability can result in operational downtime, increased greenhouse gas emissions, and higher capture costs due to frequent adsorbent replacement. According to the literature, the degradation of solid DAC adsorbents generally occurs via three primary mechanisms: thermal degradation, oxidative degradation, and hydro(thermal) degradation. While certain zeolites and MOFs exhibit high CO<sub>2</sub> uptake, most physisorbents still suffer from limited capacity at atmospheric concentrations. Nevertheless, physisorbents generally display excellent thermal and oxidative stability due to the absence of amine functionalities, although their performance is often adversely affected by humidity. In contrast, amine-functionalized adsorbents typically offer higher CO<sub>2</sub> capacities across a broader range of DAC conditions, but exhibit varying resistance to thermal, oxidative, and hydro(thermal) stressors.

Exposure to elevated temperatures during the regeneration step can lead to degradation of solid adsorbents, making thermal stability a key factor determining their long-term cyclic performance.

Consequently, numerous adsorbents have been synthesized and evaluated through TGA and/or cyclic adsorption-desorption tests under inert conditions. Most of these adsorbents consist of porous silica-based supports functionalized with amine groups, introduced either via physical impregnation of aminopolymers or through chemical grafting of aminosilanes, where the latter group exhibits enhanced thermal stability. The chemical structure of the amine component also plays a critical role in determining thermal stability; for instance, PEI has demonstrated greater thermal stability than TEPA, attributed to its lower volatility and bulkier molecular structure. Urea formation, a CO<sub>2</sub>-induced degradation pathway, is more pronounced in capture processes involving higher CO<sub>2</sub> concentrations and is less relevant under DAC conditions. This mechanism primarily occurs under dry conditions, and adsorbents containing only secondary amines are more stable toward it.

Oxidative degradation represents a critical degradation pathway for functionalized DAC adsorbents, resulting from the constant presence of oxygen during the adsorption phase and subsequent exposure to moderate or high temperatures during cooling and regeneration, where trace amounts of O<sub>2</sub> may remain in the contactor even after evacuation. The capacity loss during oxidative degradation is primarily attributed to the formation of solid byproducts, such as amides, imides, nitriles, and imines, which are less basic and exhibit lower CO<sub>2</sub> affinity. Additionally, oxidation of amine-based adsorbents leads to the release of volatile byproducts like ammonia. Oxidative degradation of amine-based adsorbents is generally driven by a radical-mediated autoxidation mechanism, which is intensified by factors such as metal contaminants within the adsorbent and the presence of water and CO<sub>2</sub> in the adsorption gas stream. Proposed degradation pathways often involve C-H bond cleavage at specific sites and it is well established that the chemical structure of the amine significantly influences its oxidative resistance, with different types of amines showing varying levels of stability. Single primary amines exhibit higher oxidation resistance than single secondary amines. In contrast, for polyamines containing a mixture of primary, secondary, and tertiary amines, reducing the proportion of primary amine groups has been shown to enhance oxidative stability. Furthermore, the length and nature of the linker also influence oxidation resistance; polyamines with propyl linkers are typically more stable than those with ethyl linkers, owing to the higher  $\alpha$ C-H BDE associated with longer alkyl chains near the primary amine groups.

The third major degradation pathway in solid adsorbents involves interaction with water, either from atmospheric moisture during operation (referred to as hydro stability) or from steam and hot water encountered during the regeneration step (known as hydrothermal stability). Mesoporous silicas with thinner pore walls are prone to structural collapse, while thicker-walled materials or silica frameworks modified with aluminum exhibit improved resistance. In addition to structural degradation, pore restructuring and surface coverage from leached amines have been reported as key contributors to the decline in adsorption performance. By comparison,  $\gamma$ -alumina demonstrates better stability, with minimal changes to its porous structure upon steam treatment. Overall, in situ polymerized and grafted adsorbents offer superior hydrothermal stability compared to impregnated ones, mainly due to the formation of strong covalent bonds between the amine groups and the support, which reduces amine leaching. Taken together, these observations demonstrate the critical influence of regeneration conditions, particularly steam temperature and exposure time, on the choice of support materials capable of long-term operation.

Although carbonate-based adsorbents exhibit good thermal and oxidative stability, their practical application in DAC systems is constrained by other performance limitations, including high regeneration energy demands and slow CO<sub>2</sub> adsorption kinetics. In addition, K<sub>2</sub>CO<sub>3</sub>-based DAC adsorbents have shown issues with active material leaching during extended humidity swing cycles. However, their capture

capacity can be restored through reimpregnation, offering a partial solution to this stability concern.

In conclusion, both process conditions and material selection play decisive roles in ensuring the economic viability of DAC systems. The trends and limitations discussed in this review provide valuable guidance for the development of improved adsorbents and processes, while also outlining research priorities that can accelerate the deployment of DAC technologies toward achieving large-scale negative emissions and contributing to global climate change mitigation.

## SUPPORTING INFORMATION

The Supporting Information is available free of charge at

<https://pubs.acs.org/doi/10.1021/acs.energyfuels.5c05460>

Chemical structures of amines employed for functionalization, comprehensive list of adsorbents and studies on stability, including detailed experimental conditions (PDF)

## NOTES

The authors declare no competing financial interest.

## ACKNOWLEDGMENTS

The authors thank the Walloon Region and European Union (NKL project, Grant C8700 financed by EU Resiliency and Recovery Fund), the Energy Transition Fund project TRILATE organized by the Belgian FPS Economy, as well as the Faculty of Applied Science at the University of Liege for supporting this project.

## ABBREVIATIONS

<sup>13</sup>C CP/MAS NMR, carbon-13 cross-polarization magic angle spinning nuclear magnetic resonance; 2-ampd, 2-(aminomethyl)piperidine; ACs, activated carbons; AEAPDMS, *N*-(2-aminoethyl)-3-aminopropylmethyldimethoxysilane; APTES, (3-aminopropyl)triethoxysilane; APTMS, 3-(aminopropyl)trimethoxysilane; Ar, argon; ASTs, accelerated stress tests; BDDPA, 4,4'-bis( $\alpha,\alpha$ -dimethylbenzyl)-diphenylamine; BDE, bond dissociation energy; BECCS, bioenergy with carbon capture and storage; BET, Brunauer-Emmett-Teller; B-ethyl, *N*<sup>1</sup>-(2-aminoethyl)-*N*<sup>1</sup>-(3-(triethoxysilyl)propyl)ethane-1,2-diamine; BJH, Barrett-Joyner-Halenda; bPEI, branched poly(ethylenimine); bPPI, branched poly(propyleneimine); B-propyl, *N*<sup>1</sup>-(3-aminopropyl)-*N*<sup>1</sup>-(3-(triethoxysilyl)propyl)propane-1,3-diamine; CAPEX, capital expenditure; CNTs, carbon nanotubes; CO<sub>2</sub>, carbon dioxide; COFs, covalent organic frameworks; COP21, 21st Conference of Parties; DAC, direct air capture; DACCS, direct air capture with carbon sequestration; den, 1,1-dimethylethylenediamine; DETA, diethylenetriamine; DI, 3-(2-aminoethylamino)propyltrimethoxysilane; DMAPS, (*N,N*-dimethylaminopropyl)trimethoxysilane; DMEDA, *N,N'*-dimethylethylenediamine; DRIFT, diffuse reflectance infrared Fourier transform; DSC, differential scanning calorimetry; EA, elemental analysis; EB, 1,2-epoxybutane; ED, ethylenediamine; een, *N*-ethylethylenediamine; EI-den, dendritic PEI; EPR, electron paramagnetic resonance; ESI-MS, electrospray ionization mass spectrometry; EW, enhanced weathering; FT-IR, Fourier-transform infrared spectroscopy; GC-MS, gas chromatography-mass spectrometry; H<sub>2</sub>O, water; HAADF-STEM, high-angle annular dark-field scanning transmission electron microscopy; He, helium; HNTs, halloysite nanotubes; H-SiO<sub>2</sub>, hierarchical meso-/macroporous silica structure; IEA, International Energy Agency; IPCC, the Intergovernmental Panel on Climate Change; KPIs, key performance indicators; LPAISi, large-pore AlMCM-41 aluminosilicate; lPEI, linear poly(ethylenimine); lPPI, linear poly(propyleneimine); L-propyl, 3-(2-aminopropylamino)propyltrimethoxysilane; MacS, macroporous silica; MAPS, (3-methylaminopropyl)trimethoxysilane; MCF, mesocellular silica foam; mm-2, *N,N*-dimethylethylenediamine; Mn, number-average molecular weight; MOF, metal-organic framework; MSA, moisture swing adsorption; MSF, mesoporous silica foam; Mw, weight-average molecular weight; N<sub>2</sub>, nitrogen; O<sub>2</sub>, oxygen; NETs, negative emission technologies; NFC, nanofibrillated cellulose; NH<sub>3</sub>, ammonia; OF, ocean fertilization; PAA, poly(allylamine); PD, propylenediamine; PEG, polyethylene glycol; PEHA, pentaethylenehexamine; PEM, proton-exchange membrane; PE-MCM-41, pore-expanded MCM-41 mesoporous silica; PGA, poly(glycidyl amine); PI-den, dendritic PPI; PO, propylene oxide; PPG, poly(propylene guanidine); PSA,

pressure swing adsorption; PVA, poly(vinyl alcohol); PXRD, powder X-ray diffraction; RH, relative humidity; ROP, ringopening polymerization; ROS, reactive oxygen species; SCXRD, single-crystal X-ray diffraction; SEM, scanning electron microscope; SPER, spermine; S-TSA, steam-assisted temperature swing adsorption; S-TVSA, steam-assisted temperature-vacuum swing adsorption; T-BRN, 4-(2-aminoethyl)-*N*-(2-aminoethyl)-*N*'-[2-[(2-aminoethyl)amino]ethyl]-1,2-ethanediamine; TCSA, temperature concentration swing adsorption; TEPA, tetraethylenepentamine; T-EPZ, 1-[2-[[2-[(2-aminoethyl)amino]ethyl]amino]ethyl]-piperazine; TETA, triethylenetetramine; TGA, thermogravimetric analysis; T-IPZ, 1-(2-aminoethyl)-4-[[[(2-aminoethyl)amino]ethyl]-piperazine; T-LIN, 1,4,7,10,13-pentaazatridecane; TMMAPS, trimethoxy[3-(methylamino)propyl]silane; TPD, temperature-programmed desorption; TPTA, tripropylenetetramine; TREN, tris(2-aminoethyl)amine; TRI, *N*<sup>1</sup>-(3-trimethoxy-silyl-propyl); TRL, technology readiness level; TRPN, tris(3-aminopropyl)amine; TSA, temperature swing adsorption; TSP, trisodiumphosphate; TVCSA, temperature-vacuum concentration swing adsorption; TVSA, temperature-vacuum swing adsorption; VT-PXRD, variable-temperature powder X-ray diffraction; XPS, X-ray photoelectron spectroscopy; XRD, X-ray diffraction;  $\gamma$ -Al<sub>2</sub>O<sub>3</sub>,  $\gamma$ -alumina

## REFERENCES

- (1) Global Monitoring Laboratory. Trends in Atmospheric Carbon Dioxide. <https://gml.noaa.gov/ccgg/trends> (accessed Feb 02, 2026).
- (2) Rogelj, J.; Shindell, D.; Jiang, K. *Chapter 2: Mitigation Pathways Compatible with 1.5°C in the Context of Sustainable Development*; IPCC Special Report, 2018.
- (3) World Meteorological Organization (WMO). WMO confirms 2024 as warmest year on record at about 1.55°C above pre-industrial level; World Meteorological Organization (WMO). <https://wmo.int/news/media-centre/wmo-confirms-2024-warmest-year-record-about-155degc-above-pre-industrial-level> (accessed Jan 08, 2026).
- (4) Low, M. Y.; Barton, L. V.; Pini, R.; Petit, C. Analytical Review of the Current State of Knowledge of Adsorption Materials and Processes for Direct Air Capture. *Chem. Eng. Res. Des.* **2023**, *189*, 745-767.
- (5) Bach, L. T.; Gill, S. J.; Rickaby, R. E. M.; Gore, S.; Renforth, P. CO<sub>2</sub> Removal With Enhanced Weathering and Ocean Alkalinity Enhancement: Potential Risks and Co-Benefits for Marine Pelagic Ecosystems. *Front. Clim.* **2019**, *1*, 7.
- (6) Gattuso, J. P.; Williamson, P.; Duarte, C. M.; Magnan, A. K. The Potential for Ocean-Based Climate Action: Negative Emissions Technologies and Beyond. *Front. Clim.* **2021**, *2*, 575716.
- (7) Minx, J. C.; Lamb, W. F.; Callaghan, M. W.; Fuss, S.; Hilaire, J.; Creutzig, F.; Amann, T.; Beringer, T.; De Oliveira Garcia, W.; Hartmann, J.; Khanna, T.; Lenzi, D.; Luderer, G.; Nemet, G. F.; Rogelj, J.; Smith, P.; Vicente Vicente, J. L.; Wilcox, J.; Del Mar Zamora Dominguez, M. Negative Emissions - Part 1: Research Landscape and Synthesis. *Environ. Res. Lett.* **2018**, *13*, 063001.
- (8) Sweet, S. K.; Schuldt, J. P.; Lehmann, J.; Bossio, D. A.; Woolf, D. Perceptions of Naturalness Predict US Public Support for Soil Carbon Storage as a Climate Solution. *Clim. Change* **2021**, *166* (1-2), 22.
- (9) Creutzig, F.; Breyer, C.; Hilaire, J.; Minx, J.; Peters, G. P.; Socolow, R. The Mutual Dependence of Negative Emission Technologies and Energy Systems. *Energy Environ. Sci.* **2019**, *12* (6), 1805-1817.
- (10) International Energy Agency (IEA). *Direct Air Capture: A Key Technology for Net Zero*: Paris, 2022.
- (11) Ozkan, M.; Nayak, S. P.; Ruiz, A. D.; Jiang, W. Current Status and Pillars of Direct Air Capture Technologies. *iScience* **2022**, *25* (4), 103990.
- (12) Ozkan, M. Direct Air Capture of CO<sub>2</sub>: A Response to Meet the Global Climate Targets. *MRS Energy Sustain.* **2021**, *8* (2), 51-56.
- (13) Wilcox, J.; Haghpanah, R.; Rupp, E. C.; He, J.; Lee, K. Advancing Adsorption and Membrane Separation Processes for the Gigaton Carbon Capture Challenge. *Annu. Rev. Chem. Biomol. Eng.* **2014**, *5*, 479-505.

- (14) Kim, S.-m.; Zaryab, S. A.; Fakhraddinfakhriazar, S.; Martelli, E.; Léonard, G. Optimization of Large-Scale Direct Air Capture (DAC) Model Using SCR Algorithm. *Comput.-Aided Chem. Eng.* **2023**, 52, 1181-1186.
- (15) Sabatino, F.; Grimm, A.; Gallucci, F.; van Sint Annaland, M.; Kramer, G. J.; Gazzani, M. A Comparative Energy and Costs Assessment and Optimization for Direct Air Capture Technologies. *Joule* **2021**, 5 (8), 2047-2076.
- (16) McQueen, N.; Gomes, K. V.; McCormick, C.; Blumanthal, K.; Pisciotta, M.; Wilcox, J. A Review of Direct Air Capture (DAC): Scaling up Commercial Technologies and Innovating for the Future. *Prog. Energy* **2021**, 3, 032001.
- (17) Yang, M.; Ma, C.; Xu, M.; Wang, S.; Xu, L. Recent Advances in CO<sub>2</sub> Adsorption from Air: A Review. *Curr. Pollut. Rep.* **2019**, 5, 272293.
- (18) Gebald, C.; Meier, W.; Repond, N.; Ruesch, T.; André Wurzbacher, J. Direct Air Capture Device. U.S. Patent 10,232,305 B2, 2019.
- (19) Suter, R.; Tschense, A.; Megerle, B.; Repond, N.; Gebald, C.; Wurzbacher, J. A. Adsorber Structure for Gas Separation Processes. U.S. Patent 20,220,193,598 A1, 2022.
- (20) Eisenberger, P.; Chichilnisky, G. Rotating Multi-Monolith Bed Movement System for Removing CO<sub>2</sub>. U.S. Patent 10,512,880 B2, 2019.
- (21) Barlow, H.; Shahi, S. STATE OF THE ART: CCS TECHNOLOGIES 2024; 2024. <https://www.globalccsinstitute.com/wp-content/uploads/2024/08/Report-CCS-Technologies-Compendium-2024-1.pdf> (accessed Dec 16, 2024).
- (22) Wu, J.; Wang, K.; Zhao, J.; Chen, Y.; Gan, Z.; Zhu, X.; Wang, R.; Wang, C. H.; Tong, Y. W.; Ge, T. A Direct Air Capture Rotary Adsorber for CO<sub>2</sub> Enrichment in Greenhouses. *Device* **2024**, 2 (11), 100510.
- (23) Klomp, J.; Srinivas, A.; Brilman, D. W. F. Design and Demonstration of a 10 kg CO<sub>2</sub>/Day DAC Pilot Facility Using Sorbent Circulation. In *Proceedings of the 16th Greenhouse Gas Control Technologies Conference (GHGT-16)*; SSRN, 2022.
- (24) Wilcox, J. An Electro-Swing Approach. *Nat. Energy* **2020**, 5, 121-122.
- (25) Erguvan, M.; Amini, S. Experimental Microwave Assisted CO<sub>2</sub> Desorption of a Solid Sorbent in a Fluidized Bed Reactor. *Sep. Purif. Technol.* **2024**, 343, 127062.
- (26) Boylu, R.; Erguvan, M.; Amini, S. Investigation of MicrowaveBased CO<sub>2</sub> Regeneration in a Packed Bed Reactor for Direct Air Capture. *Chem. Eng. Res. Des.* **2024**, 212, 391-404.
- (27) Lee, W. H.; Zhang, X.; Banerjee, S.; Jones, C. W.; Realff, M. J.; Lively, R. P. Sorbent-Coated Carbon Fibers for Direct Air Capture Using Electrically Driven Temperature Swing Adsorption. *Joule* **2023**, 7 (6), 1241-1259.
- (28) Jang, I.; Kim, S. Y.; Warner, R.; Song, M.; Potdar, S.; Rivata, A.; Lee, W. H.; Realff, M. J.; Lively, R. P. Electrically-Operated Sorbent-Coated Carbon Fiber Modules for Direct Air Capture. *Chem. Eng. J.* **2025**, 522, 167410.
- (29) Liu, W.; Huang, Y.; Zhang, X. J.; Fang, M. X.; Liu, X.; Wang, T.; Jiang, L. Steam-Assisted Temperature Swing Adsorption for Carbon Capture Integrated with Heat Pump. *Case Stud. Therm. Eng.* **2023**, 49, 103233.
- (30) Schellevis, H. M.; Brilman, D. W. F. Experimental Study of CO<sub>2</sub> Capture from Air via Steam-Assisted Temperature-Vacuum Swing Adsorption with a Compact kg-Scale Pilot Unit. *React. Chem. Eng.* **2024**, 9, 910.
- (31) Shi, X.; Xiao, H.; Kanamori, K.; Yonezu, A.; Lackner, K. S.; Chen, X. Moisture-Driven CO<sub>2</sub> Sorbents. *Joule* **2020**, 4 (8), 18231837.
- (32) Rezaei, F.; Jones, C. W. Stability of Supported Amine Adsorbents to SO<sub>2</sub> and NO<sub>x</sub> in Postcombustion CO<sub>2</sub> Capture. 2. Multicomponent Adsorption. *Ind. Eng. Chem. Res.* **2014**, 53 (30), 12103-12110.
- (33) Kim, S.-M.; Léonard, G. Performance and Sensitivity Analysis of Direct Air Capture (DAC) Model Using Solid Amine Sorbents for CO<sub>2</sub> Capture. In *Proceedings of the 16th Greenhouse Gas Control Technologies Conference (GHGT-16)*; SSRN, 2022.
- (34) Holmes, H. E.; Banerjee, S.; Wallace, A.; Lively, R. P.; Jones, C. W.; Realff, M. J. Tuning Sorbent Properties to Reduce the Cost of Direct Air Capture. *Energy Environ. Sci.* **2024**, 17 (13), 4544-4559.
- (35) Jahandar Lashaki, M.; Khiavi, S.; Sayari, A. Stability of Amine- Functionalized CO<sub>2</sub> Adsorbents: A Multifaceted Puzzle. *Chem. Soc. Rev.* **2019**, 48, 3320-3405.
- (36) Chuah, C. Y.; Ho, Y. L.; Syed, A. M. H.; Thivyalakshmi, K. G. K.; Yang, E.; Johari, K.; Yang, Y.; Poon, W. C. Applicability of Adsorbents in Direct Air Capture (DAC): Recent Progress and Future Perspectives. *Ind. Eng. Chem. Prod. Res. Dev.* **2025**, 64, 41174147.

- (37) Wu, J.; Zhu, X.; Chen, Y.; Wang, R.; Ge, T. The Analysis and Evaluation of Direct Air Capture Adsorbents on the Material Characterization Level. *Chem. Eng. J.* **2022**, *450*, 137958.
- (38) Yang, B.; Yang, W.; Du, J.; Huang, C.; Yang, J.; Wang, B.; Sun, L.; Zhang, H. Recent Progress of Solid Adsorbents on Direct Air Capture of Carbon Dioxide. *J. Environ. Chem. Eng.* **2025**, *13* (6), 119406.
- (39) Zhu, X.; Xie, W.; Wu, J.; Miao, Y.; Xiang, C.; Chen, C.; Ge, B.; Gan, Z.; Yang, F.; Zhang, M.; O'Hare, D.; Li, J.; Ge, T.; Wang, R. Recent Advances in Direct Air Capture by Adsorption. *Chem. Soc. Rev.* **2022**, *51*, 6574-6651.
- (40) Shi, Y.; Ni, R.; Zhao, Y. Review on Multidimensional Adsorbents for CO<sub>2</sub> Capture from Ambient Air: Recent Advances and Future Perspectives. *Energy Fuels* **2023**, *37* (9), 6365-6381.
- (41) Zhao, S.; Zhang, Y.; Li, L.; Feng, J.; Qiu, W.; Ning, Y.; Huang, Z.; Lin, H. Degradation of Amine-Functionalized Adsorbents in Carbon Capture and Direct Air Capture Applications: Mechanism and Solutions. *Sep. Purif. Technol.* **2025**, *354*, 129586.
- (42) Oschatz, M.; Antonietti, M. A Search for Selectivity to Enable CO<sub>2</sub> Capture with Porous Adsorbents. *Energy Environ. Sci.* **2018**, *11*, 57-70.
- (43) Cuesta, A. R.; Song, C. P. H. Swing Adsorption Process for Ambient Carbon Dioxide Capture Using Activated Carbon Black Adsorbents and Immobilized Carbonic Anhydrase Biocatalysts. *Appl. Energy* **2020**, *280*, 116003.
- (44) Jeong-Potter, C.; Abdallah, M.; Sanderson, C.; Goldman, M.; Gupta, R.; Farrauto, R. Dual Function Materials (Ru+Na<sub>2</sub>O/Al<sub>2</sub>O<sub>3</sub>) for Direct Air Capture of CO<sub>2</sub> and in Situ Catalytic Methanation: The Impact of Realistic Ambient Conditions. *Appl. Catal., B* **2022**, *307*, 120990.
- (45) Saha, D.; Kienbaum, M. J. Role of Oxygen, Nitrogen and Sulfur Functionalities on the Surface of Nanoporous Carbons in CO<sub>2</sub> Adsorption: A Critical Review. *Microporous Mesoporous Mater.* **2019**, *287*, 29-55.
- (46) Gokirmak Sogut, E.; Gulcan, M. Adsorption: Basics, Properties, and Classification. In *Adsorption through Advanced Nanoscale Materials: Applications in Environmental Remediation*; Elsevier, 2023; pp 3-21.
- (47) Saenz Cavazos, P. A.; Hunter-Sellars, E.; Iacomì, P.; McIntyre, S. R.; Danaci, D.; Williams, D. R. Evaluating Solid Sorbents for CO<sub>2</sub> Capture: Linking Material Properties and Process Efficiency via Adsorption Performance. *Front. Energy Res.* **2023**, *11*, 1167043.
- (48) Sai Bhargava Reddy, M.; Ponnamma, D.; Sadasivuni, K. K.; Kumar, B.; Abdullah, A. M. Carbon Dioxide Adsorption Based on Porous Materials. *RSC Adv.* **2021**, *11*, 12658-12681.
- (49) Zhang, Z.; Dai, Y.; Zhang, S.; Chen, L.; Gu, J.; Wang, Y.; Sun, W. Porous Framework Materials for CO<sub>2</sub> Capture. *J. Energy Chem.* **2025**, *101*, 278-297.
- (50) Pérez-Botella, E.; Valencia, S.; Rey, F. Zeolites in Adsorption Processes: State of the Art and Future Prospects. *Chem. Rev.* **2022**, *122*, 17647-17695.
- (51) Li, J.; Gao, M.; Yan, W.; Yu, J. Regulation of the Si/Al Ratios and Al Distributions of Zeolites and Their Impact on Properties. *Chem. Sci.* **2023**, *14*, 1935-1959.
- (52) Walton, K. S.; Abney, M. B.; LeVan, M. D. CO<sub>2</sub> Adsorption in  $\gamma$  and X Zeolites Modified by Alkali Metal Cation Exchange. *Microporous Mesoporous Mater.* **2006**, *91* (1-3), 78-84.
- (53) Bhati, G.; Dharanikota, N. P. S. K.; Uppaluri, R. V. S.; Mandal, B. Influence of Cation Exchange on the Selective CO<sub>2</sub> Adsorption Performance of Zeolite-Y over CH<sub>4</sub> and N<sub>2</sub>. *Microporous Mesoporous Mater.* **2025**, *387*, 113537.
- (54) Zhao', D.; Cleare, K.; Oliver, C.; Ingram, C.; Cook', D.; Szostak, R.; Kevan, L. Characteristics of the Synthetic Heulandite/Clinoptilolite Family of Zeolites. *Microporous Mesoporous Mater.* **1998**, *21*, 371-379.
- (55) Tao, Z.; Tian, Y.; Wu, W.; Liu, Z.; Fu, W.; Kung, C.-W.; Shang, J. Development of Zeolite Adsorbents for CO<sub>2</sub> Separation in Achieving Carbon Neutrality. *npj Mater. Sustain.* **2024**, *2* (1), 20.
- (56) Boer, D. G.; Langerak, J.; Pescarmona, P. P. Zeolites as Selective Adsorbents for CO<sub>2</sub> Separation. *ACS Appl. Energy Mater.* **2023**, *6*, 2634-2656.
- (57) Fu, D.; Davis, M. E. Toward the Feasible Direct Air Capture of Carbon Dioxide with Molecular Sieves by Water Management. *Cell Rep. Phys. Sci.* **2023**, *4* (5), 101389.

- (58) Fu, D.; Park, Y.; Davis, M. E. Confinement Effects Facilitate Low-Concentration Carbon Dioxide Capture with Zeolites. *Proc. Natl. Acad. Sci. U.S.A.* **2022**, *119* (39), No. e2211544119.
- (59) Song, M. G.; Rim, G.; Kong, F.; Priyadarshini, P.; Rosu, C.; Lively, R. P.; Jones, C. W. Cold-Temperature Capture of Carbon Dioxide with Water Coproduction from Air Using Commercial Zeolites. *Ind. Eng. Chem. Res.* **2022**, *61* (36), 13624-13634.
- (60) Wilson, S. M. W. The Potential of Direct Air Capture Using Adsorbents in Cold Climates. *iScience* **2022**, *25* (12), 105564.
- (61) Wilson, S. M. W. High Purity CO<sub>2</sub> from Direct Air Capture Using a Single TVSA Cycle with Na-X Zeolites. *Sep. Purif. Technol.* **2022**, *294*, 121186.
- (62) Ye, Z. M.; Xie, Y.; Kirlikovali, K. O.; Xiang, S.; Farha, O. K.; Chen, B. Architecting Metal-Organic Frameworks at Molecular Level toward Direct Air Capture. *J. Am. Chem. Soc.* **2025**, *147*, 5495-5514.
- (63) Wilson, S. M. W.; Tezel, F. H. Direct Dry Air Capture of CO<sub>2</sub> Using VTSA with Faujasite Zeolites. *Ind. Eng. Chem. Res.* **2020**, *59* (18), 8783-8794.
- (64) Lyadov, I.; Lusardi, M. Characterization of K-MER and 13X Zeolites for Humid Direct Air Capture of CO<sub>2</sub> under Equilibrium and Cycling Conditions. *Chem. Eng. J.* **2025**, *524*, 168648.
- (65) Kim, D. Y.; Bae, W. B.; Min, H.; Ryu, K. H.; Kweon, S.; Tran, L. M.; Kim, Y. J.; Park, M. B.; Kang, S. B. Sodium Cation Exchanged Zeolites for Direct Air Capture of CO<sub>2</sub>. *Appl. Surf. Sci. Adv.* **2025**, *25*, 100664.
- (66) Serafin, J.; Dziejarski, B. Activated Carbons-Preparation, Characterization and Their Application in CO<sub>2</sub> Capture: A Review. *Environ. Sci. Pollut. Res.* **2024**, *31* (28), 40008-40062.
- (67) Ramar, V.; Balraj, A. Critical Review on Carbon-Based Nanomaterial for Carbon Capture: Technical Challenges, Opportunities, and Future Perspectives. *Energy Fuels* **2022**, *36*, 1347913505.
- (68) Isah, M.; Lawal, R.; Onaizi, S. A. CO<sub>2</sub> Capture and Conversion Using Graphene-Based Materials: A Review on Recent Progresses and Future Outlooks. *Green Chem. Eng.* **2025**, *6*, 305-334.
- (69) Blankenship, L. S.; Mokaya, R. Modulating the Porosity of Carbons for Improved Adsorption of Hydrogen, Carbon Dioxide, and Methane: A Review. *Mater. Adv.* **2022**, *3*, 1905-1930.
- (70) Singh, R.; Wang, L.; Ostrikov, K.; Huang, J. Designing CarbonBased Porous Materials for Carbon Dioxide Capture. *Adv. Mater. Interfaces* **2024**, *11*, 2202290.
- (71) Petrovic, B.; Gorbounov, M.; Masoudi Soltani, S. Impact of Surface Functional Groups and Their Introduction Methods on the Mechanisms of CO<sub>2</sub> Adsorption on Porous Carbonaceous Adsorbents. *Carbon Capture Sci. Technol.* **2022**, *3*, 100045.
- (72) Zhang, Z.; Zhang, W.; Chen, X.; Xia, Q.; Li, Z. Adsorption of CO<sub>2</sub> on Zeolite 13X and Activated Carbon with Higher Surface Area. *Sep. Sci. Technol.* **2010**, *45* (5), 710-719.
- (73) McEwen, J.; Hayman, J. D.; Ozgur Yazaydin, A. A Comparative Study of CO<sub>2</sub>, CH<sub>4</sub> and N<sub>2</sub> Adsorption in ZIF-8, Zeolite-13X and BPL Activated Carbon. *Chem. Phys.* **2013**, *412*, 72-76.
- (74) Sircar, S.; Golden, T. C.; Rao, M. B. Activated Carbon for Gas Separation and Storage. *Carbon* **1996**, *34* (1), 1-12.
- (75) Siriwardane, R. V.; Shen, M. S.; Fisher, E. P.; Poston, J. A. Adsorption of CO<sub>2</sub> on Molecular Sieves and Activated Carbon. *Energy Fuels* **2001**, *15* (2), 279-284.
- (76) Xu, D.; Xiao, P.; Zhang, J.; Li, G.; Xiao, G.; Webley, P. A.; Zhai, Y. Effects of Water Vapour on CO<sub>2</sub> Capture with Vacuum Swing Adsorption Using Activated Carbon. *Chem. Eng. J.* **2013**, *230*, 64-72.
- (77) Lopes, F. V. S.; Grande, C. A.; Ribeiro, A. M.; Loureiro, J. M.; Evaggelos, O.; Nikolakis, V.; Rodrigues, A. E. Adsorption of H<sub>2</sub>, CO<sub>2</sub>, CH<sub>4</sub>, CO, N<sub>2</sub> and H<sub>2</sub>O in Activated Carbon and Zeolite for Hydrogen Production. *Sep. Sci. Technol.* **2009**, *44* (5), 1045-1073.
- (78) Cheon, G.; Youn, J.; Kim, N.; Choe, J. H.; Lee, N.; Lee, D.; Hong, C. S. MOF-carbon Fiber Composites for Electrically Driven CO<sub>2</sub> Regeneration under Direct Air Capture Conditions. *Chem. Eng. J.* **2025**, *525*, 170309.
- (79) Bose, S.; Sengupta, D.; Rayder, T. M.; Wang, X.; Kirlikovali, K. O.; Sekizkardes, A. K.; Islamoglu, T.; Farha, O. K. Challenges and Opportunities: Metal-Organic Frameworks for Direct Air Capture. *Adv. Funct. Mater.* **2024**, *34*, 2307478.

- (80) Yu, C. H.; Huang, C. H.; Tan, C. S. A Review of CO<sub>2</sub> Capture by Absorption and Adsorption. *Aerosol Air Qual. Res.* **2012**, *12*, 745769.
- (81) Sayari, A.; Belmabkhout, Y.; Serna-Guerrero, R. Flue Gas Treatment via CO<sub>2</sub> Adsorption. *Chem. Eng. J.* **2011**, *171* (3), 760774.
- (82) Sumida, K.; Rogow, D. L.; Mason, J. A.; McDonald, T. M.; Bloch, E. D.; Herm, Z. R.; Bae, T. H.; Long, J. R. Carbon Dioxide Capture in Metal-Organic Frameworks. *Chem. Rev.* **2012**, *112* (2), 724-781.
- (83) Kumar, A.; Madden, D. G.; Lusi, M.; Chen, K.; Daniels, E. A.; Curtin, T.; Perry, J. J.; Zaworotko, M. J. Direct Air Capture of CO<sub>2</sub> by Physisorbent Materials. *Angew. Chem., Int. Ed.* **2015**, *54*, 14372.
- (84) Vrtovec, N.; Mazaj, M.; Buscarino, G.; Terracina, A.; Agnello, S.; Arcò n, I.; Kováč, J.; Zabukovec Logar, N. Structural and CO<sub>2</sub> Capture Properties of Ethylenediamine-Modified HKUST-1 Metal-Organic Framework. *Cryst. Growth Des.* **2020**, *20* (8), 5455-5465.
- (85) McDonald, T. M.; Lee, W. R.; Mason, J. A.; Wiers, B. M.; Hong, C. S.; Long, J. R. Capture of Carbon Dioxide from Air and Flue Gas in the Alkylamine-Appended Metal-Organic Framework Mmen- Mg<sub>2</sub>(Dobpdc). *J. Am. Chem. Soc.* **2012**, *134* (16), 7056-7065.
- (86) Vitillo, J. G.; Bordiga, S. Increasing the Stability of Mg<sub>2</sub>(Dobpdc) Metal-Organic Framework in Air through Solvent Removal. *Mater. Chem. Front.* **2017**, *1*, 444-448.
- (87) Caskey, S. R.; Wong-Foy, A. G.; Matzger, A. J. Dramatic Tuning of Carbon Dioxide Uptake via Metal Substitution in a Coordination Polymer with Cylindrical Pores. *J. Am. Chem. Soc.* **2008**, *130* (33), 10870-10871.
- (88) Britt, D.; Furukawa, H.; Wang, B.; Glover, T. G.; Yaghi, O. M. Highly Efficient Separation of Carbon Dioxide by a Metal-Organic Framework Replete with Open Metal Sites. *Proceedings of the National Academy of Sciences*; Vol. *106*(49), pp 20637-20640.
- (89) Liu, J.; Benin, A. I.; Furtado, A. M. B.; Jakubczak, P.; Willis, R. R.; Levan, M. D. Stability Effects on CO<sub>2</sub> Adsorption for the DOBDC Series of Metal-Organic Frameworks. *Langmuir* **2011**, *27* (18), 11451-11456.
- (90) Queen, W. L.; Hudson, M. R.; Bloch, E. D.; Mason, J. A.; Gonzalez, M. I.; Lee, J. S.; Gygi, D.; Howe, J. D.; Lee, K.; Darwish, T. A.; James, M.; Peterson, V. K.; Teat, S. J.; Smit, B.; Neaton, J. B.; Long, J. R.; Brown, C. M. Comprehensive Study of Carbon Dioxide Adsorption in the Metal-Organic Frameworks M<sub>2</sub>(Dobdc) (M = Mg, Mn, Fe, Co, Ni, Cu, Zn). *Chem. Sci.* **2014**, *5* (12), 4569-4581.
- (91) Choe, J. H.; Kim, H.; Hong, C. S. MOF-74 Type Variants for CO<sub>2</sub> Capture. *Mater. Chem. Front.* **2021**, *5*, 5172-5185.
- (92) Llewellyn, P. L.; Bourrelly, S.; Serre, C.; Vimont, A.; Daturi, M.; Hamon, L.; De Weireld, G.; Chang, J. S.; Hong, D. Y.; Kyu Hwang, Y.; Hwa Jhung, S.; Férey, G. High Uptakes of CO<sub>2</sub> and CH<sub>4</sub> in Mesoporous Metal-Organic Frameworks MIL-100 and MIL-101. *Langmuir* **2008**, *24* (14), 7245-7250.
- (93) Ye, S.; Jiang, X.; Ruan, L. W.; Liu, B.; Wang, Y. M.; Zhu, J. F.; Qiu, L. G. Post-Combustion CO<sub>2</sub> Capture with the HKUST-1 and MIL-101(Cr) Metal-Organic Frameworks: Adsorption, Separation and Regeneration Investigations. *Microporous Mesoporous Mater.* **2013**, *179*, 191-197.
- (94) Morelli Venturi, D.; Costantino, F. Recent Advances in the Chemistry and Applications of Fluorinated Metal-Organic Frameworks (F-MOFs). *RSC Adv.* **2023**, *13*, 29215-29230.
- (95) Shekhah, O.; Belmabkhout, Y.; Chen, Z.; Guillerm, V.; Cairns, A.; Adil, K.; Eddaoudi, M. Made-to-Order Metal-Organic Frameworks for Trace Carbon Dioxide Removal and Air Capture. *Nat. Commun.* **2014**, *5*, 4228.
- (96) Mukherjee, S.; Sikdar, N.; O'nolan, D.; Franz, D. M.; Gascón, V.; Kumar, A.; Kumar, N.; Scott, H. S.; Madden, D. G.; Kruger, P. E.; Space, B.; Zaworotko, M. J. Trace CO<sub>2</sub> Capture by an Ultra- microporous Physisorbent with Low Water Affinity. *Sci. Adv.* **2019**, *5*, No. eaax9171.
- (97) Kumar, A.; Hua, C.; Madden, D. G.; O'Nolan, D.; Chen, K. J.; Keane, L. A. J.; Perry, J. J.; Zaworotko, M. J. Hybrid Ultramicroporous Materials (HUMs) with Enhanced Stability and Trace Carbon Capture Performance. *Chem. Commun.* **2017**, *53* (44), 5946-5949.
- (98) Bhatt, P. M.; Belmabkhout, Y.; Cadiau, A.; Adil, K.; Shekhah, O.; Shkurenko, A.; Barbour, L. J.; Eddaoudi, M. A Fine-Tuned Fluorinated MOF Addresses the Needs for Trace CO<sub>2</sub> Removal and Air Capture Using Physisorption.

*J. Am. Chem. Soc.* **2016**, 138 (29), 9301-9307.

- (99) Low, M. Y. A.; Danaci, D.; Azzan, H.; Jiayi, A. L.; Yong, G. W. S.; Itskou, I.; Petit, C. Physicochemical Properties, Equilibrium Adsorption Performance, Manufacturability, and Stability of TIFSIX- 3-Ni for Direct Air Capture of CO<sub>2</sub>. *Energy Fuels* **2024**, 38 (13), 11947-11965.
- (100) Barsoum, M. L.; Hofmann, J.; Xie, H.; Chen, Z.; Vornholt, S. M.; dos Reis, R.; Burns, N.; Kycia, S.; Chapman, K. W.; Dravid, V. P.; Farha, O. K. Probing Structural Transformations and Degradation Mechanisms by Direct Observation in SIFSIX-3-Ni for Direct Air Capture. *J. Am. Chem. Soc.* **2024**, 146 (10), 6557-6565.
- (101) Bayati, B.; Keshavarz, F.; Rezaei, N.; Zendejboudi, S.; Barbiellini, B. New Insight into Impact of Humidity on Direct Air Capture Performance by SIFSIX-3-Cu MOF. *Phys. Chem. Chem. Phys.* **2024**, 26 (25), 17645-17659.
- (102) Åhlén, M.; Cheung, O.; Xu, C. Low-Concentration CO<sub>2</sub> Capture Using Metal-Organic Frameworks - Current Status and Future Perspectives. *Dalton Trans.* **2023**, 52, 1841-1856.
- (103) Zhang, Z.; Ding, Q.; Cui, J.; Cui, X.; Xing, H. High and Selective Capture of Low-Concentration CO<sub>2</sub> with an Anion- Functionalized Ultramicroporous Metal-Organic Framework. *Sci. China Mater.* **2021**, 64 (3), 691-697.
- (104) Geng, K.; He, T.; Liu, R.; Dalapati, S.; Tan, K. T.; Li, Z.; Tao, S.; Gong, Y.; Jiang, Q.; Jiang, D. Covalent Organic Frameworks: Design, Synthesis, and Functions. *Chem. Rev.* **2020**, 120, 8814-8933.
- (105) Feng, X.; Ding, X.; Jiang, D. Covalent Organic Frameworks. *Chem. Soc. Rev.* **2012**, 41 (18), 6010-6022.
- (106) Diercks, C. S.; Yaghi, O. M. The Atom, the Molecule, and the Covalent Organic Framework. *Science* **2017**, 355, No. eaal1585.
- (107) Liu, X.; Huang, D.; Lai, C.; Zeng, G.; Qin, L.; Wang, H.; Yi, H.; Li, B.; Liu, S.; Zhang, M.; Deng, R.; Fu, Y.; Li, L.; Xue, W.; Chen, S. Recent Advances in Covalent Organic Frameworks (COFs) as a Smart Sensing Material. *Chem. Soc. Rev.* **2019**, 48, 5266-5302.
- (108) Mähringer, A.; Medina, D. D. Taking Stock of Stacking. *Nat. Chem.* **2020**, 12 (11), 985-987.
- (109) Côté, A. P.; Benin, A. I.; Ockwig, N. W.; O'Keeffe, M.; Matzger, A. J.; Yaghi, O. M. Porous, Crystalline, Covalent Frameworks. *Science* **2005**, 310 (5751), 1166-1170.
- (110) El-Kaderi, H. M.; Hunt, J. R.; Mendoza-Cortés, J. L.; Côté, A. P.; Taylor, R. E.; O'Keeffe, M.; Yaghi, O. M. Designed Synthesis of 3D Covalent Organic Frameworks. *Science* **2007**, 316 (5822), 268272.
- (111) Waller, P. J.; Gándara, F.; Yaghi, O. M. Chemistry of Covalent Organic Frameworks. *Acc. Chem. Res.* **2015**, 48 (12), 3053-3063.
- (112) Gui, B.; Lin, G.; Ding, H.; Gao, C.; Mal, A.; Wang, C. ThreeDimensional Covalent Organic Frameworks: From Topology Design to Applications. *Acc. Chem. Res.* **2020**, 53 (10), 2225-2234.
- (113) Alenazi, M. H.; Helal, A.; Khan, M. Y.; Khalil, A.; Khan, A.; Usman, M.; Zahir, M. H. Covalent Organic Frameworks (COFs) for CO<sub>2</sub> Utilizations. *Carbon Capture Sci. Technol.* **2025**, 14, 100365.
- (114) Ozdemir, J.; Mosleh, I.; Abolhassani, M.; Greenlee, L. F.; Beitle, R. R.; Beyzavi, M. H. Covalent Organic Frameworks for the Capture, Fixation, or Reduction of CO<sub>2</sub>. *Front. Energy Res.* **2019**, 7, 77.
- (115) Wang, X.; Liu, H.; Zhang, J.; Chen, S. Covalent Organic Frameworks (COFs): A Promising CO<sub>2</sub> Capture Candidate Material. *Polym. Chem.* **2023**, 14, 1293-1317.
- (116) Li, R. Z.; Yu, S. C.; Jiang, W.; Zhou, J.; Wang, Z. C.; Ren, X. R.; Feng, W.; Zhou, Y.; Wang, D.; Wan, L. J. Direct Synthesis of Amide-Linked COFs via Ester-Amine Exchange Reaction. *J. Am. Chem. Soc.* **2025**, 147 (34), 31016-31024.
- (117) Chen, H.; Qin, J.; Ruan, X.; Zhang, Q.; Zhu, H.; Zhu, S. Linkage Engineering of Covalent-Organic Frameworks for CO<sub>2</sub> Capture. *Sep. Purif. Technol.* **2025**, 354, 129378.
- (118) Kang, C.; Zhang, Z.; Xi, S.; Li, H.; Usadi, A. K.; Calabro, D. C.; Baugh, L. S.; Wang, Y.; Zhao, D. Insertion of CO<sub>2</sub> in Metal Ion- Doped Two-Dimensional Covalent Organic Frameworks. *Proc. Natl. Acad. Sci. U.S.A.* **2023**, 120 (9), No. e2217081120.
- (119) Liu, J.; Hao, C.; Zhang, H.; Chen, H.; Zhang, L.; Chen, X.; Wang, J.; Wang, M.; Wei, S.; Lu, X.; Wang, Z.; Liu, S. Alkali Metal- Functionalized Covalent Organic Frameworks for CO<sub>2</sub> Adsorption and CO<sub>2</sub>/N<sub>2</sub> Separation. *ACS Appl. Polym. Mater.* **2025**, 7 (3), 1729-1740.
- (120) Sarkar, P.; Chowdhury, I. H.; Das, S.; Islam, S. M. Recent Trends in Covalent Organic Frameworks (COFs) for Carbon Dioxide Reduction. *Mater. Adv.* **2022**, 3, 8063-8080.

- (121) Li, H.; Dilipkumar, A.; Abubakar, S.; Zhao, D. Covalent Organic Frameworks for CO<sub>2</sub> Capture: From Laboratory Curiosity to Industry Implementation. *Chem. Soc. Rev.* **2023**, *52*, 6294-6329.
- (122) Wei, W.; Wang, Z.; Xu, C.; Li, Z.; Bai, H.; Liu, Z. Advances in the Structural Design of Covalent Organic Frameworks for Direct Air Capture of CO<sub>2</sub>. *Ind. Eng. Chem. Res.* **2025**, *64* (51), 24276-24299.
- (123) Zhao, Y.; Yao, K. X.; Teng, B.; Zhang, T.; Han, Y. A Perfluorinated Covalent Triazine-Based Framework for Highly Selective and Water-Tolerant CO<sub>2</sub> Capture. *Energy Environ. Sci.* **2013**, *6* (12), 3684-3692.
- (124) Uribe-Romo, F. J.; Hunt, J. R.; Furukawa, H.; Klöck, C.; O'Keeffe, M.; Yaghi, O. M. A Crystalline Imine-Linked 3-D Porous Covalent Organic Framework. *J. Am. Chem. Soc.* **2009**, *131* (13), 4570-4571.
- (125) Fang, Q.; Zhuang, Z.; Gu, S.; Kaspar, R. B.; Zheng, J.; Wang, J.; Qiu, S.; Yan, Y. Designed Synthesis of Large-Pore Crystalline Polyimide Covalent Organic Frameworks. *Nat. Commun.* **2014**, *5*, 4503.
- (126) Ozkan, M.; Akhavi, A. A.; Coley, W. C.; Shang, R.; Ma, Y. Progress in Carbon Dioxide Capture Materials for Deep Decarbonization. *Chem* **2022**, *8*, 141-173.
- (127) Cherevotan, A.; Raj, J.; Peter, S. C. An Overview of Porous Silica Immobilized Amines for Direct Air CO<sub>2</sub> capture. *J. Mater. Chem. A* **2021**, *9*, 27271-27303.
- (128) Hack, J.; Maeda, N.; Meier, D. M. Review on CO<sub>2</sub> Capture Using Amine-Functionalized Materials. *ACS Omega* **2022**, *7*, 3952039530.
- (129) Petrovic, B.; Gorbounov, M.; Masoudi Soltani, S. Influence of Surface Modification on Selective CO<sub>2</sub> Adsorption: A Technical Review on Mechanisms and Methods. *Microporous Mesoporous Mater.* **2021**, *312*, 110751.
- (130) Said, R. B.; Kolle, J. M.; Essalah, K.; Tangour, B.; Sayari, A. A Unified Approach to CO<sub>2</sub>-Amine Reaction Mechanisms. *ACS Omega* **2020**, *5* (40), 26125-26133.
- (131) Bacsik, Z.; Ahlsten, N.; Ziadi, A.; Zhao, G.; Garcia-Bennett, A. E.; Martín-Matute, B.; Hedin, N. Mechanisms and Kinetics for Sorption of CO<sub>2</sub> on Bicontinuous Mesoporous Silica Modified with N-Propylamine. *Langmuir* **2011**, *27* (17), 11118-11128.
- (132) Srikanth, C. S.; Chuang, S. S. C. Spectroscopic Investigation into Oxidative Degradation of Silica-Supported Amine Sorbents for CO<sub>2</sub> Capture. *ChemSusChem* **2012**, *5* (8), 1435-1442.
- (133) Priyadarshini, P.; Rim, G.; Rosu, C.; Song, M. G.; Jones, C. W. Direct Air Capture of CO<sub>2</sub> Using Amine/Alumina Sorbents at Cold Temperature. *ACS Environ. Au* **2023**, *3* (5), 295-307.
- (134) Navik, R.; Wang, E.; Ding, X.; Qiu, K. X.; Li, J. Atmospheric Carbon Dioxide Capture by Adsorption on Amine-Functionalized Silica Composites: A Review. *Environ. Chem. Lett.* **2024**, *22*, 17911830.
- (135) Surkatti, R.; Abdullatif, Y. M.; Muhammad, R.; Sodiq, A.; Mroue, K.; Al-Ansari, T.; Amhamed, A. I. Comparative Analysis of Amine-Functionalized Silica for Direct Air Capture (DAC): Material Characterization, Performance, and Thermodynamic Efficiency. *Sep. Purif. Technol.* **2025**, *354*, 128641.
- (136) Kumar, R.; Ohtani, S.; Tsunoji, N. Direct Air Capture on Amine-Impregnated FAU Zeolites: Exploring for High Adsorption Capacity and Low-Temperature Regeneration. *Microporous Mesoporous Mater.* **2023**, *360*, 112714.
- (137) Jia, S.; Gao, M.; Yang, L.; Chen, K.; Xi, L.; Wu, X.; Nagasaka, T. Amine Functionalized Zeolites: Modification Strategy and Application. *ChemistrySelect* **2025**, *10*, No. e00362.
- (138) Chen, Z.; Deng, S.; Wei, H.; Wang, B.; Huang, J.; Yu, G. Polyethylenimine-Impregnated Resin for High CO<sub>2</sub> Adsorption: An Efficient Adsorbent for CO<sub>2</sub> Capture from Simulated Flue Gas and Ambient Air. *ACS Appl. Mater. Interfaces* **2013**, *5* (15), 6937-6945.
- (139) Yang, M.; Wang, S.; Xu, L. Hydrophobic Functionalized Amine-Impregnated Resin for CO<sub>2</sub> Capture in Humid Air. *Sep. Purif. Technol.* **2023**, *315*, 123606.
- (140) Zhao, S.; Zhang, Y.; Li, L.; Feng, J.; Qiu, W.; Wang, Y.; Huang, Z.; Lin, H. Amine-Functionalized Macroporous Resin for Direct Air Capture with High CO<sub>2</sub> Capacity in Real Atmospheric Conditions: Effects of Moisture and Oxygen. *Sep. Purif. Technol.* **2024**, *350*, 127999.
- (141) Choi, S.; Watanabe, T.; Bae, T. H.; Sholl, D. S.; Jones, C. W. Modification of the Mg/DOBDC MOF with Amines to Enhance CO<sub>2</sub> Adsorption from Ultradilute Gases. *J. Phys. Chem. Lett.* **2012**, *3* (9), 1136-1141.
- (142) Lee, W. R.; Hwang, S. Y.; Ryu, D. W.; Lim, K. S.; Han, S. S.; Moon, D.; Choi, J.; Hong, C. S. Diamine-Functionalized MetalOrganic Framework: Exceptionally High CO<sub>2</sub> Capacities from Ambient Air and Flue Gas, Ultrafast

CO<sub>2</sub> Uptake Rate, and Adsorption Mechanism. *Energy Environ. Sci.* **2014**, 7 (2), 744-751.

- (143) Li, H.; Wang, K.; Feng, D.; Chen, Y. P.; Verdegaal, W.; Zhou, H. C. Incorporation of Alkylamine into Metal-Organic Frameworks through a Brønsted Acid-Base Reaction for CO<sub>2</sub> Capture. *ChemSusChem* **2016**, 9 (19), 2832-2840.
- (144) Lyu, H.; Li, H.; Hanikel, N.; Wang, K.; Yaghi, O. M. Covalent Organic Frameworks for Carbon Dioxide Capture from Air. *J. Am. Chem. Soc.* **2022**, 144 (28), 12989-12995.
- (145) Zhou, Z.; Ma, T.; Zhang, H.; Chheda, S.; Li, H.; Wang, K.; Ehrling, S.; Giovine, R.; Li, C.; Alawadhi, A. H.; Abduljawad, M. M.; Alawad, M. O.; Gagliardi, L.; Sauer, J.; Yaghi, O. M. Carbon Dioxide Capture from Open Air Using Covalent Organic Frameworks. *Nature* **2024**, 635 (8037), 96-101.
- (146) Choi, S.; Drese, J. H.; Jones, C. W. Adsorbent Materials for Carbon Dioxide Capture from Large Anthropogenic Point Sources. *ChemSusChem* **2009**, 2, 796-854.
- (147) Ahmadian Hosseini, A.; Jahandar Lashaki, M. A Comprehensive Evaluation of Amine-Impregnated Silica Materials for Direct Air Capture of Carbon Dioxide. *Sep. Purif. Technol.* **2023**, 325, 124580.
- (148) Panda, D.; Kulkarni, V.; Singh, S. K. Evaluation of AmineBased Solid Adsorbents for Direct Air Capture: A Critical Review. *React. Chem. Eng.* **2022**, 8, 10-40.
- (149) Rao, N.; Wang, M.; Shang, Z.; Hou, Y.; Fan, G.; Li, J. CO<sub>2</sub> Adsorption by Amine-Functionalized MCM-41: A Comparison between Impregnation and Grafting Modification Methods. *Energy Fuels* **2018**, 32 (1), 670-677.
- (150) Chen, C.; Zhang, S.; Row, K. H.; Ahn, W. S. Amine-Silica Composites for CO<sub>2</sub> Capture: A Short Review. *J. Energy Chem.* **2017**, 26, 868-880.
- (151) Chaikittisilp, W.; Lunn, J. D.; Shantz, D. F.; Jones, C. W. Poly(L-Lysine) Brush-Mesoporous Silica Hybrid Material as a Biomolecule-Based Adsorbent for CO<sub>2</sub> Capture from Simulated Flue Gas and Air. *Chem.—Eur. J.* **2011**, 17 (38), 10556-10561.
- (152) Wamba, A. G. N.; Kofa, G. P.; Koungou, S. N.; Thue, P. S.; Lima, E. C.; Dos Reis, G. S.; Kayem, J. G. Grafting of Amine Functional Group on Silicate Based Material as Adsorbent for Water Purification: A Short Review. *J. Environ. Chem. Eng.* **2018**, 6, 31923203.
- (153) Shi, X.; Xiao, H.; Azarabadi, H.; Song, J.; Wu, X.; Chen, X.; Lackner, K. S. Sorbenten Zur Direkten Gewinnung von CO<sub>2</sub> Aus Der Umgebungsluft. *Angew. Chem., Int. Ed.* **2020**, 59, 6984.
- (154) Sanz-Pérez, E. S.; Murdock, C. R.; Didas, S. A.; Jones, C. W. Direct Capture of CO<sub>2</sub> from Ambient Air. *Chem. Rev.* **2016**, 116, 11840-11876.
- (155) Al-Absi, A. A.; Ogungbenro, A. E.; Benneker, A. M.; Mahinpey, N. Review of Polyethylenimine through Ring-Opening Polymerization Reactions and Its Application in CO<sub>2</sub> Capture. *J. Environ. Chem. Eng.* **2024**, 12, 112739.
- (156) Gleede, T.; Reisman, L.; Rieger, E.; Mbarushimana, P. C.; Rupar, P. A.; Wurm, F. R. Aziridines and Azetidines: Building Blocks for Polyamines by Anionic and Cationic Ring-Opening Polymerization. *Polym. Chem.* **2019**, 10, 3257-3283.
- (157) Shi, X.; Lee, G. A.; Liu, S.; Kim, D.; Alahmed, A.; Jamal, A.; Wang, L.; Park, A. H. A. Water-Stable MOFs and Hydrophobically Encapsulated MOFs for CO<sub>2</sub> Capture from Ambient Air and Wet Flue Gas. *Mater. Today* **2023**, 65, 207-226.
- (158) Kumar, R.; Bandyopadhyay, M.; Pandey, M.; Tsunaji, N. Amine-Impregnated Nanoarchitectonics of Mesoporous Silica for Capturing Dry and Humid 400 Ppm Carbon Dioxide: A Comparative Study. *Microporous Mesoporous Mater.* **2022**, 338, 111956.
- (159) Chaikittisilp, W.; Khunsupat, R.; Chen, T. T.; Jones, C. W. Poly(Allylamine)-Mesoporous Silica Composite Materials for CO<sub>2</sub> Capture from Simulated Flue Gas or Ambient Air. *Ind. Eng. Chem. Res.* **2011**, 50 (24), 14203-14210.
- (160) Goepfert, A.; Zhang, H.; Czaun, M.; May, R. B.; Prakash, G. K. S.; Olah, G. A.; Narayanan, S. R. Easily Regenerable Solid Adsorbents Based on Polyamines for Carbon Dioxide Capture from the Air. *ChemSusChem* **2014**, 7 (5), 1386-1397.
- (161) Kwon, H. T.; Sakwa-Novak, M. A.; Pang, S. H.; Sujana, A. R.; Ping, E. W.; Jones, C. W. Aminopolymer-Impregnated Hierarchical Silica Structures: Unexpected Equivalent CO<sub>2</sub> Uptake under Simulated Air Capture and Flue Gas Capture Conditions. *Chem. Mater.* **2019**, 31 (14), 5229-5237.

- (162) Spinu, D.; Rout, K. R.; Chen, D. Unveiling the Desorption Performance and Thermal Stability of Unmodified Polyamine-Containing CO<sub>2</sub> Adsorbents. *Energy Fuels* **2024**, *38* (14), 131761-13185.
- (163) Chaikittisilp, W.; Kim, H. J.; Jones, C. W. Mesoporous Alumina-Supported Amines as Potential Steam-Stable Adsorbents for Capturing CO<sub>2</sub> from Simulated Flue Gas and Ambient Air. *Energy Fuels* **2011**, *25* (11), 5528-5537.
- (164) Pang, S. H.; Lively, R. P.; Jones, C. W. Oxidatively-Stable Linear Poly(Propylenimine)-Containing Adsorbents for CO<sub>2</sub> Capture from Ultradilute Streams. *ChemSusChem* **2018**, *11* (15), 2628-2637.
- (165) Zhang, H.; Goepfert, A.; Prakash, G. K. S.; Olah, G. Applicability of Linear Polyethylenimine Supported on Nano-Silica for the Adsorption of CO<sub>2</sub> from Various Sources Including Dry Air. *RSC Adv.* **2015**, *5* (65), 52550-52562.
- (166) Sarazen, M. L.; Sakwa-Novak, M. A.; Ping, E. W.; Jones, C. W. Effect of Different Acid Initiators on Branched Poly(Propylenimine) Synthesis and CO<sub>2</sub> Sorption Performance. *ACS Sustain. Chem. Eng.* **2019**, *7* (7), 7338-7345.
- (167) Park, S. J.; Lee, J. J.; Hoyt, C. B.; Kumar, D. R.; Jones, C. W. Silica Supported Poly(Propylene Guanidine) as a CO<sub>2</sub> Sorbent in Simulated Flue Gas and Direct Air Capture. *Adsorption* **2020**, *26* (1), 89-101.
- (168) Sujan, A. R.; Kumar, D. R.; Sakwa-Novak, M.; Ping, E. W.; Hu, B.; Park, S. J.; Jones, C. W. Poly(Glycidyl Amine)-Loaded SBA-15 Sorbents for CO<sub>2</sub> Capture from Dilute and Ultradilute Gas Mixtures. *ACS Appl. Polym. Mater.* **2019**, *1* (11), 3137-3147.
- (169) Miao, Y.; He, Z.; Zhu, X.; Izkowitz, D.; Li, J. Operating Temperatures Affect Direct Air Capture of CO<sub>2</sub> in Polyamine-Loaded Mesoporous Silica. *Chem. Eng. J.* **2021**, *426*, 131875.
- (170) Zhao, M.; Xiao, J.; Gao, W.; Wang, Q. Defect-Rich Mg-Al MMOs Supported TEPA with Enhanced Charge Transfer for Highly Efficient and Stable Direct Air Capture. *J. Energy Chem.* **2022**, *68*, 401-410.
- (171) Kulkarni, V.; Panda, D.; Singh, S. K. Direct Air Capture of CO<sub>2</sub> over Amine-Modified Hierarchical Silica. *Ind. Eng. Chem. Res.* **2023**, *62* (8), 3800-3811.
- (172) Pang, S. H.; Lee, L. C.; Sakwa-Novak, M. A.; Lively, R. P.; Jones, C. W. Design of Aminopolymer Structure to Enhance Performance and Stability of CO<sub>2</sub> Sorbents: Poly(Propylenimine) vs Poly(Ethylenimine). *J. Am. Chem. Soc.* **2017**, *139* (10), 3627-3630.
- (173) Potter, M. E.; Cho, K. M.; Lee, J. J.; Jones, C. W. Exploring the Acid Gas Sorption Properties of Oxidatively Degraded Supported Amine Sorbents. *Energy Fuels* **2019**, *33* (2), 1372-1382.
- (174) Kulkarni, V.; Parthiban, J.; Singh, S. K. Direct CO<sub>2</sub> Capture from Simulated and Ambient Air over Aminosilane-Modified Hierarchical Silica. *Microporous Mesoporous Mater.* **2024**, *368*, 112998.
- (175) Abhilash, K. A. S.; Deepthi, T.; Sadhana, R. A.; Benny, K. G. Functionalized Polysilsesquioxane-Based Hybrid Silica Solid Amine Sorbents for the Regenerative Removal of CO<sub>2</sub> from Air. *ACS Appl. Mater. Interfaces* **2015**, *7* (32), 17969-17976.
- (176) Kong, Y.; Jiang, G.; Wu, Y.; Cui, S.; Shen, X. Amine Hybrid Aerogel for High-Efficiency CO<sub>2</sub> Capture: Effect of Amine Loading and CO<sub>2</sub> Concentration. *Chem. Eng. J.* **2016**, *306*, 362-368.
- (177) Yoo, C. J.; Park, S. J.; Jones, C. W. CO<sub>2</sub> Adsorption and Oxidative Degradation of Silica-Supported Branched and Linear Aminosilanes. *Ind. Eng. Chem. Res.* **2020**, *59* (15), 7061-7071.
- (178) Anyanwu, J. T.; Wang, Y.; Yang, R. T. CO<sub>2</sub> Capture (Including Direct Air Capture) and Natural Gas Desulfurization of Amine-Grafted Hierarchical Bimodal Silica. *Chem. Eng. J.* **2022**, *427*, 131561.
- (179) Anyanwu, J. T.; Wang, Y.; Yang, R. T. Amine-Grafted Silica Gels for CO<sub>2</sub> Capture Including Direct Air Capture. *Ind. Eng. Chem. Res.* **2020**, *59* (15), 7072-7079.
- (180) Chen, Y.; Zhu, L.; Wu, J.; Wang, K.; Ge, T. Feasibility and Effectivity of an Amine-Grafted Alumina Adsorbent for Direct Air Capture. *Langmuir* **2024**, *40*, 26166.
- (181) Gebald, C.; Wurzbacher, J. A.; Tingaut, P.; Steinfeld, A. Stability of Amine-Functionalized Cellulose during Temperature-Vacuum-Swing Cycling for CO<sub>2</sub> Capture from Air. *Environ. Sci. Technol.* **2013**, *47* (17), 10063-10070.
- (182) Gebald, C.; Wurzbacher, J. A.; Borgschulte, A.; Zimmermann, T.; Steinfeld, A. Single-Component and Binary CO<sub>2</sub> and H<sub>2</sub>O Adsorption of Amine-Functionalized Cellulose. *Environ. Sci. Technol.* **2014**, *48* (4), 2497-2504.
- (183) Al-Absi, A. A.; Benneker, A. M.; Mahinpey, N. Amine Sorbents for Sustainable Direct Air Capture: Long-

Term Stability and Extended Aging Study. *Energy Fuels* **2024**, 38 (10), 8938-8950.

(184) Flaig, R. W.; Osborn Popp, T. M.; Fracaroli, A. M.; Kapustin, E. A.; Kalmutzki, M. J.; Altamimi, R. M.; Fathieh, F.; Reimer, J. A.; Yaghi, O. M. The Chemistry of CO<sub>2</sub> Capture in an Amine- Functionalized Metal-Organic Framework under Dry and Humid Conditions. *J. Am. Chem. Soc.* **2017**, 139 (35), 12125-12128.

(185) McDonald, T. M.; Mason, J. A.; Kong, X.; Bloch, E. D.; Gygi, D.; Dani, A.; Crocella, V.; Giordanino, F.; Odoh, S. O.; Drisdell, W. S.; Vlasisavljevich, B.; Dzubak, A. L.; Poloni, R.; Schnell, S. K.; Planas, N.; Lee, K.; Pascal, T.; Wan, L. F.; Prendergast, D.; Neaton, J. B.; Smit, B.; Kortright, J. B.; Gagliardi, L.; Bordiga, S.; Reimer, J. A.; Long, J. R. Cooperative Insertion of CO<sub>2</sub> in Diamine-Appended Metal-Organic Frameworks. *Nature* **2015**, 519 (7543), 303-308.

(186) Darunte, L. A.; Oetomo, A. D.; Walton, K. S.; Sholl, D. S.; Jones, C. W. Direct Air Capture of CO<sub>2</sub> Using Amine Functionalized MIL-101(Cr). *ACS Sustain. Chem. Eng.* **2016**, 4 (10), 5761-5768.

(187) Choe, J. H.; Kim, H.; Yun, H.; Kurisingal, J. F.; Kim, N.; Lee, D.; Lee, Y. H.; Hong, C. S. Extended MOF-74-Type Variant with an Azine Linkage: Efficient Direct Air Capture and One-Pot Synthesis. *J. Am. Chem. Soc.* **2024**, 146 (28), 19337-19349.

(188) Chen, O. I. F.; Liu, C. H.; Wang, K.; Borrego-Marin, E.; Li, H.; Alawadhi, A. H.; Navarro, J. A. R.; Yaghi, O. M. Water-Enhanced Direct Air Capture of Carbon Dioxide in Metal-Organic Frameworks. *J. Am. Chem. Soc.* **2024**, 146 (4), 2835-2844.

(189) Jo, H.; Lee, W. R.; Kim, N. W.; Jung, H.; Lim, K. S.; Kim, J. E.; Kang, D. W.; Lee, H.; Hiremath, V.; Seo, J. G.; Jin, H.; Moon, D.; Han, S. S.; Hong, C. S. Fine-Tuning of the Carbon Dioxide Capture Capability of Diamine-Grafted Metal-Organic Framework Adsorbents Through Amine Functionalization. *ChemSusChem* **2017**, 10 (3), 541-550.

(190) Lee, W. R.; Kim, J. E.; Lee, S. J.; Kang, M.; Kang, D. W.; Lee, H. Y.; Hiremath, V.; Seo, J. G.; Jin, H.; Moon, D.; Cho, M.; Jung, Y.; Hong, C. S. Diamine-Functionalization of a Metal-Organic Framework Adsorbent for Superb Carbon Dioxide Adsorption and Desorption Properties. *ChemSusChem* **2018**, 11 (10), 1694-1707.

(191) Park, J.; Park, J. R.; Choe, J. H.; Kim, S.; Kang, M.; Kang, D. W.; Kim, J. Y.; Jeong, Y. W.; Hong, C. S. Metal-Organic Framework Adsorbent for Practical Capture of Trace Carbon Dioxide. *ACS Appl. Mater. Interfaces* **2020**, 12 (45), 50534-50540.

(192) Mahajan, S.; Lahtinen, M. Recent Progress in Metal-Organic Frameworks (MOFs) for CO<sub>2</sub> capture at Different Pressures. *J. Environ. Chem. Eng.* **2022**, 10, 108930.

(193) Xie, F.; Wang, N.; Chen, H.; Li, M.; Li, Y.; Leng, L.; Qu, W.; Yang, J.; Yang, Z.; Li, H. Advances in Amine-Functionalized Metal Organic Frameworks for Carbon Capture. *J. Mater. Chem. A* **2025**, 13, 41653.

(194) Zhao, F.; Xu, F.; García, H.; Yu, J. Amine-Functionalized Covalent Organic Frameworks for High-Performance Carbon Dioxide Capture. *J. Colloid Interface Sci.* **2025**, 700, 138532.

(195) Zhang, S. Y.; Tang, X. H.; Yan, Y. L.; Li, S. Q.; Zheng, S.; Fan, J.; Li, X.; Zhang, W. G.; Cai, S. Facile and Site-Selective Synthesis of an Amine-Functionalized Covalent Organic Framework. *ACS Macro Lett.* **2021**, 10 (12), 1590-1596.

(196) Li, H.; Zhou, Z.; Ma, T.; Wang, K.; Zhang, H.; Alawadhi, A. H.; Yaghi, O. M. Bonding of Polyethylenimine in Covalent Organic Frameworks for CO<sub>2</sub> Capture from Air. *J. Am. Chem. Soc.* **2024**, 146 (51), 35486-35492.

(197) Wang, Q.; Lin, L.; Jiang, L.; Wang, Z.; Zhang, Y.; Han, Q.; Huang, X.; Zhu, C.; Jia, J.; Bian, Z.; Zhu, G. A New Post-Synthetic Route to Graft Amino Groups in Porous Organic Polymers for CO<sub>2</sub> Capture. *Chem. Sci.* **2025**, 16 (33), 15121-15128.

(198) Fracaroli, A. M.; Furukawa, H.; Suzuki, M.; Dodd, M.; Okajima, S.; Gándara, F.; Reimer, J. A.; Yaghi, O. M. Metal-Organic Frameworks with Precisely Designed Interior for Carbon Dioxide Capture in the Presence of Water. *J. Am. Chem. Soc.* **2014**, 136 (25), 8863-8866.

(199) Mahajan, S.; Elfving, J.; Lahtinen, M. Evaluating the Viability of Ethylenediamine-Functionalized Mg-MOF-74 in Direct Air Capture: The Challenges of Stability and Slow Adsorption Rate. *J. Environ. Chem. Eng.* **2024**, 12 (2), 112193.

(200) Siegelman, R. L.; Milner, P. J.; Forse, A. C.; Lee, J. H.; Colwell, K. A.; Neaton, J. B.; Reimer, J. A.; Weston, S. C.; Long, J. R.

Water Enables Efficient CO<sub>2</sub> Capture from Natural Gas Flue Emissions in an Oxidation-Resistant Diamine-

Appended Metal-Organic Framework. *J. Am. Chem. Soc.* **2019**, *141* (33), 13171-13186.

- (201) Young, J.; García-Díez, E.; Garcia, S.; Van Der Spek, M. The Impact of Binary Water-CO<sub>2</sub> Isotherm Models on the Optimal Performance of Sorbent-Based Direct Air Capture Processes. *Energy Environ. Sci.* **2021**, *14* (10), 5377-5394.
- (202) Lanxess Corporation. Product Information LEWATIT® VP OC 1065, 2022. <https://lanxess.com/en/products-and-brands/brands/lewatit/product-search/lewatit--vp-oc-1065> (accessed June 03, 2025).
- (203) Bos, M. J.; Pietersen, S.; Brilman, D. W. F. Production of High Purity CO<sub>2</sub> from Air Using Solid Amine Sorbents. *Chem. Eng. Sci.* **2019**, *2*, 100020.
- (204) Low, M. Y. A.; Danaci, D.; Azzan, H.; Woodward, R. T.; Petit, C. Measurement of Physicochemical Properties and CO<sub>2</sub>, N<sub>2</sub>, Ar, O<sub>2</sub>, and H<sub>2</sub>O Unary Adsorption Isotherms of Purolite A110 and Lewatit VP OC 1065 for Application in Direct Air Capture. *J. Chem. Eng. Data* **2023**, *68* (12), 3499-3511.
- (205) Parvazinia, M.; Garcia, S.; Maroto-Valer, M. CO<sub>2</sub> Capture by Ion Exchange Resins as Amine Functionalised Adsorbents. *Chem. Eng. J.* **2018**, *331*, 335-342.
- (206) Guo, Y.; Sun, J.; Wang, R.; Li, W.; Zhao, C.; Li, C.; Zhang, J. Recent Advances in Potassium-Based Adsorbents for CO<sub>2</sub> Capture and Separation: A Review. *Carbon Capture Sci. Technol.* **2021**, *1*, 100011.
- (207) Rodríguez-Mosqueda, R.; Rutgers, J.; Bramer, E. A.; Brem, G. Low Temperature Water Vapor Pressure Swing for the Regeneration of Adsorbents for CO<sub>2</sub> Enrichment in Greenhouses via Direct Air Capture. *J. CO<sub>2</sub> Util.* **2019**, *29*, 65-73.
- (208) Guo, Y.; Zhao, C.; Sun, J.; Li, W.; Lu, P. Facile Synthesis of Silica Aerogel Supported K<sub>2</sub>CO<sub>3</sub> Sorbents with Enhanced CO<sub>2</sub> Capture Capacity for Ultra-Dilute Flue Gas Treatment. *Fuel* **2018**, *215*, 735-743.
- (209) Veselovskaya, J. V.; Derevschikov, V. S.; Shalygin, A. S.; Yatsenko, D. A. K<sub>2</sub>CO<sub>3</sub>-Containing Composite Sorbents Based on a ZrO<sub>2</sub> Aerogel for Reversible CO<sub>2</sub> Capture from Ambient Air. *Microporous Mesoporous Mater.* **2021**, *310*, 110624.
- (210) Rodríguez-Mosqueda, R.; Bramer, E. A.; Brem, G. CO<sub>2</sub> Capture from Ambient Air Using Hydrated Na<sub>2</sub>CO<sub>3</sub> Supported on Activated Carbon Honeycombs with Application to CO<sub>2</sub> Enrichment in Greenhouses. *Chem. Eng. Sci.* **2018**, *189*, 114-122.
- (211) Rodríguez-Mosqueda, R.; Bramer, E. A.; Roestenberg, T.; Brem, G. Parametrical Study on CO<sub>2</sub> Capture from Ambient Air Using Hydrated K<sub>2</sub>CO<sub>3</sub> Supported on an Activated Carbon Honeycomb. *Ind. Eng. Chem. Res.* **2018**, *57* (10), 3628-3638.
- (212) Meis, N. N. A. H.; Frey, A. M.; Bitter, J. H.; De Jong, K. P. Carbon Nanofiber-Supported K<sub>2</sub>CO<sub>3</sub> as an Efficient Low-Temperature Regenerable CO<sub>2</sub> Sorbent for Post-Combustion Capture. *Ind. Eng. Chem. Res.* **2013**, *52* (36), 12812-12818.
- (213) Bali, S.; Sakwa-Novak, M. A.; Jones, C. W. Potassium Incorporated Alumina Based CO<sub>2</sub> Capture Sorbents: Comparison with Supported Amine Sorbents under Ultra-Dilute Capture Conditions. *Colloids Surf., A* **2015**, *486*, 78-85.
- (214) Zheng, S.; Cheng, X.; Zhou, W.; Wang, T.; Zhu, L.; Xiao, H.; Chen, X. K<sub>2</sub>CO<sub>3</sub> on Porous Supports for Moisture-Swing CO<sub>2</sub> Capture from Ambient Air. *Asia-Pac. J. Chem. Eng.* **2024**, *19* (3), No. e3058.
- (215) Masoud, N.; Bordanaba-Florit, G.; van Haasterecht, T.; Bitter, J. H. Effect of Support Surface Properties on CO<sub>2</sub> Capture from Air by Carbon-Supported Potassium Carbonate. *Ind. Eng. Chem. Res.* **2021**, *60* (38), 13749-13755.
- (216) Masoud, N.; Bordanaba Florit, G.; Van Haasterecht, T.; Bitter, H. Direct CO<sub>2</sub> Capture from Air-What Is the Best Sorbent? In *International Symposium on Green Chemistry (ISGC)*; 2019.
- (217) Veselovskaya, J. V.; Lysikov, A. I.; Netskina, O. V.; Kuleshov, D. V.; Okunev, A. G. K<sub>2</sub>CO<sub>3</sub>-Containing Composite Sorbents Based on Thermally Modified Alumina: Synthesis, Properties, and Potential Application in a Direct Air Capture/Methanation Process. *Ind. Eng. Chem. Res.* **2020**, *59* (15), 7130-7139.
- (218) Cruciani, G. Zeolites upon Heating: Factors Governing Their Thermal Stability and Structural Changes. *J.*

*Phys. Chem. Solids* **2006**, 67 (9-10), 1973-1994.

(219) Simancas, R.; Chokkalingam, A.; Elangovan, S. P.; Liu, Z.; Sano, T.; Iyoki, K.; Wakihara, T.; Okubo, T. Recent Progress in the Improvement of Hydrothermal Stability of Zeolites. *Chem. Sci.* **2021**, 12, 7677-7695.

(220) Zhou, J.; Wang, X.; Xing, W. Carbon-Based CO<sub>2</sub> Adsorbents. In *Post-combustion Carbon Dioxide Capture Material*; Wang, Q., Ed.; Royal Society of Chemistry, 2018; pp 1-75.

(221) Escobar-Hernandez, H. U.; Pérez, L. M.; Hu, P.; Soto, F. A.; Papadaki, M. I.; Zhou, H. C.; Wang, Q. Thermal Stability of Metal-Organic Frameworks (MOFs): Concept, Determination, and Model Prediction Using Computational Chemistry and Machine Learning. *Ind. Eng. Chem. Res.* **2022**, 61 (17), 5853-5862.

(222) Healy, C.; Patil, K. M.; Wilson, B. H.; Hermanspahn, L.; Harvey-Reid, N. C.; Howard, B. I.; Kleinjan, C.; Koliën, J.; Payet, F.; Telfer, S. G.; Kruger, P. E.; Bennett, T. D. The Thermal Stability of Metal-Organic Frameworks. *Coord. Chem. Rev.* **2020**, 419, 213388.

(223) Feng, L.; Wang, K. Y.; Day, G. S.; Ryder, M. R.; Zhou, H. C. Destruction of Metal-Organic Frameworks: Positive and Negative Aspects of Stability and Lability. *Chem. Rev.* **2020**, 120, 13087-13133.

(224) Lin, K. S.; Adhikari, A. K.; Ku, C. N.; Chiang, C. L.; Kuo, H. Synthesis and Characterization of Porous HKUST-1 Metal Organic Frameworks for Hydrogen Storage. *Int. J. Hydrogen Energy* **2012**, 37, 13865-13871.

(225) Diaz-Garcia, M.; Mayoral, A. I.; Diaz, I.; Sánchez-Sánchez, M. Nanoscaled M-MOF-74 Materials Prepared at Room Temperature. *Cryst. Growth Des.* **2014**, 14 (5), 2479-2487.

(226) Healy, C.; Harvey-Reid, N. C.; Howard, B. I.; Kruger, P. E. Thermal Decomposition of Hybrid Ultramicroporous Materials (HUMs). *Dalton Trans.* **2020**, 49 (47), 17433-17439.

(227) Wang, X.; Ma, X.; Schwartz, V.; Clark, J. C.; Overbury, S. H.; Zhao, S.; Xu, X.; Song, C. A Solid Molecular Basket Sorbent for CO<sub>2</sub> Capture from Gas Streams with Low CO<sub>2</sub> Concentration under Ambient Conditions. *Phys. Chem. Chem. Phys.* **2012**, 14 (4), 14851492.

(228) Sandhu, N. K.; Pudasainee, D.; Sarkar, P.; Gupta, R. Steam Regeneration of Polyethylenimine-Impregnated Silica Sorbent for Postcombustion CO<sub>2</sub> Capture: A Multicyclic Study. *Ind. Eng. Chem. Res.* **2016**, 55 (7), 2210-2220.

(229) Sanz-Pérez, E. S.; Arencibia, A.; Calleja, G.; Sanz, R. Tuning the Textural Properties of HMS Mesoporous Silica. Functionalization towards CO<sub>2</sub> Adsorption. *Microporous Mesoporous Mater.* **2018**, 260, 235-244.

(230) Zhao, Y.; Zhou, J.; Fan, L.; Chen, L.; Li, L.; Xu, Z. P.; Qian, G. Indoor CO<sub>2</sub> Control through Mesoporous Amine-Functionalized Silica Monoliths. *Ind. Eng. Chem. Res.* **2019**, 58 (42), 19465-19474.

(231) Goepfert, A.; Zhang, H.; Sen, R.; Dang, H.; Prakash, G. K. S. Oxidation-Resistant, Cost-Effective Epoxide-Modified Polyamine Adsorbents for CO<sub>2</sub> Capture from Various Sources Including Air. *ChemSusChem* **2019**, 12 (8), 1712-1723.

(232) White, C.; Wan, Z.; Wood, C.; Czapla, J. Ultra-Low Volatility Solid Polyamine CO<sub>2</sub> Capture Materials for Greenhouse CO<sub>2</sub> Enrichment. *Chem. Eng. J.* **2025**, 504, 158741.

(233) Liu, L.; Chen, J.; Tao, L.; Li, H.; Yang, Q. Aminopolymer Confined in Ethane-Silica Nanotubes for CO<sub>2</sub> Capture from Ambient Air. *ChemNanoMat* **2020**, 6 (7), 1096-1103.

(234) Kumar, D. R.; Rosu, C.; Sujan, A. R.; Sakwa-Novak, M. A.; Ping, E. W.; Jones, C. W. Alkyl-Aryl Amine-Rich Molecules for CO<sub>2</sub> Removal via Direct Air Capture. *ACS Sustain. Chem. Eng.* **2020**, 8 (29), 10971-10982.

(235) Wang, X.; Ma, X.; Song, C.; Locke, D. R.; Siefert, S.; Winans, R. E.; Möllmer, J.; Lange, M.; Möller, A.; Gläser, R. Molecular Basket Sorbents Polyethylenimine-SBA-15 for CO<sub>2</sub> Capture from Flue Gas: Characterization and Sorption Properties. *Microporous Mesoporous Mater.* **2013**, 169, 103-111.

(236) Sehaqui, H.; Gálvez, M. E.; Becatinni, V.; Cheng Ng, Y.; Steinfeld, A.; Zimmermann, T.; Tingaut, P. Fast and Reversible Direct CO<sub>2</sub> Capture from Air onto All-Polymer Nanofibrillated Cellulose- Polyethylenimine Foams. *Environ. Sci. Technol.* **2015**, 49 (5), 31673174.

(237) Liu, Z.; Teng, Y.; Zhang, K.; Chen, H.; Yang, Y. CO<sub>2</sub> Adsorption Performance of Different Amine-Based Siliceous MCM-41 Materials. *J. Energy Chem.* **2015**, 24 (3), 322-330.

(238) Wang, W.; Liu, F.; Zhang, Q.; Yu, G.; Deng, S. Efficient Removal of CO<sub>2</sub> from Indoor Air Using a Polyethyleneimine-Impregnated Resin and Its Low-Temperature Regeneration. *Chem. Eng. J.* **2020**, 399, 125734.

- (239) Qi, G.; Wang, Y.; Estevez, L.; Duan, X.; Anako, N.; Park, A. H. A.; Li, W.; Jones, C. W.; Giannelis, E. P. High Efficiency Nanocomposite Sorbents for CO<sub>2</sub> Capture Based on Amine- Functionalized Mesoporous Capsules. *Energy Environ. Sci.* **2011**, 4 (2), 444-452.
- (240) Zhang, G.; Zhao, P.; Hao, L.; Xu, Y. Amine-Modified SBA- 15(P): A Promising Adsorbent for CO<sub>2</sub> Capture. *J. CO<sub>2</sub> Util.* **2018**, 24, 22-33.
- (241) Ye, W.; Tang, Y.; Liang, X.; Luo, Q.; Liang, W.; Chen, C.; Zhang, K. Amine-Impregnated as-Synthesized Silicas for CO<sub>2</sub> Capture: Experimental Study and Mechanism Analysis. *Chem. Eng. Sci.* **2024**, 300, 120614.
- (242) Cai, H.; Bao, F.; Gao, J.; Chen, T.; Wang, S.; Ma, R. Preparation and Characterization of Novel Carbon Dioxide Adsorbents Based on Polyethylenimine-Modified Halloysite Nanotubes. *Environ. Technol.* **2015**, 36 (10), 1273-1280.
- (243) Chaikittisilp, W.; Kim, H. J.; Jones, C. W. Mesoporous Alumina-Supported Amines as Potential Steam-Stable Adsorbents for Capturing CO<sub>2</sub> from Simulated Flue Gas and Ambient Air. *Energy Fuels* **2011**, 25 (11), 5528-5537.
- (244) Keller, L.; Ohs, B.; Lenhart, J.; Abduly, L.; Blanke, P.; Wessling, M. High Capacity Polyethylenimine Impregnated Microtubes Made of Carbon Nanotubes for CO<sub>2</sub> Capture. *Carbon* **2018**, 126, 338-345.
- (245) Zhu, S.; Zhao, B.; Su, Y. Multiple-Amine Functionalized  $\gamma$ - Al<sub>2</sub>O<sub>3</sub> for Post-Combustion CO<sub>2</sub> Capture: Performance, Mechanism, and Kinetics. *Fuel* **2025**, 380, 133186.
- (246) Irani, M.; Gasem, K. A. M.; Dutcher, B.; Fan, M. CO<sub>2</sub> Capture Using Nanoporous TiO(OH)<sub>2</sub>/Tetraethylenepentamine. *Fuel* **2016**, 183, 601-608.
- (247) Irani, M.; Jacobson, A. T.; Gasem, K. A. M.; Fan, M. Modified Carbon Nanotubes/Tetraethylenepentamine for CO<sub>2</sub> Capture. *Fuel* **2017**, 206, 10-18.
- (248) Choi, S.; Gray, M. L.; Jones, C. W. Amine-Tethered Solid Adsorbents Coupling High Adsorption Capacity and Regenerability for CO<sub>2</sub> Capture from Ambient Air. *ChemSusChem* **2011**, 4 (5), 628-635.
- (249) Kuwahara, Y.; Kang, D. Y.; Copeland, J. R.; Brunelli, N. A.; Didas, S. A.; Bollini, P.; Sievers, C.; Kamegawa, T.; Yamashita, H.; Jones, C. W. Dramatic Enhancement of CO<sub>2</sub> Uptake by Poly(Ethyleneimine) Using Zirconosilicate Supports. *J. Am. Chem. Soc.* **2012**, 134 (26), 10757-10760.
- (250) Kuwahara, Y.; Kang, D. Y.; Copeland, J. R.; Bollini, P.; Sievers, C.; Kamegawa, T.; Yamashita, H.; Jones, C. W. Enhanced CO<sub>2</sub> Adsorption over Polymeric Amines Supported on Heteroatom- Incorporated SBA-15 Silica: Impact of Heteroatom Type and Loading on Sorbent Structure and Adsorption Performance. *Chem. — Eur. J.* **2012**, 18 (52), 16649-16664.
- (251) Liu, S. H.; Hsiao, W. C.; Sie, W. H. Tetraethylenepentamine- Modified Mesoporous Adsorbents for CO<sub>2</sub> Capture: Effects of Preparation Methods. *Adsorption* **2012**, 18, 431-437.
- (252) Jung, H.; Lee, C. H.; Jeon, S.; Jo, D. H.; Huh, J.; Kim, S. H. Effect of Amine Double-Functionalization on CO<sub>2</sub> Adsorption Behaviors of Silica Gel-Supported Adsorbents. *Adsorption* **2016**, 22 (8), 1137-1146.
- (253) Zhang, G.; Zhao, P.; Hao, L.; Xu, Y.; Cheng, H. A Novel Amine Double Functionalized Adsorbent for Carbon Dioxide Capture Using Original Mesoporous Silica Molecular Sieves as Support. *Sep. Purif. Technol.* **2019**, 209, 516-527.
- (254) Adegoke, K. A.; Akpomie, K. G.; Okeke, E. S.; Olisah, C.; Malloum, A.; Maxakato, N. W.; Ighalo, J. O.; Conradie, J.; Ohoro, C. R.; Amaku, J. F.; Oyedotun, K. O. UiO-66-Based Metal-Organic Frameworks for CO<sub>2</sub> Catalytic Conversion, Adsorption and Separation. *Sep. Purif. Technol.* **2024**, 331, 125456.
- (255) Katz, M. J.; Brown, Z. J.; Colón, Y. J.; Siu, P. W.; Scheidt, K. A.; Snurr, R. Q.; Hupp, J. T.; Farha, O. K. A Facile Synthesis of UiO- 66, UiO-67 and Their Derivatives. *Chem. Commun.* **2013**, 49 (82), 9449-9451.
- (256) Decoste, J. B.; Peterson, G. W.; Jasuja, H.; Glover, T. G.; Huang, Y. G.; Walton, K. S. Stability and Degradation Mechanisms of Metal-Organic Frameworks Containing the Zr<sub>6</sub>O<sub>4</sub>(OH)<sub>4</sub> Secondary Building Unit. *J. Mater. Chem. A* **2013**, 1 (18), 5642-5650.
- (257) Siegelman, R. L.; McDonald, T. M.; Gonzalez, M. I.; Martell, J. D.; Milner, P. J.; Mason, J. A.; Berger, A. H.; Bhowan, A. S.; Long, J. R. Controlling Cooperative CO<sub>2</sub> Adsorption in Diamine-Appended Mg<sub>2</sub>(Dobpdc) Metal-Organic Frameworks. *J. Am. Chem. Soc.* **2017**, 139 (30), 10526-10538.

- (258) Milner, P. J.; Martell, J. D.; Siegelman, R. L.; Gygi, D.; Weston, S. C.; Long, J. R. Overcoming Double-Step CO<sub>2</sub> Adsorption and Minimizing Water Co-Adsorption in Bulky Diamine-Appended Variants of Mg<sub>2</sub>(Dobpdc). *Chem. Sci.* **2018**, 9 (1), 160-174.
- (259) Rim, G.; Kong, F.; Song, M.; Rosu, C.; Priyadarshini, P.; Lively, R. P.; Jones, C. W. Sub-Ambient Temperature Direct Air Capture of CO<sub>2</sub> using Amine-Impregnated MIL-101(Cr) Enables Ambient Temperature CO<sub>2</sub> Recovery. *JACS Au* **2022**, 2 (2), 380393.
- (260) Wang, Y.; Rim, G.; Song, M. G.; Holmes, H. E.; Jones, C. W.; Lively, R. P. Cold Temperature Direct Air CO<sub>2</sub> Capture with Amine-Loaded Metal-Organic Framework Monoliths. *ACS Appl. Mater. Interfaces* **2024**, 16 (1), 1404-1415.
- (261) Lawson, S.; Griffin, C.; Rapp, K.; Rownaghi, A. A.; Rezaei, F. Amine-Functionalized MIL-101 Monoliths for CO<sub>2</sub> Removal from Enclosed Environments. *Energy Fuels* **2019**, 33 (3), 2399-2407.
- (262) Gadipelli, S.; Patel, H. A.; Guo, Z. An Ultrahigh Pore Volume Drives Up the Amine Stability and Cyclic CO<sub>2</sub> Capacity of a Solid- Amine@Carbon Sorbent. *Adv. Mater.* **2015**, 27 (33), 4903-4909.
- (263) Evans, A. M.; Ryder, M. R.; Ji, W.; Strauss, M. J.; Corcos, A. R.; Vitaku, E.; Flanders, N. C.; Bisbey, R. P.; Dichtel, W. R. Trends in the Thermal Stability of Two-Dimensional Covalent Organic Frameworks. *Faraday Discuss.* **2021**, 225, 226-240.
- (264) Alesi, W. R.; Kitchin, J. R. Evaluation of a Primary Amine-Functionalized Ion-Exchange Resin for CO<sub>2</sub> Capture. *Ind. Eng. Chem. Res.* **2012**, 51 (19), 6907-6915.
- (265) Hunt, R.; Gillbanks, J.; Czaplá, J.; Wan, Z.; Karmelich, C.; White, C.; Wood, C. Representative Longevity Testing of Direct Air Capture Materials. *Chem. Eng. J.* **2024**, 481, 148901.
- (266) Yu, Q.; Delgado, J. D. L. P.; Veneman, R.; Brilman, D. W. F. Stability of a Benzyl Amine Based CO<sub>2</sub> Capture Adsorbent in View of Regeneration Strategies. *Ind. Eng. Chem. Res.* **2017**, 56 (12), 32593269.
- (267) Elfving, J.; Bajamundi, C.; Kauppinen, J. Characterization and Performance of Direct Air Capture Sorbent. *Energy Procedia* **2017**, 114, 6087-6101.
- (268) Elfving, J.; Kauppinen, J.; Jegoroff, M.; Ruuskanen, V.; Järvinen, L.; Sainio, T. Experimental Comparison of Regeneration Methods for CO<sub>2</sub> Concentration from Air Using Amine-Based Adsorbent. *Chem. Eng. J.* **2021**, 404, 126337.
- (269) Min, Y. J.; Ganesan, A.; Realf, M. J.; Jones, C. W. Direct Air Capture of CO<sub>2</sub> Using Poly(Ethyleneimine)-Functionalized Expanded Poly(Tetrafluoroethylene)/Silica Composite Structured Sorbents. *ACS Appl. Mater. Interfaces* **2022**, 14 (36), 40992-41002.
- (270) Min, K.; Choi, W.; Kim, C.; Choi, M. Oxidation-Stable Amine-Containing Adsorbents for Carbon Dioxide Capture. *Nat. Commun.* **2018**, 9 (1), 726.
- (271) Drage, T. C.; Arenillas, A.; Smith, K. M.; Snape, C. E. Thermal Stability of Polyethylenimine Based Carbon Dioxide Adsorbents and Its Influence on Selection of Regeneration Strategies. *Microporous Mesoporous Mater.* **2008**, 116 (1-3), 504-512.
- (272) Guta, Y. A.; Carneiro, J.; Li, S.; Innocenti, G.; Pang, S. H.; Sakwa-Novak, M. A.; Sievers, C.; Jones, C. W. Contributions of CO<sub>2</sub>, O<sub>2</sub>, and H<sub>2</sub>O to the Oxidative Stability of Solid Amine Direct Air Capture Sorbents at Intermediate Temperature. *ACS Appl. Mater. Interfaces* **2023**, 15 (40), 46790-46802.
- (273) Li, S.; Guta, Y.; Calegari Andrade, M. F.; Hunter-Sellars, E.; Maiti, A.; Varni, A. J.; Tang, P.; Sievers, C.; Pang, S. H.; Jones, C. W. Competing Kinetic Consequences of CO<sub>2</sub> on the Oxidative Degradation of Branched Poly(Ethyleneimine). *J. Am. Chem. Soc.* **2024**, jacs.4c08126.
- (274) Sayari, A.; Belmabkhout, Y. Stabilization of Amine-Containing CO<sub>2</sub> Adsorbents: Dramatic Effect of Water Vapor. *J. Am. Chem. Soc.* **2010**, 132 (18), 6312-6314.
- (275) Sayari, A.; Belmabkhout, Y.; Da'Na, E. CO<sub>2</sub> Deactivation of Supported Amines: Does the Nature of Amine Matter? *Langmuir* **2012**, 28 (9), 4241-4247.
- (276) Sayari, A.; Heydari-Gorji, A.; Yang, Y. CO<sub>2</sub>-Induced Degradation of Amine-Containing Adsorbents: Reaction Products and Pathways. *J. Am. Chem. Soc.* **2012**, 134 (33), 13834-13842.
- (277) Chen, Z.; Yan, X.; Hu, X.; Feng, R.; Lu, S.; Liu, L.; Kang, G. Amine-Functionalized High-Surface-Area Al<sub>2</sub>O<sub>3</sub>

Adsorbent for CO<sub>2</sub> Capture: Effect of the Support Calcination Conditions. *Sep. Purif. Technol.* **2024**, 342, 127064.

(278) Jo, S. B.; Lee, S. C.; Chae, H. J.; Cho, M. S.; Lee, J. B.; Baek, J. I.; Kim, J. C. Regenerable Potassium-Based Alumina Sorbents Prepared by CO<sub>2</sub> Thermal Treatment for Post-Combustion Carbon Dioxide Capture. *Korean J. Chem. Eng.* **2016**, 33 (11), 3207-3215.

(279) Derevschikov, V. S.; Veselovskaya, J. V.; Shalygin, A. S.; Yatsenko, D. A.; Sheshkovas, A. Z.; Martyanov, O. N. Operating Limits and Features of Direct Air Capture on K<sub>2</sub>CO<sub>3</sub>/ZrO<sub>2</sub> Composite Sorbent. *Chin. J. Chem. Eng.* **2022**, 46, 11-20.

(280) Carneiro, J. S. A.; Innocenti, G.; Moon, H. J.; Guta, Y.; Proaño, L.; Sievers, C.; Sakwa-Novak, M. A.; Ping, E. W.; Jones, C. W. Insights into the Oxidative Degradation Mechanism of Solid Amine Sorbents for CO<sub>2</sub> Capture from Air: Roles of Atmospheric Water. *Angew. Chem., Int. Ed.* **2023**, 62 (24), No. e202302887.

(281) Heydari-Gorji, A.; Sayari, A. Thermal, Oxidative, and CO<sub>2</sub>- Induced Degradation of Supported Polyethylenimine Adsorbents. *Ind. Eng. Chem. Res.* **2012**, 51 (19), 6887-6894.

(282) Léonard, G.; Voice, A.; Toye, D.; Heyen, G. Influence of Dissolved Metals and Oxidative Degradation Inhibitors on the Oxidative and Thermal Degradation of Monoethanolamine in Postcombustion CO<sub>2</sub> Capture. *Ind. Eng. Chem. Res.* **2014**, 53 (47), 18121-18129.

(283) Léonard, G.; Crosset, C.; Toye, D.; Heyen, G. Influence of Process Operating Conditions on Solvent Thermal and Oxidative Degradation in Post-Combustion CO<sub>2</sub> Capture. *Comput. Chem. Eng.* **2015**, 83, 121-130.

(284) Buvik, V.; Vevelstad, S. J.; Brakstad, O. G.; Knuutila, H. K. Stability of Structurally Varied Aqueous Amines for CO<sub>2</sub> Capture. *Ind. Eng. Chem. Res.* **2021**, 60 (15), 5627-5638.

(285) Meng, Y.; Jiang, J.; Aihemaiti, A.; Ju, T.; Gao, Y.; Liu, J.; Han, S. Feasibility of CO<sub>2</sub> Capture from O<sub>2</sub>-Containing Flue Gas Using a Poly(Ethylenimine)-Functionalized Sorbent: Oxidative Stability in Long-Term Operation. *ACS Appl. Mater. Interfaces* **2019**, 11 (37), 33781-33791.

(286) Vu, Q. T.; Yamada, H.; Yogo, K. Oxidative Degradation of Tetraethylenepentamine-Impregnated Silica Sorbents for CO<sub>2</sub> Capture. *Energy Fuels* **2019**, 33 (4), 3370-3379.

(287) Krishna, R. Describing the Diffusion of Guest Molecules inside Porous Structures. *J. Phys. Chem. C* **2009**, 113 (46), 1975619781.

(288) Goff, G. S.; Rochelle, G. T. Monoethanolamine Degradation: O<sub>2</sub>Mass Transfer Effects under CO<sub>2</sub> Capture Conditions. *Ind. Eng. Chem. Res.* **2004**, 43 (20), 6400-6408.

(289) Lepaumier, H.; Picq, D.; Carrette, P. L. New Amines for CO<sub>2</sub> Capture. II. Oxidative Degradation Mechanisms. *Ind. Eng. Chem. Res.* **2009**, 48 (20), 9068-9075.

(290) Vu, Q. T.; Yamada, H.; Yogo, K. Effects of Amine Structures on Oxidative Degradation of Amine-Functionalized Adsorbents for CO<sub>2</sub>Capture. *Ind. Eng. Chem. Res.* **2021**, 60 (13), 4942-4950.

(291) Ahmadalinezhad, A.; Sayari, A. Oxidative Degradation of Silica-Supported Polyethylenimine for CO<sub>2</sub> Adsorption: Insights into the Nature of Deactivated Species. *Phys. Chem. Chem. Phys.* **2014**, 16 (4), 1529-1535.

(292) Miao, Y.; Wang, Y.; Zhu, X.; Chen, W.; He, Z.; Yu, L.; Li, J. Minimizing the Effect of Oxygen on Supported Polyamine for Direct Air Capture. *Sep. Purif. Technol.* **2022**, 298, 121583.

(293) Bali, S.; Chen, T. T.; Chaikittisilp, W.; Jones, C. W. Oxidative Stability of Amino Polymer-Alumina Hybrid Adsorbents for Carbon Dioxide Capture. *Energy Fuels* **2013**, 27 (3), 1547-1554.

(294) Buvik, V.; Høisæter, K. K.; Vevelstad, S. J.; Knuutila, H. K. A Review of Degradation and Emissions in Post-Combustion CO<sub>2</sub> Capture Pilot Plants. *Int. J. Greenhouse Gas Control* **2021**, 106, 103246.

(295) Nezam, I.; Xie, J.; Golub, K. W.; Carneiro, J.; Olsen, K.; Ping, E. W.; Jones, C. W.; Sakwa-Novak, M. A. Chemical Kinetics of the Autoxidation of Poly(Ethylenimine) in CO<sub>2</sub> Sorbents. *ACS Sustain. Chem. Eng.* **2021**, 9 (25), 8477-8486.

(296) Racicot, J.; Li, S.; Clabaugh, A.; Hertz, C.; Akhade, S. A.; Ping, E. W.; Pang, S. H.; Sakwa-Novak, M. A. Volatile Products of the Autoxidation of Poly(Ethylenimine) in CO<sub>2</sub> Sorbents. *J. Phys. Chem. C* **2022**, 126 (20), 8807-8816.

(297) Bedell, S. A. Amine Autoxidation in Flue Gas CO<sub>2</sub> Capture- Mechanistic Lessons Learned from Other Gas Treating Processes. *Int. J. Greenhouse Gas Control* **2011**, 5 (1), 1-6.

- (298) Fredriksen, S. B.; Jens, K. J. Oxidative Degradation of Aqueous Amine Solutions of MEA, AMP, MDEA, Pz: A Review. *Energy Procedia* **2013**, *37*, 1770-1777.
- (299) Yan, C.; Sayari, A. Spectroscopic Investigation into the Oxidation of Polyethylenimine for CO<sub>2</sub> Capture: Mitigation Strategies and Mechanism. *Chem. Eng. J.* **2024**, *479*, 147498.
- (300) Wang, Y.; Hu, X.; Guo, T.; Tian, W.; Hao, J.; Guo, Q. The Competitive Adsorption Mechanism of CO<sub>2</sub>, H<sub>2</sub>O and O<sub>2</sub> on a Solid Amine Adsorbent. *Chem. Eng. J.* **2021**, *416*, 129007.
- (301) Rosu, C.; Pang, S. H.; Sujan, A. R.; Sakwa-Novak, M. A.; Ping, E. W.; Jones, C. W. Effect of Extended Aging and Oxidation on Linear Poly(Propylenimine)-Mesoporous Silica Composites for CO<sub>2</sub> Capture from Simulated Air and Flue Gas Streams. *ACS Appl. Mater. Interfaces* **2020**, *12* (34), 38085-38097.
- (302) Guta, Y. A.; Tang, P.; Li, S.; Zhang, J.; Sakwa-Novak, M. A.; Pang, S. H.; Sievers, C.; Jones, C. W. Evaluating Autoxidation Radical Scavengers and Additives to Enhance Aminopolymer Sorbent Stability. *Energy Fuels* **2025**, *39* (49), 23141-23152.
- (303) Calleja, G.; Sanz, R.; Arencibia, A.; Sanz-Pérez, E. S. Influence of Drying Conditions on Amine-Functionalized SBA-15 as Adsorbent of CO<sub>2</sub>. *Top. Catal.* **2011**, *54*, 135-145.
- (304) Heydari-Gorji, A.; Belmabkhout, Y.; Sayari, A. Degradation of Amine-Supported CO<sub>2</sub> Adsorbents in the Presence of Oxygen-Containing Gases. *Microporous Mesoporous Mater.* **2011**, *145* (1-3), 146-149.
- (305) Ahmadalinezhad, A.; Tailor, R.; Sayari, A. Molecular-Level Insights into the Oxidative Degradation of Grafted Amines. *Chem. — Eur. J.* **2013**, *19* (32), 10543-10550.
- (306) Bollini, P.; Choi, S.; Drese, J. H.; Jones, C. W. Oxidative Degradation of Aminosilica Adsorbents Relevant to Postcombustion CO<sub>2</sub> Capture. *Energy Fuels* **2011**, *25* (5), 2416-2425.
- (307) Didas, S. A.; Zhu, R.; Brunelli, N. A.; Sholl, D. S.; Jones, C. W. Thermal, Oxidative and CO<sub>2</sub> Induced Degradation of Primary Amines Used for CO<sub>2</sub> Capture: Effect of Alkyl Linker on Stability. *J. Phys. Chem. C* **2014**, *118* (23), 12302-12311.
- (308) Xiong, S.; Sterling, A. J.; Tkachenko, N. V.; Reyes, R. D.; Tsai, H.; Lee, J.; Chen, Y.; Wang, Y.; Dods, M. N.; Lu, D.; Zhu, Z.; Börgel, J.; Kim, J. W.; Schmeiser, A. J.; Meng, J.; Furukawa, H.; Peters, A. W.; McCloskey, B. D.; Reimer, J. A.; Weston, S. C.; Head-Gordon, M.; Long, J. R. Mechanistic Studies of Oxidative Degradation in Diamine-Appended Metal-Organic Frameworks Exhibiting Cooperative CO<sub>2</sub> Capture. *J. Am. Chem. Soc.* **2025**, *147*, 25761.
- (309) Sujan, A. R.; Pang, S. H.; Zhu, G.; Jones, C. W.; Lively, R. P. Direct CO<sub>2</sub> Capture from Air Using Poly(Ethylenimine)-Loaded Polymer/Silica Fiber Sorbents. *ACS Sustain. Chem. Eng.* **2019**, *7* (5), 5264-5273.
- (310) Zhao, J.; Deng, S.; Zhao, L.; Yuan, X.; Wang, B.; Chen, L.; Wu, K. Synergistic and Competitive Effect of H<sub>2</sub>O on CO<sub>2</sub> Adsorption Capture: Mechanism Explanations Based on Molecular Dynamic Simulation. *J. CO<sub>2</sub> Util.* **2021**, *52*, 101662.
- (311) Lee, T. S.; Cho, J. H.; Chi, S. H. Carbon Dioxide Removal Using Carbon Monolith as Electric Swing Adsorption to Improve Indoor Air Quality. *Build. Environ.* **2015**, *92*, 209-221.
- (312) Korah, M. M.; Culp, K.; Lackner, K. S.; Green, M. D. Activated Carbon Fiber Felt Composites for the Direct Air Capture of Carbon Dioxide. *ChemSusChem* **2025**, *18* (3), No. e202401188.
- (313) Li, W. L.; Shuai, Q.; Yu, J. Recent Advances of Carbon Capture in Metal-Organic Frameworks: A Comprehensive Review. *Small* **2024**, *20*, 2402783.
- (314) Zuluaga, S.; Fuentes-Fernandez, E. M. A.; Tan, K.; Xu, F.; Li, J.; Chabal, Y. J.; Thonhauser, T. Understanding and Controlling Water Stability of MOF-74. *J. Mater. Chem. A* **2016**, *4* (14), 51765183.
- (315) Tan, K.; Zuluaga, S.; Gong, Q.; Canepa, P.; Wang, H.; Li, J.; Chabal, Y. J.; Thonhauser, T. Water Reaction Mechanism in Metal Organic Frameworks with Coordinatively Unsaturated Metal Ions: MOF-74. *Chem. Mater.* **2014**, *26* (23), 6886-6895.
- (316) Xiao, C.; Tian, J.; Chen, Q.; Hong, M. Water-Stable Metal-Organic Frameworks (MOFs): Rational Construction and Carbon Dioxide Capture. *Chem. Sci.* **2024**, *15*, 1570-1610.
- (317) Boone, P.; He, Y.; Lieber, A. R.; Steckel, J. A.; Rosi, N. L.; Hornbostel, K. M.; Wilmer, C. E. Designing Optimal Core-Shell MOFs for Direct Air Capture. *Nanoscale* **2022**, *14* (43), 1608516096.

- (318) He, Y.; Boone, P.; Lieber, A. R.; Tong, Z.; Das, P.; Hornbostel, K. M.; Wilmer, C. E.; Rosi, N. L. Implementation of a Core-Shell Design Approach for Constructing MOFs for CO<sub>2</sub> Capture. *ACS Appl. Mater. Interfaces* **2023**, *15* (19), 23337-23342.
- (319) Tompkins, J. T.; Mokaya, R. Steam Stable Mesoporous Silica MCM-41 Stabilized by Trace Amounts of Al. *ACS Appl. Mater. Interfaces* **2014**, *6* (3), 1902-1908.
- (320) Li, W.; Bollini, P.; Didas, S. A.; Choi, S.; Drese, J. H.; Jones, C. W. Structural Changes of Silica Mesocellular Foam Supported Amine- Functionalized CO<sub>2</sub> Adsorbents upon Exposure to Steam. *ACS Appl. Mater. Interfaces* **2010**, *2* (11), 3363-3372.
- (321) Ziaei-Azad, H.; Kolle, J. M.; Al-Yasser, N.; Sayari, A. One-Pot Synthesis of Large-Pore AlMCM-41 Aluminosilicates with High Stability and Adjustable Acidity. *Microporous Mesoporous Mater.* **2018**, *262*, 166-174.
- (322) Jahandar Lashaki, M.; Ziaei-Azad, H.; Sayari, A. Unprecedented Improvement of the Hydrothermal Stability of Amine-Grafted MCM-41 Silica for CO<sub>2</sub> Capture via Aluminum Incorporation. *Chem. Eng. J.* **2022**, *450*, 138393.
- (323) Jahandar Lashaki, M.; Ziaei-Azad, H.; Sayari, A. Insights into the Hydrothermal Stability of Triamine-Functionalized SBA-15 Silica for CO<sub>2</sub> Adsorption. *ChemSusChem* **2017**, *10* (20), 4037-4045.
- (324) Hammache, S.; Hoffman, J. S.; Gray, M. L.; Fauth, D. J.; Howard, B. H.; Pennline, H. W. Comprehensive Study of the Impact of Steam on Polyethyleneimine on Silica for CO<sub>2</sub> Capture. *Energy Fuels* **2013**, *27* (11), 6899-6905.
- (325) Min, K.; Choi, W.; Choi, M. Macroporous Silica with Thick Framework for Steam-Stable and High-Performance Poly- (Ethyleneimine)/Silica CO<sub>2</sub> Adsorbent. *ChemSusChem* **2017**, *10* (11), 2518-2526.
- (326) Kim, J. M.; Jun, S.; Ryoo, R. Improvement of Hydrothermal Stability of Mesoporous Silica Using Salts: Reinvestigation for Time-Dependent Effects. *J. Phys. Chem. B* **1999**, *103* (30), 6200-6205.
- (327) Ryoo, R.; Jun, S. Improvement of Hydrothermal Stability of MCM-41 Using Salt Effects during the Crystallization Process. *J. Phys. Chem. B* **1997**, *101* (3), 317-320.
- (328) Masika, E.; Mokaya, R. Mesoporous Aluminosilicates from a Zeolite BEA Recipe. *Chem. Mater.* **2011**, *23* (9), 2491-2498.
- (329) Mokaya, R. Improving the Stability of Mesoporous MCM-41 Silica via Thicker More Highly Condensed Pore Walls. *J. Phys. Chem. B* **1999**, *103* (46), 10204-10208.
- (330) Mokaya, R. On the Extended Recrystallisation of Mesoporous Silica: Characterisation of Restructured Pure Silica MCM-41. *J. Mater. Chem.* **2002**, *12* (10), 3027-3033.
- (331) Sakwa-Novak, M. A.; Jones, C. W. Steam Induced Structural Changes of a Poly(Ethyleneimine) Impregnated  $\gamma$ -Alumina Sorbent for CO<sub>2</sub> Extraction from Ambient Air. *ACS Appl. Mater. Interfaces* **2014**, *6* (12), 9245-9255.
- (332) Kuhnert, E.; Hacker, V.; Bodner, M. A Review of Accelerated Stress Tests for Enhancing MEA Durability in PEM Water Electrolysis Cells. *Int. J. Energy Res.* **2023**, *2023*, 1.
- (333) Wallnöfer-Ogris, E.; Grimmer, I.; Ranz, M.; Höglinger, M.; Kartusch, S.; Rauh, J.; Macherhammer, M. G.; Grabner, B.; Trattner, A. A Review on Understanding and Identifying Degradation Mechanisms in PEM Water Electrolysis Cells: Insights for Stack Application, Development, and Research. *Int. J. Hydrogen Energy* **2024**, *65*, 381-397.
- (334) Thiele, P.; Gouveia, L.; Ulrich, O.; Yang, Y.; Liu, Y.; Wick, M.; Pischinger, S. Realistic Accelerated Stress Tests for PEM Fuel Cells: Operation Condition Dependent Load Profile Optimization. *J. Power Sources* **2024**, *617*, 234959.
- (335) Hydrogen and Fuel Cell Technologies Office. DOE Cell Component Accelerated Stress Test Protocols for PEM Fuel Cells, 2007. [https://www1.eere.energy.gov/hydrogenandfuelcells/fuelcells/pdfs/component\\_durability\\_profile.pdf](https://www1.eere.energy.gov/hydrogenandfuelcells/fuelcells/pdfs/component_durability_profile.pdf) (accessed Jan 23, 2026).
- (336) Goswami, N.; Rao, S.; Abad, S. D.; Ruba, A.; Thakkar, H.; Mukherjee, P. P.; Singh, R. P.; Spendelow, J. S.; Holby, E. F.; Zelenay, P.; Kang, Q. Role of Hierarchical Porosity in Dictating Adsorption Dynamics in Direct Air Capture Systems. *ACS Appl. Energy Mater.* **2025**, *8* (15), 11758-11770.
- (337) Verstreken, M. F. K.; Chanut, N.; Magnin, Y.; Landa, H. O. R.; Denayer, J. F. M.; Baron, G. V.; Ameloot, R. Mind the Gap: The Role of Mass Transfer in Shaped Nanoporous Adsorbents for Carbon Dioxide Capture. *J. Am. Chem.*

*Soc.* **2024**, 146, 23633-23648.

(338) Sriram, A.; Choi, S.; Yu, X.; Brabson, L. M.; Das, A.; Ulissi, Z.; Uyttendaele, M.; Medford, A. J.; Sholl, D. S. The Open DAC 2023 Dataset and Challenges for Sorbent Discovery in Direct Air Capture. *ACS Cent. Sci.* **2024**, 10 (5), 923-941.

(339) Park, H.; Majumdar, S.; Zhang, X.; Kim, J.; Smit, B. Inverse Design of Metal-Organic Frameworks for Direct Air Capture of CO<sub>2</sub> via Deep Reinforcement Learning. *Digital Discovery* **2024**, 3 (4), 728-741.

(340) Lim, Y.; Park, H.; Walsh, A.; Kim, J. Accelerating CO<sub>2</sub> Direct Air Capture Screening for Metal-Organic Frameworks with a Transferable Machine Learning Force Field. *Matter* **2025**, 8 (7), 102203.

(341) Davis, M. C.; Kort-Kamp, W. J. M.; Matanovic, I.; Zelenay, P.; Holby, E. F. Design of Active Sites for Amine-Functionalized Direct Air Capture Materials Using Integrated High-Throughput Calculations and Machine Learning. *Commun. Chem.* **2026**, 9 (1), 12.